



# Studies towards the synthesis of oligoaryl- based ApoA1-mimetics

MASTERARBEIT

Zur Erlangung des akademischen Grades  
Master of Science (MSc)  
der Studienrichtung „Chemie“

an der  
Technischen Universität Graz

vorgelegt von

**Patrick Dobrounig, BSc**

unter der Betreuung von  
Univ.-Prof. Dipl.-Ing. Dr.rer.nat. Rolf Breinbauer  
(Institut für Organische Chemie, TU Graz)

Graz, 30.07.2014

Die vorliegende Arbeit wurde unter der Betreuung von Prof. Dr. Rolf Breinbauer in der Zeit von November 2013 bis Juli 2014 im Fachbereich Chemie am Institut für Organische Chemie der Technischen Universität Graz angefertigt

*„Ein Gelehrter in seinem Laboratorium ist nicht nur ein Techniker; er steht auch vor den Naturgesetzen wie ein Kind vor der Märchenwelt.“*

Marie Curie

---

|   |    |
|---|----|
| 1 Introduction .....  | 7  |
| 2 Theoretical Background .....                                      | 8  |
| 2.1 Apolipoprotein A1 .....   | 8  |
| 2.1.1 Physiological role of ApoA1 and HDL .....                     | 8  |
| 2.1.2 Structural properties of ApoA1 .....                          | 10 |
| 2.2 Protein-protein interactions .....                              | 12 |
| 2.2.1 General concepts .....  | 12 |
| 2.2.2 Protein-protein interactions with ApoA1/HDL .....             | 13 |
| 2.3 Inhibitors of protein-protein interactions .....                | 14 |
| 2.3.1 Inhibitors based on small peptides .....                      | 14 |
| 2.3.2 Non-peptidic inhibitors - $\alpha$ -helix mimetics .....      | 15 |
| 2.3.3 ApoA1 mimetics .....  | 18 |
| 2.4 Targeted drug delivery .....                                    | 21 |
| 2.4.1 Why targeted drug delivery? .....                             | 21 |
| 2.4.2 HDL as a drug carrier .....                                   | 22 |
| 3 Scientific Task .....   | 25 |
| 4 Results and Discussion .....                                      | 26 |
| 4.1 Synthesis of the Glu-building block .....                       | 26 |
| 4.1.1 Pechmann coumarin synthesis .....                             | 26 |
| 4.1.2 The Heck-Mizoroki reaction .....                              | 29 |
| 4.1.3 The Sonogashira reaction .....                                | 34 |
| 4.1.4 Heterogeneously catalyzed hydrogenation .....                 | 36 |
| 4.1.5 Iodination .....  | 39 |
| 4.1.6 Reesterification .....  | 39 |
| 4.1.7 Introduction of the trifluoromethane sulfonate group .....    | 41 |
| 4.2 Synthesis of the Lys-building block .....                       | 42 |
| 4.2.1 Heck reaction of 3-bromophenol .....                          | 44 |
| 4.2.2 Wittig reaction with benzyltriphenylphosphonium bromide ..... | 46 |
| 4.2.3 Horner-Wadsworth-Emmons reaction .....                        | 47 |
| 4.2.4 Claisen rearrangement .....                                   | 48 |
| 4.2.5 Heck reaction with a diazonium salt .....                     | 49 |
| 4.2.6 Silylation .....  | 52 |
| 4.2.7 Appel reaction .....  | 52 |

---

|   |    |
|---|----|
| 4.2.8 Synthesis of (3-(( <i>tert</i> -butoxycarbonyl)amino)propyl)triphenylphosphonium iodide ..... | 53 |
| 4.2.9 Finkelstein reaction .....  | 54 |
| 4.2.10 Organozinc chemistry .....   | 55 |
| 5 Summary .....   | 57 |
| 6 Outlook.....  | 59 |
| 7 Experimental Section .....  | 61 |
| 7.1 General .....   | 61 |
| 7.2 Solvents .....  | 61 |
| 7.3 Separation techniques.....  | 62 |
| 7.3.1 Thin layer chromatography .....   | 62 |
| 7.3.2 Flash chromatography .....  | 63 |
| 7.3.3 Gas chromatography .....  | 63 |
| 7.4 Nuclear Magnetic Resonance.....   | 64 |
| 7.5 Melting points .....  | 64 |
| 7.6 High resolution mass spectroscopy .....   | 64 |
| 7.7 Experimental procedures.....  | 65 |
| 7.7.1 7-Hydroxy-2 <i>H</i> -chromen-2-one (1).....  | 65 |
| 7.7.2 2-Oxo-2 <i>H</i> -chromen-7-yl trifluoromethanesulfonate (2).....                             | 67 |
| 7.7.3 7-(Phenylethynyl)-2 <i>H</i> -chromen-2-one (3) .....   | 68 |
| 7.7.4 7-Phenethylchroman-2-one (4) .....  | 70 |
| 7.7.5 6-Iodo-7-phenethylchroman-2-one (5).....  | 71 |
| 7.7.5 6-Iodo-7-phenethylchroman-2-one (5).....  | 71 |
| 7.7.6 Methyl 3-(2-hydroxy-5-iodo-4-phenethylphenyl)propanoate (6) .....                             | 73 |
| 7.7.7 Methyl-3-(5-iodo-4-phenethyl-2-(((trifluoromethyl)sulfonyl)oxy) .....                         | 74 |
| phenyl)propanoate (7) .....   | 74 |
| 7.7.8 Diethyl benzylphosphonate (8) .....   | 76 |
| 7.7.9 <i>tert</i> -Butyl (3-chloropropyl)carbamate (9) .....  | 77 |
| 7.7.10 <i>tert</i> -Butyl (3-hydroxypropyl)carbamate (10) .....                                     | 78 |
| 7.7.11 Methyl 4-amino-2-hydroxybenzoate (11) .....  | 79 |
| 7.7.12 3-Hydroxy-4-(methoxycarbonyl)benzenediazoniumtetrafluoro borate (12) .....                   | 80 |
| 7.7.13 3-Iodopropanenitrile (13) .....  | 81 |
| 7.7.14 Methyl 2-(( <i>tert</i> -butyldimethylsilyl)oxy)-4-phenethylbenzoate (14) .....              | 82 |
| 8 References .....  | 84 |

|                       |    |
|-----------------------|----|
| 9 Abbreviations ..... | 90 |
| 10 Danksagung .....   | 94 |
| 11 Appendix .....     | 97 |

## 1 Introduction

No matter how large an organism is, all functions are carried out by small units, called cells. Nature has designed cells and their modes of action in unmentionable efficiency and elegance. Communication between cells and their function have been improved and are still improving during the evolution.<sup>[1]</sup>

If a cell has a malfunction the results can lead to serious diseases of the organism. To some amount an organism has repair mechanisms to fix such malfunctions, but in many cases repair mechanisms fail. In many cases chemicals, called drugs, can cure such diseases. Therefore humans have been using natural products like herbs throughout history as medicine. Natural products still are very important as potential drugs or as starting material for the synthesis of other compounds.<sup>[2]</sup>

The mode of action of a drug is mostly through inhibition of an enzyme or a receptor. By inhibition a malfunction of those can often be repaired. When we are talking of such enzymes or receptors which we want to address with a drug we speak of targets. Not every target is easily druggable, an example are interactions between proteins, which control many processes in organisms. Other difficult targets are cancer cells.<sup>[3,4]</sup>

A cancer cell is in many aspects similar to a healthy cell. For instance cancer cells do also undergo mitosis, but do not undergo apoptosis, the programmed cell death. Therefore tumors keep growing. A cancer cell has mostly the same sort of enzymes as a healthy cell has, but some are interacting in different mode or are overexpressed. This leads to the main problem of treating cancer: how to kill a cancer cell without killing healthy ones?<sup>[4]</sup>

One promising answer is targeted drug delivery. A drug carrier, which delivers a drug selectively to the cancer cell, releases the drug, which then kills the cancer cell without hurting any healthy cell.<sup>[4]</sup>

A lot of research is going on in that field and the first promising results have been published.<sup>[4-7]</sup> The goal of this thesis is to contribute to this field of research.

## 2 Theoretical Background

### 2.1 Apolipoprotein A1

Apolipoprotein A1 (ApoA1) is the main protein compartment of high-density lipoprotein (HDL), which is responsible for the transport of cholesterol to the liver.<sup>[8]</sup> ApoA1 consists of 243 amino acid residues, which form ten  $\alpha$ -helices as a secondary structure. Most of these helices show a class A amphipathic character. In class A amphipathic helices positive charges are located on the water lipid interface and the negative ones are located in the middle of the hydrophilic side.<sup>[9,10]</sup> Two ApoA1 molecules form an antiparallel stacked double-belt dimer, which encircles HDL (Figure 1).<sup>[11]</sup>

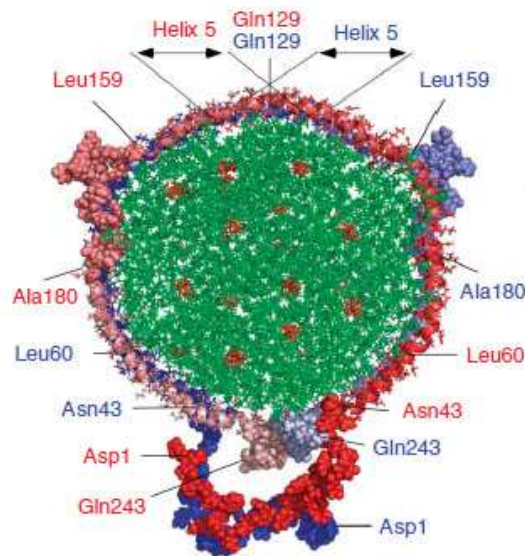


**Figure 1: On-top-view of a solar-flares model of the antiparallel stacked double-belt ApoA1 dimer. One ApoA1 molecule in red (*N*-terminus) and pink (*C*-terminus). The second ApoA1 molecule in dark blue (*N*-terminus) and light blue (*C*-terminus). Picture taken from Ref. [11].**

#### 2.1.1 Physiological role of ApoA1 and HDL

The ApoA1/HDL complex works as a transporter of cholesterol from peripheral cells to the liver. This process is known as reverse cholesterol efflux, which contains three major steps (Figure 2). Reverse cholesterol efflux starts with lipid-free or lipid-poor ApoA1 interacting with ATP-binding cassette transporter ABCA1. There cholesterol is transferred from peripheral cells via ABCA1 to ApoA1 forming or enlarging HDL. In the next step cholesterol esterification of HDL's lipid core takes place, resulting in mature HDL. This happens through a lecithin-cholesterol acyltransferase (LCAT) mediated process. LCAT is interacting with



ApoA1, which is essential for successful esterification. In the final step cholesterol of mature HDL is off-loaded to liver cells by the scavenger receptor B1 (SR-B1). After the off-loading lipid-free or lipid-poor ApoA1 is obtained, which can reenter the reverse cholesterol efflux in step one. SR-B1 has the ability to off-load cholesterol from various sources, including HDL, low-density lipoprotein (LDL) and very-low-density lipoprotein (VLDL). SR-B1 also interacts with ApoA1 to off-load cholesterol. [8,10,12,13]

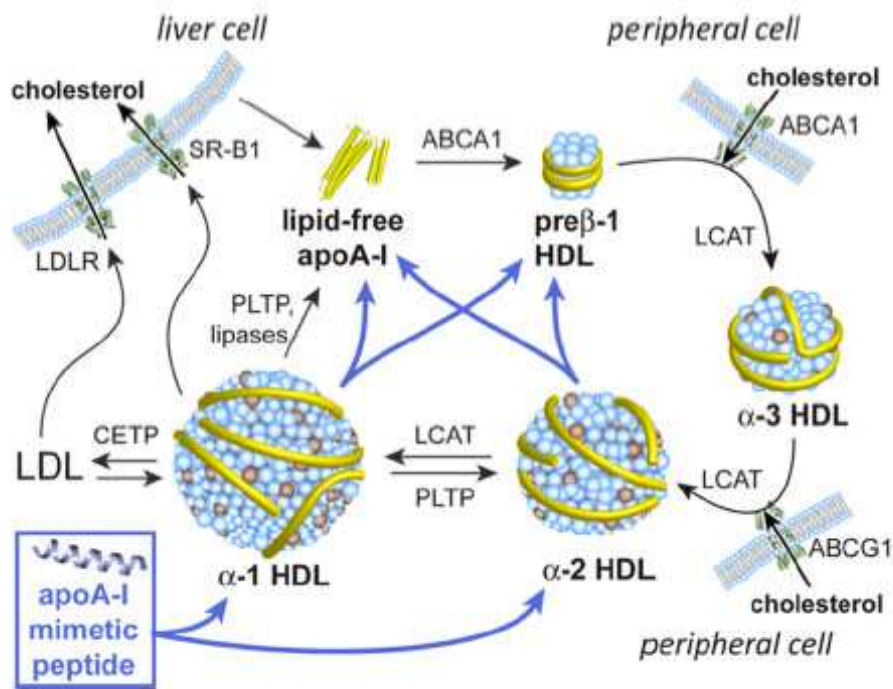


**Figure 2: Reverse cholesterol efflux, including the effects of ApoA1 mimetics (blue arrows). Picture taken from Ref. [13]**

The artery wall is thickened due to accumulation of cholesterol loaded macrophages in atherosclerosis. Therefore HDL/ApoA1 has a positive effect due to reverse cholesterol efflux and is seen as a potential therapeutic. [12,13]

Beside its role in reverse cholesterol efflux, ApoA1/HDL shows other biological properties, such as anti-inflammatory, anti-apoptotic and anti-oxidative properties. [8] Anti-inflammatory and anti-oxidative properties are thought to be mediated in some part by ApoA1 and in some part by HDL associated proteins, such as paraoxonase-1 (PON1). An anti-oxidative effect is achieved by reducing the amount of oxidized LDL-associated lipids. [8,14]

ApoA1 has shown to be very suitable as a biomarker for the onset of Parkinson's disease. There low ApoA1 concentration correlates to an earlier Parkinson's disease onset. [15] ApoA1,

apolipoprotein B (ApoB) and ApoB/ApoA1 ratio have been shown to be very suitable for the prediction of stroke. High ApoB and ApoB/ApoA1 values and low ApoA1 values correlate to a higher risk for suffering of stroke.<sup>[16]</sup>

Zamanian-Daryoush *et al.* have investigated the effect of ApoA1 on tumor growth and metastasis development in mice. In vitro experiments showed no direct effect of ApoA1 or HDL on tumor growth, but ApoA1 knock-out (KO) mice showed a ten times higher tumor burden compared to ApoA1 overexpressing mice. The same trend was seen for metastasis. When ApoA1 KO mice were treated with ApoA1, tumor growth and metastasis were inhibited more than a 100-fold compared to saline treated ApoA1 KO mice. Not a single ApoA1 treated ApoA1 KO mouse died during the test time (35 d), whereas all saline treated ApoA1 KO mice had died after day 29. ApoA1 treatment on ApoA1 KO mice, which already had had tumor burden and had developed metastasis, led to a reduction in metastasis and a shrinking of the tumor. Further experiments with immune deficient mice have shown, that most of the anti-tumor activity of ApoA1 seems to originate from an immune dependent pathway.<sup>[8]</sup>

### **2.1.2 Structural properties of ApoA1**

As said before, ApoA1 consists of 243 amino acid residues, which form ten  $\alpha$ -helices as secondary structure. Many experiments have been done to identify the ApoA1 structural elements, which are required to mediate reverse cholesterol efflux. Helix 1 and helix 10 are the smallest helices of ApoA1 and show the highest lipid affinity. Helix 1 alone is able to mediate reverse cholesterol efflux with 50 % efficiency compared to full length ApoA1 whereas helix 10 alone was not able to mediate reverse cholesterol efflux. In combination with helix 9, as a bihelical 9/10 peptide, reverse cholesterol efflux was mediated with 68 % efficiency.<sup>[17]</sup> That means lipophilicity alone is not sufficient to interact with ABCA1. A synthetic peptide, corresponding to helix 1, did not promote cholesterol efflux in an ABCA1 dependent manner. Just at high concentrations of that helix 1 peptide cholesterol efflux was observed, but just with 15 % efficiency. A helix 1/9 chimera promoted cholesterol efflux, whereas helix 9 alone did not. A mixture of helices 1 and 9 also did not promote cholesterol efflux indicating that the covalent linkage between helix 1 and 9 is essential for interacting with ABCA1. A helix 9/10 peptide promoted cholesterol efflux twice as efficient as the 1/9 chimera. A closer look on the structural properties shows, that peptide 9/10 is a class Y amphipathic peptide, which means that there is also one positive charge in the middle of the

hydrophilic side, whereas in class A amphipathic peptides positive charges are just on the lipid/water interface. Peptide 1/9 belongs to class A amphipathic peptides, which indicates that class Y is not necessarily needed for ABCA1 interaction. Both peptides have the same net charge of -1 and the positions of negatively charged amino acid residues over the length of the joined peptide are nearly the same by both. Three of those negative charges form an alignment spanning  $\sim 32\text{\AA}$  down the length of the joined helices (Figure 3).<sup>[9]</sup>

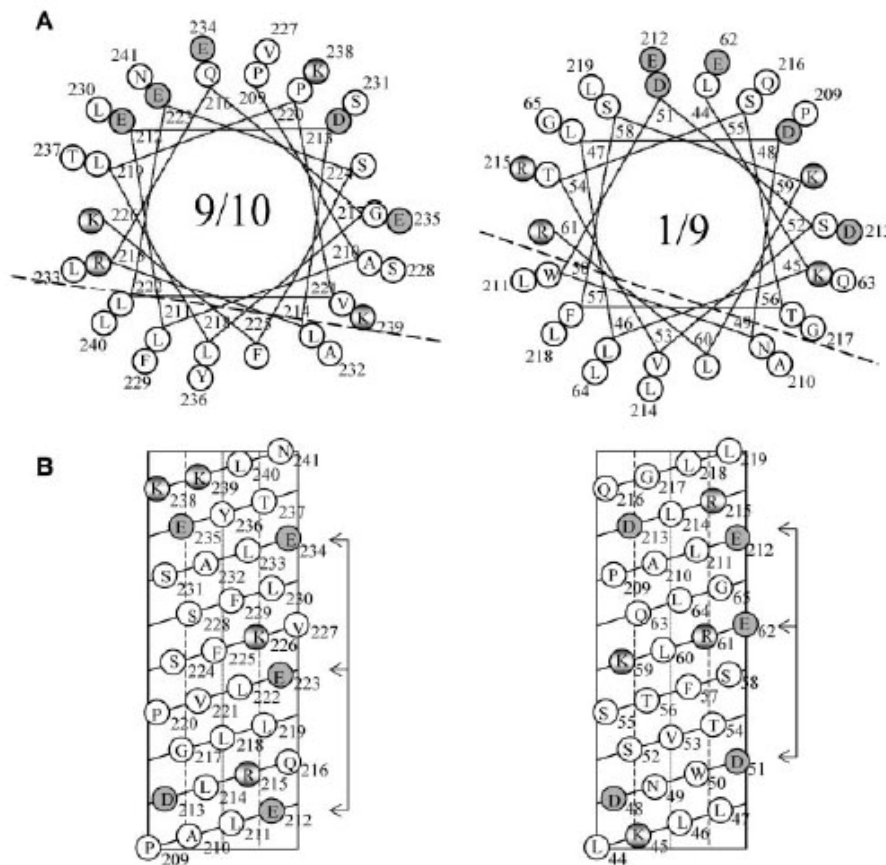


**Figure 3: Peptide 9/10 and 1/9 chimera; Shaded circles represent negative and partially shaded circles represent positive charges; A: Edmundson helical wheel projection, dashed line: lipid/water interface; B:  $\alpha$ -helices shown as cylinders, the arrows show the aligned negative charges ( $\sim 32\text{\AA}$ ). Picture taken from Ref.[9]**

Combinations of other helices failed to promote cholesterol efflux. Some combination give no amphipathic peptide (1/3 chimera) or give highly charged peptides (2/9 chimera) resulting in poor lipid affinity. Some combinations give good lipid affinities, but fail to promote cholesterol efflux. These peptides lack aligned negative charges and there are positive charges between the negative ones (4/9 chimera, 10/9 chimera). A 9/1 chimera resulted also in a peptide with aligned negative charges and was therefore able to promote cholesterol efflux. Those results indicate that the topology of negative charges is essential for the affinity to ABCA1.<sup>[9]</sup>

## 2.2 Protein-protein interactions

### 2.2.1 General concepts

Many processes in organisms occur via higher protein complexes. Those complexes are formed via protein-protein interactions (PPI). One example for PPI is the interaction between cytokine proteins with its cell-surface receptor regulating transduction. Another example is aggregation of proteins forming insoluble fibres leading to amyloidogenic disease, which is an undesirable PPI.<sup>[18]</sup> There are many other PPIs which are essential for diseases, for instance HIV-1 Protease and Gp41 in HIV<sup>[3,19]</sup> or the interaction between the protein p53 and the Human Double Minute 2 protein (HDM2) in cancer.<sup>[19]</sup> The interaction domain between two proteins is rather huge having an interaction area of over  $1100\text{\AA}^2$ , which seems to make it impossible for small molecules to inhibit such PPI. Fortunately, most of the binding energy of PPI results from just a few amino acid residues topologically close to each other. Those so called "hot spots" are essential for successful PPI and are therefore attractive targets for inhibitor design.<sup>[3,18]</sup>

An analysis of the protein database (PDB) has shown that 62 % of all higher protein complexes are interacting over a helical domain.<sup>[14]</sup> The  $\alpha$ -helix is the most common secondary structure motif which has 3.6 amino acids per turn. As a consequence amino acid residues  $i$ ,  $i+3$  or  $i+4$ ,  $i+7$  and  $i+11$  are on the same side of an  $\alpha$ -helix (Figure 4).<sup>[3,18,21]</sup>

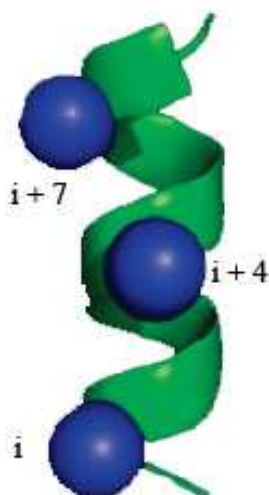
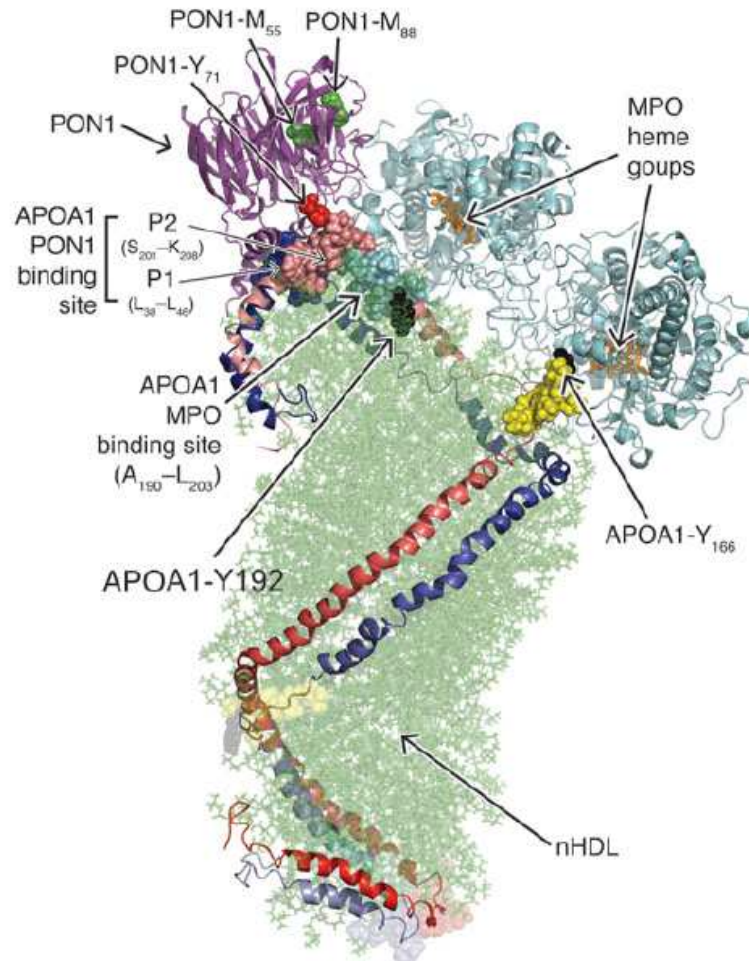


Figure 4:  $\alpha$ -Helix. Picture taken from Ref. [21]

## 2.2.2 Protein-protein interactions with ApoA1/HDL

Interactions between ApoA1/HDL and ABCA1, LCAT Myeloperoxidase (MPO) and PON1 are also PPIs,<sup>[22]</sup> although they are not a PPI in a classical way. The PPI cannot be classical, because also mimetics consisting of D-amino acids successfully interact with those (see 2.3.3).<sup>[9]</sup> Wu *et al.* investigated a ternary complex of MPO, PON1 and nascent HDL (Figure 5).<sup>[14]</sup>



**Figure 5: Hypothetical ternary complex of MPO and PON1 bound to nascent HDL, presumed LCAT interaction side in solid yellow. Picture taken from Ref. [14]**

MPO promotes lipid oxidation and is catalytically active on site of inflammation. MPO is mechanistically linked to oxidative stress and atherosclerosis. It is bound to HDL and oxidizes sitespecifically ApoA1 at Tyr166 and Tyr192, which is linked to the impairment in cholesterol efflux and LCAT binding. It also inhibits the anti-inflammatory properties of HDL and makes it pro-inflammatory.<sup>[14,22]</sup> PON1 deactivates MPO and restores the biological properties of HDL. Several experiments give hint to a ternary complex (Figure 5).<sup>[14]</sup>

The interaction between ApoA1/HDL and SR-B1 is highly dependent on the lipid loading of ApoA1/HDL, because lipid rich mature HDL has a great affinity towards SR-B1, whereas lipid-free ApoA1 or lipid-poor HDL has a lower binding affinity towards SR-B1.<sup>[12,23]</sup> Deletion of either the carboxyl-terminal sequence (amino acids 185-243) or the amino-terminal sequence (amino acids 1-59) of ApoA1 has hardly any effect on the affinity of the corresponding reconstituted HDL (rHDL) towards SR-B1. However, if both sequences are deleted (amino acid sequence 1-59 and 185-243) a very poor affinity of the resulting rHDL towards SR-B1 is observed. That gives a hint towards the necessity of at least one of the highly lipophilic helices. Another important parameter regarding affinity is the density of HDL. Experiments have shown, that higher density spherical HDL has a lower affinity towards SR-B1 compared to HDL lower in density.<sup>[23]</sup>

## 2.3 Inhibitors of protein-protein interactions

### 2.3.1 Inhibitors based on small peptides

Isolated small peptides show a broad degree of freedom in solution as they have no specific folding. As this leads to many undesirable side effects, such as unspecific interaction to other biomolecules, preorganisation towards a helical structure of these peptides has to occur. Besides gaining specificity, preorganisation has the great advantage, that the loss of entropy is not as high as it is in unorganised peptides by binding to its target. Preorganisation towards a helical structure can be achieved via covalent or non-covalent bonds. Some examples are salt bridges, interactions between aromatic systems and charged residues, hydrophobic interactions, aromatic systems and sulfur containing groups, disulfide-bridges, metal-coordination on Cys or His, lactam forming or ring closure via metathesis (Figure 6).<sup>[24-26]</sup>

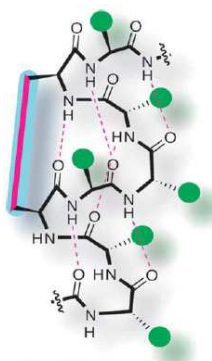


**Figure 6: Preorganisation of a small peptide through ring closure. Picture taken from Ref. [26]**

One crucial disadvantage of peptides is, that they are readily degraded by proteases in organisms. One way to avoid this problem is using unnatural amino acid oligomers such as

peptoids. In contrast to peptides, peptoids have their side chains not linked to the  $\alpha$ -C-atom, but to the amidic N-atom (Figure 7B). This leads to an  $\alpha$ -helix with a periodicity of 3 amino acids per turn and a pitch of 6 Å. An  $\alpha$ -helix, consisting of natural amino acids (Figure 7A), has a periodicity of 3.6 amino acids per turn and a pitch of 4.5 Å.<sup>[24,27]</sup>

Another alternative to peptides are  $\beta$ -peptides-foldamers (Figure 7C). These  $\beta$ -peptides-foldamers have an additional C-atom in the peptide backbone on which the amino acid side-chain is attached. This results in an  $\alpha$ -helical structure with a periodicity of 3 amino acids per turn and a pitch of 4.7 Å.<sup>[24, 26]</sup>

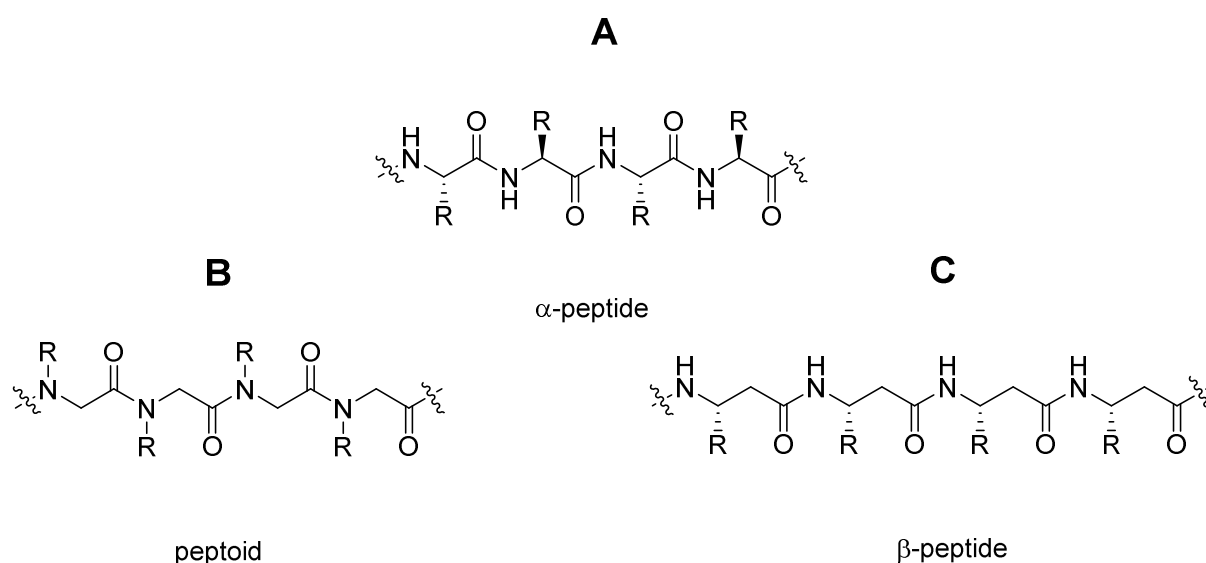


Figure 7: Comparison of A: an  $\alpha$ -peptide, B: a peptoid and C: a  $\beta$ -peptide<sup>[26,27]</sup>

Peptoids, as well as  $\beta$ -peptides-foldamers, have been proven to be very resistant against degradation through proteases. Also foldamers, consisting of a mixture of  $\alpha/\beta$  peptides, have proven to be very effective.<sup>[18,24]</sup>

### 2.3.2 Non-peptidic inhibitors - $\alpha$ -helix mimetics

Hamilton *et al.* have shown, that 3,2',2'' trisubstituted terphenyl-derivatives (Figure 8) are able to mimic amino acids  $i$ ,  $i+3$  or  $i+4$  and  $i+7$  of an  $\alpha$ -helix. The first example of a terphenyl inhibiting PPI was in mimicking smooth muscle myosin light-chain kinase (smMLCK). smMLCK interacts with calmodulin over a helical domain, in which amino acids Trp800, Thr803 and Val807 of smMLCK form the hot spot of the interaction. A terphenyl, with the analogous side chains of above mentioned amino acids, was able to mimic smMLCK's  $\alpha$ -helix and bound to calmodulin, which inhibited the interaction between smMLCK and calmodulin successfully.<sup>[18,28]</sup>



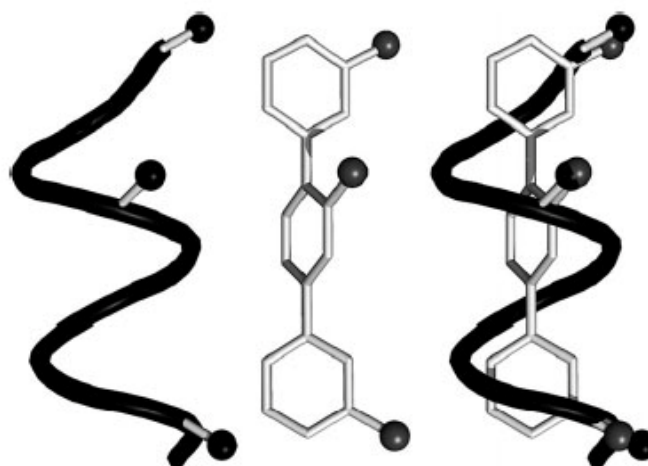


Figure 8: Scheme of an  $\alpha$ -helix mimetic based on a terphenyl scaffold. Picture taken from Ref. [29]

The distance between two substituents of the terphenyl scaffold is 4.3 Å (Figure 9). This is 5 % shorter than the  $i, i+3$  distance and 30 % shorter than the  $i, i+4$  distance in an  $\alpha$ -helix.<sup>[24]</sup>

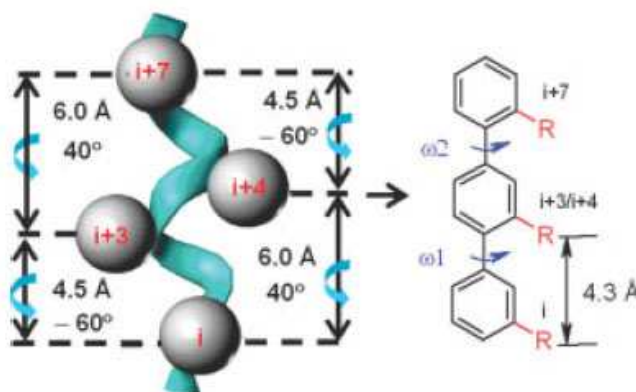


Figure 9: Distances of the amino acid residues in an  $\alpha$ -helix and the substituents of a terphenyl respectively.<sup>[24]</sup>

Due to the freely rotatable aryl-aryl single-bond the  $i+3$  and the  $i+4$  position of an  $\alpha$ -helix cannot be distinguished effectively. By shifting the substituent on the central ring by one position towards the axial direction, a distance of 6.5 Å is achieved, which matches the distance between  $i$ , and  $i+4$  much better. However such a modification leads to steric repulsion, resulting in tilting away of the substituents from the desired twist angle. To avoid this, one phenylring can be exchanged with a substituted naphthalene. According to the position of the naphthalene and its substitution pattern  $i, i+3$  and  $i+7$  or  $i, i+4$  and  $i+7$  amino acid residues can be selectively mimicked (Figure 10).<sup>[24]</sup>



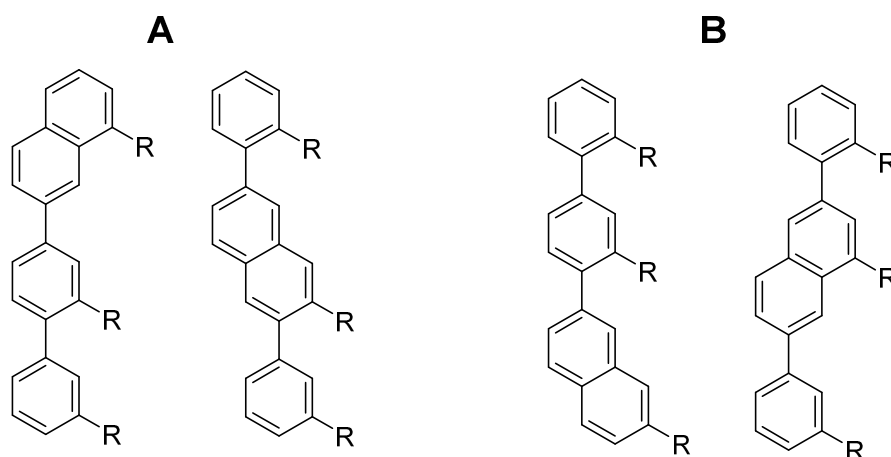


Figure 10: Terphenyl scaffold with naphthalene; A: i, i+3 and i+7 mimetics; B: i, i+4 and i+7 mimetics<sup>[24]</sup>

There are two major drawbacks with terphenyls. First of all, they are highly hydrophobic resulting in poor water solubility. Secondly, the synthesis is rather complex in most cases. Many approaches towards improvement of water solubility have been done (Figure 11). One approach is the exchange of the phenyls with pyridines towards a terpyridine scaffold. Others are pyridyl-pyridone scaffolds, central pyridazines, benzamides or H-bridge forming groups such as enamino or benzoylurea groups.<sup>[18,19,24,30,31]</sup>

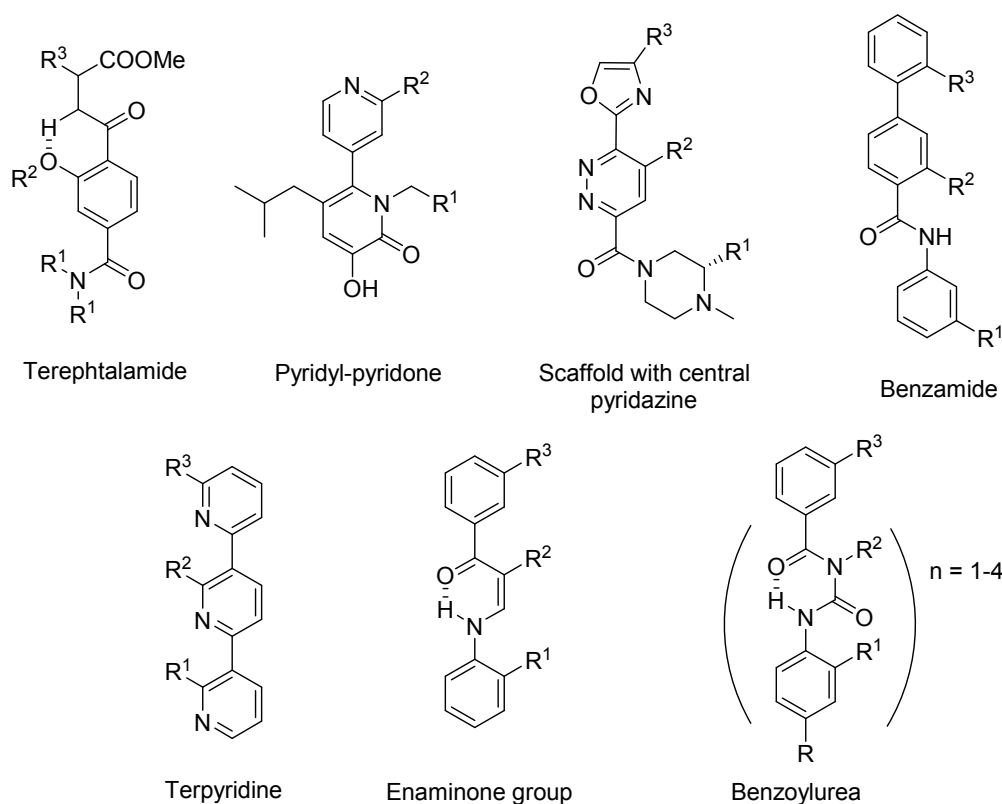
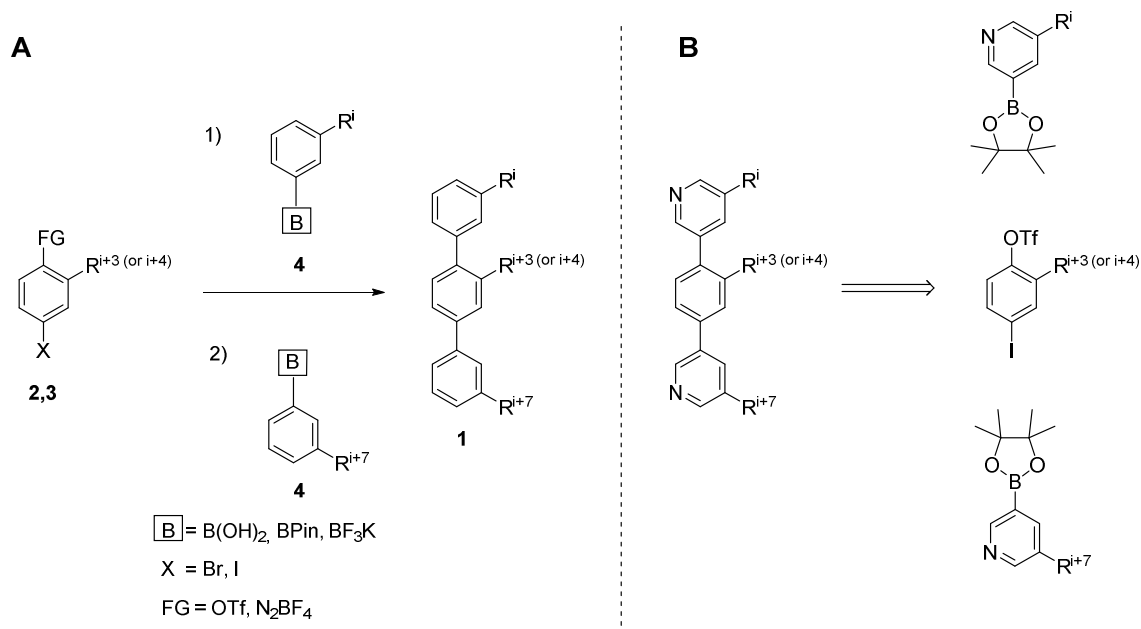


Figure 11:  $\alpha$ -helix mimetics with improved water solubility<sup>[18,19,24,30,31]</sup>

Breinbauer *et al.* have developed a modular synthesis of teraryls. On the one hand for terphenyls and on the other hand for teraryls, where the two terminal phenyls are exchanged by pyridines (Figure 12). This approach gives the opportunity to synthesize teraryls via Pd cross-coupling from two sets of building blocks, each consisting of 18 amino acid analogs.<sup>[29,32]</sup>



**Figure 12: A: Modular synthesis for terphenyls (2: FG = N<sub>2</sub>BF<sub>4</sub>, X = Br; 3: FG = OTf, X = I); B: Retrosynthesis of teraryls using pyridine as top/bottom building block<sup>[29,32]</sup>**

### 2.3.3 ApoA1 mimetics

Small helical amphipathic peptides have shown to mimic the properties of ApoA1, although these peptides show no homology to the amino acid sequence of ApoA1.<sup>[10,33]</sup> The class A amphipathic peptide 18A was one of the first peptides recognized to mimic ApoA1. The biological activity and lipid affinity of 18A could be increased by neutralizing the terminal charges of 18A (Ac-18A-NH<sub>2</sub> or 2F). Therefore several studies were performed with derivatives of 18A by exchanging some of its amino acids on the hydrophobic side with Phe. This leads to class A amphipathic peptides with a higher hydrophobicity named 2F, 3F, 4F, 5F, 6F and 7F according to the number of Phe residues in the peptide. According to their retention time on an HPLC with C<sub>18</sub>-column they can be classified into two main groups. On the one hand 2F-4F with retention times between 21 and 22 min and on the other hand 5F-7F with retention times between 26 and 27 min. Those data fit perfectly to the theoretical lipid affinity, where the lipid affinity increases gradually from 2F towards 4F, then has a sudden increase from 4F to 5F and thereon increases gradually from 5F towards 7F. The same trend is seen in solubility, which decreases with higher lipid affinity, whereas the monolayer

exclusion pressure increases with higher lipid affinity. The ability to clarify a suspension of egg phosphatidylcholine multilamellar vesicles (EPC MLV) was best for 4F. An explanation for this fact might be the optimal hydrophobicity of 4F for interacting with lipids rather than to form aggregates via hydrophobic peptide-peptide interaction. The best LCAT activation property of these peptides had 5F. LCAT activation is a complex process which cannot be predicted by lipid affinity alone, as ApoA1 itself does not clarify an EPC MLV suspension.<sup>[10,34]</sup>

As ApoA1 consists of more helices and (as said in 2.1.2) a peptide of two helices from ApoA1 gives cholesterol efflux in similar efficiency as full length, ApoA1 bihelical peptides have become very attractive as mimetics.<sup>[9,13]</sup> One approach was a peptide in which two 18A were linked via a Pro residue (37pA). It has a higher lipid affinity than 18A and in promoting cholesterol efflux 37pA is 18-fold more efficient than 18A, but still 8-fold poorer than ApoA1. In LCAT activating 37pA exceeds ApoA1 by 40 %. Two other bihelical peptides were compared to 37pA according to their lipid affinity. On the one hand a peptide consisting of two 18A (36A) and on the other hand a peptide consisting of two 18A linked via an Ala-residue (37aA). The ability to bind to the phospholipid DMPC is decreasing from 37pA to 37aA to 36A.<sup>[13]</sup> Creating an asymmetric version of 37pA, by substituting the hydrophobic side of the C-terminal helix with Ala residues, results in a helix with lower lipid affinity. This asymmetric version of 37pA has a higher specificity towards ABCA1.<sup>[35,36]</sup> Many proline-linked bihelical peptides were tested and compared by D'Souza *et al.* according to their abilities as ApoA1 mimetics. The most efficient cholesterol efflux was achieved with the peptides ELK-2A2K2E and ELK-2F which reached about the same efficiency in cholesterol efflux as ApoA1 from THP-1 cells.<sup>[13,37]</sup>

The interaction between ApoA1 and ApoA1 mimetics towards their ligands seems to be independent of stereochemistry as their stereoisomers consisting of D-amino acids are as efficient as the L-isomers. This gives a hint that the PPI's with ApoA1/ApoA1-mimetics is not a PPI in a classical way. The efficiency of PPI with several ligands is strongly dependent on the nature of the hydrophobic side and the nature and charge distribution of the hydrophilic side. In 3F, for instance, the position of the Phe residue is crucial for biological activity.<sup>[9,34,37]</sup> D'Souza *et al.* have summarized, which structural properties of bihelical amphipathic peptides are, according to their experiments, important for different biological activities (Table1).<sup>[37]</sup>

**Table 1: Influence of peptides' structural feature towards their activity<sup>[37]</sup>**

| Function                          | Hydrophobicity | Size of hydrophobic face      | Charge              | Maintaining Pro bridge | Type of helix                     | Inclusion of Cys/His residues                                  | Asymmetry                            |
|-----------------------------------|----------------|-------------------------------|---------------------|------------------------|-----------------------------------|--|--------------------------------------|
| Efficiency of cholesterol efflux  | Optimal (-0.5) | Increased size is beneficial  | Neutral             | Essential              | Limited effect                    | Detrimental in the first helix, beneficial in the second helix | Beneficial in 5A, detrimental in ELK |
| Specificity of cholesterol efflux | Limited effect | Limited effect                | Neutral or negative | Essential              | Limited effect                    | Limited effect   | Beneficial in 5A, detrimental in ELK |
| Anti-inflammatory, monocytes      | Limited effect | Increased size is detrimental | Neutral or negative | Limited effect         | Changing to G or Y is detrimental | Limited effect   | Beneficial                           |
| Anti-inflammatory, endothelium    | Limited effect | Increased size is beneficial  | Neutral or positive | Limited effect         | Limited effect                    | C + H detrimental, C beneficial                                | Limited effect                       |
| Antioxidant                       | Limited effect | Limited effect                | Limited effect      | Detrimental            | Changing to G or Y is beneficial  | Beneficial   | Limited effect                       |

In the case of reverse cholesterol efflux, one of the promoting effects of ApoA1 mimetics is their high lipid affinity. Lipid-free ApoA1 or lipid-poor ApoA1 takes up cholesterol from peripheral cells, whereas mature HDL does not. ApoA1 has to dissociate from mature HDL to form new lipid-free or lipid-poor ApoA1. Lipophilic ApoA1 mimetics (especially D4F, the D-amino acid stereoisomer of 4F) have a higher affinity towards HDL than ApoA1 and can therefore accelerate the dissociation process of ApoA1 from mature HDL (Figure 2).<sup>[13,34,38]</sup>

In some kind ApoA1 mimetics differ from ApoA1 in their anti-inflammatory properties and in their mode of action as anti-oxidants. For instance 4F binds much more effectively to oxidized lipids than ApoA1. In experiments on cultured human artery walls, ApoA1 has shown to reduce LDL induced monocyte chemotactic activity (MCA) when ApoA1 was pre-incubated. MCA is produced by the artery cell wall when a critical threshold of lipid hydroperoxides is trapped within LDL. When LDL and ApoA1 are coincubated, however, no reduction of MCA is observed. This indicates that oxidized lipids are able to dissociate again from the lipid

hydroperoxide/ApoA1 complex, if the complex is not removed. A coincubation of LDL and ApoA1 mimetics on the other side resulted in a successful inhibition of MCA. ApoA1 mimetics successfully sequester oxidized lipids.<sup>[10,34,39]</sup> The ability to bind to oxidized lipids is also seen as the main reason for the anti tumor role of mimetics in ovarian cancer, by binding to lysophosphatidic acid (LPA).<sup>[40,41]</sup>

4F and D4F have shown to possess many desirable properties in many diseases. Mostly those are reported for D4F, because the advantage of D4F is the possibility to be taken orally, whereas 4F is rapidly degraded by proteases in digestion systems and have therefore to be injected.<sup>[34]</sup> In the case of Influenza A oral administration of D4F restores the anti-inflammatory properties of HDL.<sup>[39]</sup> In sepsis 4F also shows an anti-inflammatory effect by inhibiting the binding of bacterial lipopolysaccharide to its binding protein.<sup>[39,42]</sup> In diabetic mice and rats the use of 4F or D4F decreases superoxide levels. The reduction of superoxide levels is linked to heme oxygenase 1 (HO-1). In insulin resistant mice 4F could improve insulin sensitivity. Therefore D4F and 4F generally prevent oxidative stress.<sup>[39,43-45]</sup> 4F also shows positive effects in a murine lupus model. 4F treated mice suffering of lupus showed reduced IgG anti-dsDNA and antiOxPLs values and had a higher bone density.<sup>[40,46]</sup>

As animal tests of 4F were very promising, Watson and colleagues made a clinical trial with patients suffering cardiovascular disease. 4F was administered either subcutaneously (SC) or intravenously (IV) and was very well tolerated at all doses tested. The half-lives of 4F were 1.5 h (IV) and 2.5-3.0 h (SC) respectively. According to the short half-lives no accumulation of 4F has to be expected. As a result of this trial no improvement of anti-inflammatory properties could be detected.<sup>[47]</sup>

## **2.4 Targeted drug delivery**

### **2.4.1 Why targeted drug delivery?**

Small interfering RNAs (siRNAs) are highly selective in gene silencing towards their target. Therefore siRNAs are very interesting as potential drugs, especially for targets, which are difficult to inhibit by small molecules. Unfortunately, siRNAs are unstable in biological fluids and due to their polyanionic character, they have a poor intracellular penetration. Therefore a carrier is needed to transport siRNA to its target.<sup>[5, 48]</sup>

Gene silencing is achieved by siRNA binding to its complementary messenger RNA (mRNA) resulting in a double stranded RNA (dsRNA). dsRNAs are detected by biological organisms as foreign and are rapidly degraded. As mRNA has been destroyed, no translation of this specific gene can occur, which means that the biosynthesis of a specific protein is blocked (Figure 13).<sup>[48,49,50]</sup>

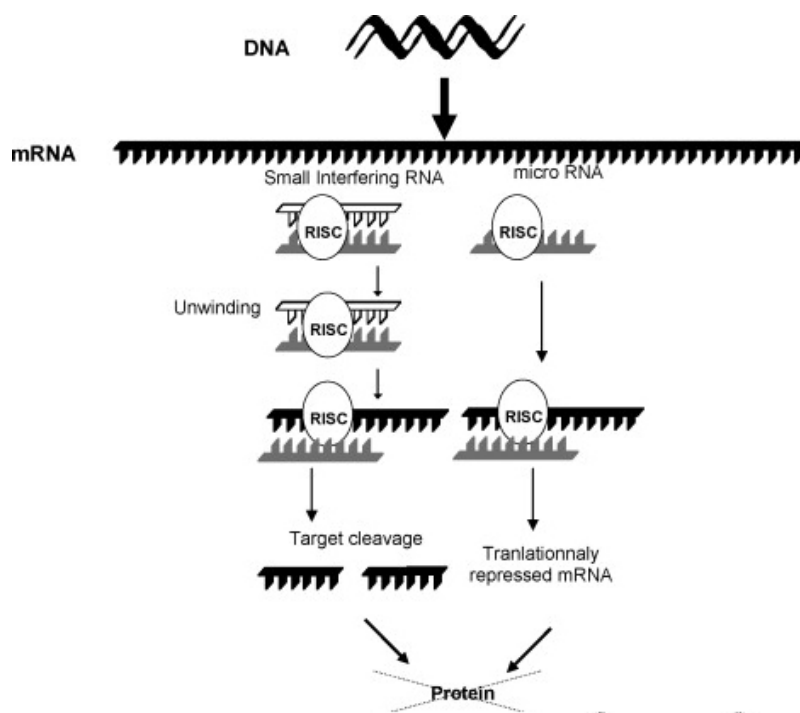


**Figure 13: Mechanism of action of siRNA. Picture taken from Ref. [48]**

Another reason for the need of targeted drug delivery can be shown by the case of Signal Transducer and Activator of Transcription 3 (STAT3). STAT3 is a cytoplasmic protein which can be activated by various extracellular ligands. When it is activated it enters the cell nucleus where STAT3 regulates many gene transcriptions. STAT3 is also known for playing a crucial role in many tumor cells which makes STAT3 an interesting target for cancer therapy. If a STAT3 mRNA specific siRNA is applied, it would also silence the STAT3 gene in healthy tissue, which would be fatal. Therefore targeted delivery of such a siRNA must be provided.<sup>[4,51,52]</sup>

#### 2.4.2 HDL as a drug carrier

Many nanoparticles have been used as drug carriers of siRNA, nanoparticles such as neutral and charged liposomes or superparamagnetic iron oxide particles. Also polycationic peptides have been used. Those all are able to deliver siRNA, but due to their toxicity and other effects alternative carriers are desirable. Especially polycationic peptides have, due to their positive

charge, many side effects, such as unspecific interactions, cytotoxicity and aggregation with serum proteins.<sup>[4,5,53-57]</sup>

HDL has properties, such as it is non-cytotoxic, long-lasting in the circulation and selectively taken up by cells expressing SR-B1 (Figure 14B), which are very promising for the use as a drug carrier. As SR-B1 is overexpressed in many cancer cells HDL is a very promising targeted drug carrier for cancer therapy. Experiments with paclitaxel (PTX) have shown, that PTX can be successfully incorporated into rHDL and is selectively delivered to cancer cells resulting in a 5-20 times lower IC<sub>50</sub> value compared to free PTX drug. This approach also works for siRNA. siRNA bound to cholesterol (chol-siRNA) was successfully incorporated into the lipophilic core of rHDL (Figure 14A). The binding cholesterol is important to increase the solubility of the highly charged siRNA in the lipid core of rHDL. Another approach to incorporate siRNA into rHDL is to complex siRNA with oligolysines peptides.<sup>[4,5,7]</sup>

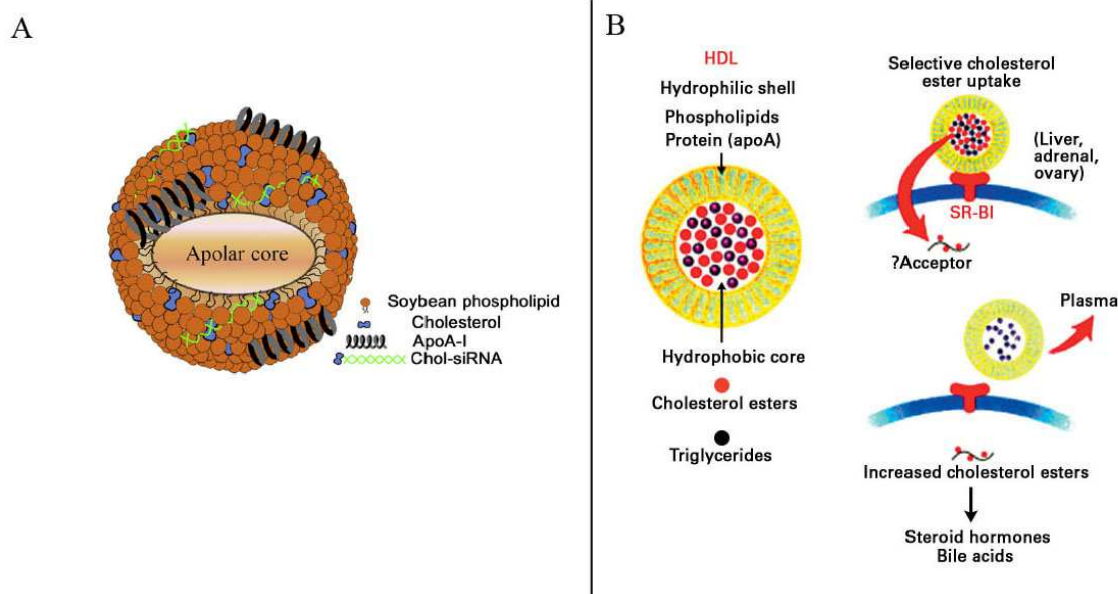


**Figure 14: A: rHDL with incorporated Chol-siRNA. Picture taken from Ref. [5], B:SR-B1 mediated selective cholesterol ester uptake. Picture taken from Ref. [7]**

Shazad *et al.* could successfully silence STAT3 selectively and focal adhesion kinase (FAK), another protein with a crucial role in tumor survival, in ovarian tumor cells in vivo in mice by incorporating the corresponding chol-siRNA into rHDL. After single injection, 80 % of the siRNA was located inside the tumor cells. Beside the tumor the highest uptake of rHDL was in the liver.<sup>[4]</sup> Another protein, which is overexpressed in many cancers is pokémon. Ding *et*

*al.* could successfully silence the pokemon gene by targeted drug delivery of chol-siRNA in rHDL.<sup>[5]</sup>

Nakayama and colleagues have shown that chol-siRNA can also be transported with mimetic lipoprotein particles. For this they used recombinant ApoA1 or recombinant lipoprotein E3 (ApoE3) and formed lipoparticles with phospholipids. The ApoA1 containing particle (A-lip) and the ApoE3 containing particle (E-lip) were both able to transport chol-siRNA, whereas the best results were obtained with E-lip.<sup>[6]</sup>



### 3 Scientific Task

In many studies ApoA1 mimetic peptides have shown to bind to HDL and ApoA1/HDL presents itself as a successful drug carrier of siRNA.<sup>[4,5,6]</sup> Those two facts combined with the concept of PPI mimetics by Hamilton *et al.* lead to the idea of a synthesis concept towards a drug carrier.<sup>[28]</sup> The aim of this project was the design of ApoA1 mimetics based on an oligoaryl scaffold.

Design of possible ApoA1 mimetics was inspired by the structure of already existing ApoA1 mimetic peptides and by the structure of ApoA1 itself.<sup>[9,10,34]</sup>

To achieve a modular synthesis with high flexibility in the synthesis of oligoaryls, building blocks have to be synthesized with a benzene core unit featuring two leaving groups in an 1,4-arrangement differing in their reactivity to allow oligomerization via iterative Pd-catalyzed cross coupling (Figure 15).<sup>[58]</sup> These building blocks are equipped with side chains mimicking on one side the corresponding polar amino acid (Lys, Glu) and on the other side a phenylalanine mimetic.

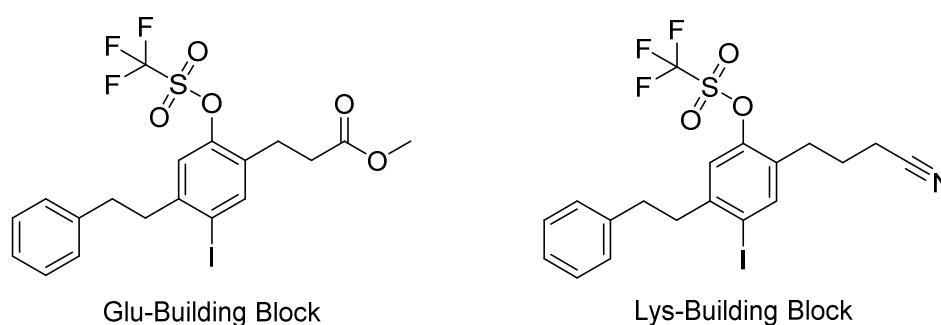
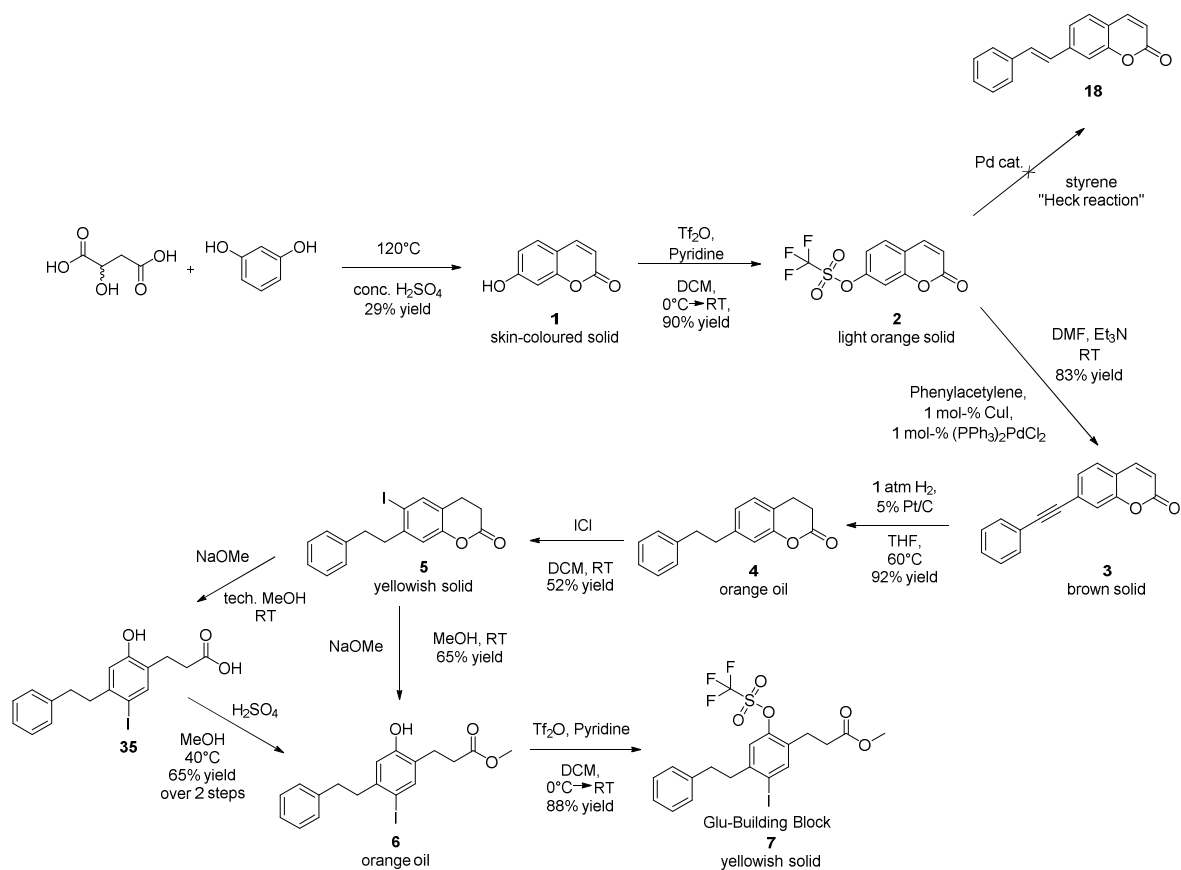


Figure 15: Building blocks

The aim of this master thesis is the synthesis of the two building blocks (Figure 15).

## 4 Results and Discussion

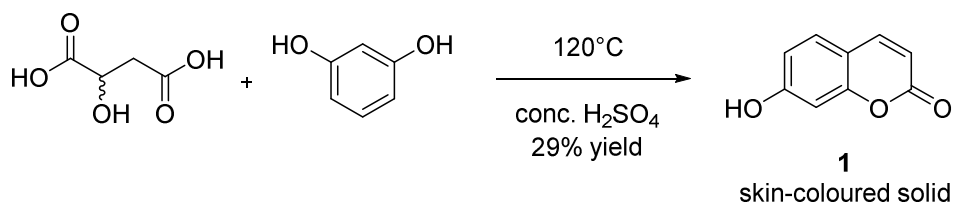
### 4.1 Synthesis of the Glu-building block



Scheme 1: Synthesis route to the Glu-building block

The synthesis of the Glu-building block (Scheme 1) will be discussed in detail in the following section.

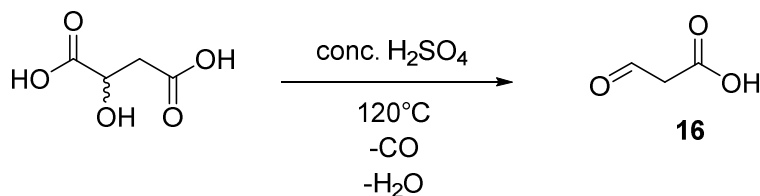
#### 4.1.1 Pechmann coumarin synthesis



Scheme 2: Pechmann coumarin synthesis

Intermediate **1** was synthesized in a Pechmann coumarin synthesis (Scheme 2). In a Pechmann synthesis electron rich phenol derivatives are reacting with β-ketoacids to the corresponding coumarin. In Scheme 2 malic acid is shown as educt, but the species, which is

actually reacting with resorcinol, is 3-oxopropanoic acid (**16**), which is formed in situ under these conditions (Scheme 3). As CO is developed during this reaction, the reaction has to be carried out in a fume hood with a gas exhaust.<sup>[59]</sup>



**Scheme 3: In situ formation of 3-oxopropanoic acid (16)**

The yield of the reaction is very low, in our case 29 % yield, even lower as reported in literature.<sup>[59]</sup> As **16** is an excellent electrophile, it is not surprising that it is not very stable. Therefore it has to be generated in situ as it is not well storable and it is not commercially available.

Procedures differing in the stoichiometry of reactants are published for the synthesis of **1**.<sup>[60,61]</sup> We also tried that and additionally varied the work-up. In our experiments we have seen that by using malic acid in excess, one other compound was obtained as a side product. According to GC-MS data the other compound seemed to be **17** (Figure 16). The by-product could be successfully separated from the desired coumarin by recrystallization from ethanol. <sup>1</sup>H-NMR analysis of the by-product could clearly falsify that the by-product is **17**. NMR-data showed that the by-product had definitely more hydrogens than **17** and had more hydrogens coupling to each other (HH-COSY). What cannot be excluded is that the actual by-product decomposes thermally to **17** in the inlet of the GC-MS. Further characterization and identification of that by-product have not been done due to time issues. The best results were obtained by using resorcinol in excess. There the by-product was not formed at all and the excess resorcinol was removed during the work-up.

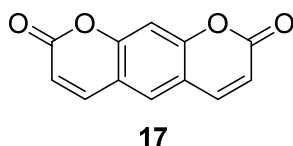


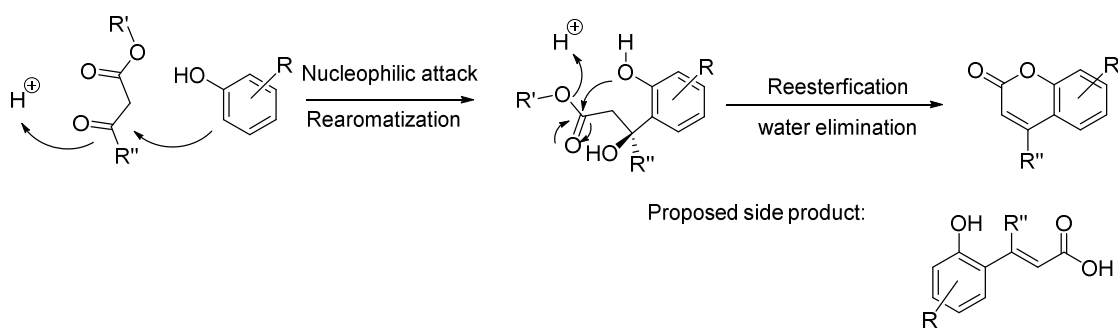
**Figure 16: 2H,8H-pyrano[3,2-g]chromene-2,8-dione (17)**

Many procedures described a simple work-up by pouring the reaction mixture on a water/ice mixture, followed by filtrating off the precipitate. The outcome of that work-up could not be

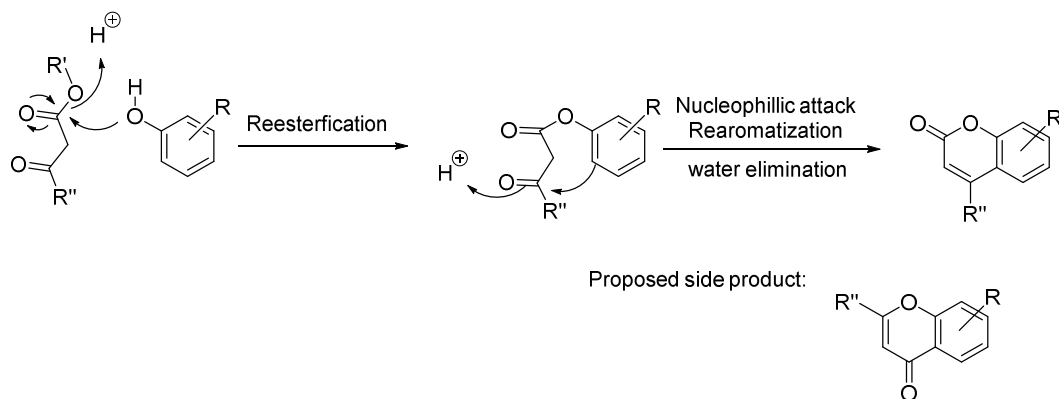
reproduced in our experiments. A solid had also precipitated in our experiments, but it was shown to be very hard to filtrate. Additionally the yield and the purity of the isolated solid was very poor. Further purification of the solid was achieved by dissolving it in 2 M NaOH, filtration and acidifying with 1 M HCl. A light orange solid precipitated by this method. Another disadvantage of this work-up in our experiments was that a huge amount of **1** stayed dissolved in the mother liquor in the pouring step as well as in the base treatment with the following acidifying step. Therefore further extraction of the aqueous layers with EtOAc was needed. All in all that made a very time consuming and ineffective work-up. Finally a more effective work up was found by extracting the mixture after the pouring step in the first place without any filtration (Compare 7.7.1). The impure crude product could be further purified by washing with saturated NaHCO<sub>3</sub> solution giving **1** in satisfactory purity for the next step. The additional solution step of the crude product would be obsolete, if the combined organic layers were washed with saturated NaHCO<sub>3</sub> solution more frequently. This was not tested, because no more amount of **1** was needed for this thesis.

Although the Pechmann reaction has been known for a long time, the reaction mechanism is still under discussion. Two mechanisms are most frequently discussed in literature<sup>[62,63]</sup> (Scheme 4).

A:



B:



**Scheme 4: Simplified possible reaction mechanisms of the Pechmann synthesis A: Mechanism proposed by Robertson *et al.*<sup>[62]</sup> B: Mechanism proposed by Ahmed and Dasai<sup>[63]</sup>**

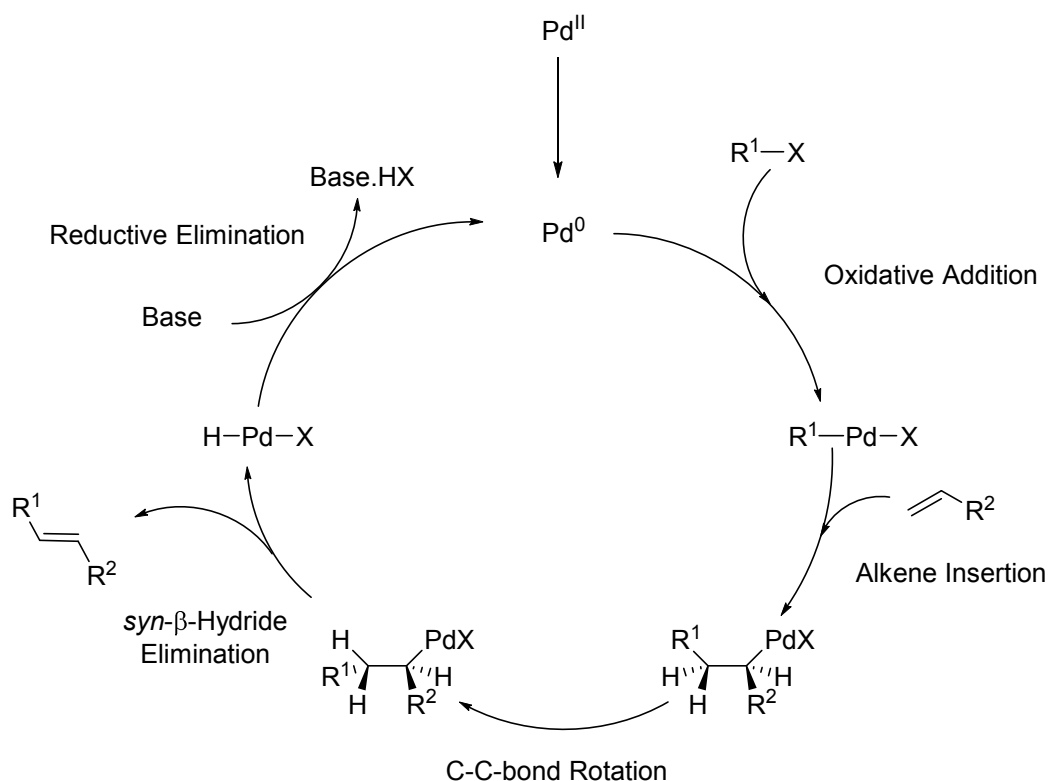
A theoretical study towards the mechanism of the Pechmann synthesis were made by Daru *et al.* The result was that these two mechanisms shown above and a third one, which is actually a mixture of the two mechanisms, are very similar according to their free energy profile calculated by density functional calculations. As a result it is possible that those three mechanisms can operate simultaneously.<sup>[63]</sup>

The low yield of the Pechmann synthesis originates probably from three reasons. First of all the rather harsh reaction conditions which are needed for the in situ formation of **16**. At these conditions degradation of starting material and product cannot be excluded. Secondly, the high reactivity of **16**, which could be the reason for some side reactions, as for instance self-condensation. Finally, side reactions can occur through the possible reaction mechanisms themselves, which is further discussed by Daru *et al.*<sup>[63]</sup> As it would have been beyond the scope of this thesis, side products have not been further characterized, but they seem to have a high water solubility, as a sufficient purity could be achieved just through washing steps.

A higher yield (81 %) of the Pechmann synthesis was described in literature by using 70% HClO<sub>4</sub> as a solvent at 90°C.<sup>[64]</sup> As HClO<sub>4</sub> is explosive at higher temperatures that experiment has not been carried out due safety issues.

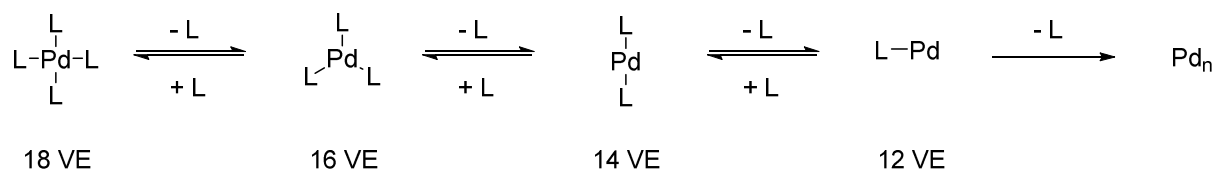
#### **4.1.2 The Heck-Mizoroki reaction**

The Heck reaction, is a Pd-catalyzed coupling of an olefin and an aryl halide, an alkenyl halide or the corresponding triflates. Mechanistically a Heck reaction is a sequence of oxidative addition, carbometalation,  $\beta$ -hydride elimination and reductive elimination (Scheme 5).<sup>[65]</sup>



**Scheme 5: Catalytic cycle of a Heck reaction; Ligands were omitted<sup>[65]</sup>**

In some cases the formation of a black precipitate was obtained. Especially at higher temperatures or after prolonged reaction times that formation was observed. Black precipitate has been reported to be Pd nanoparticles. Those form when ligands dissociate from Pd(0) complexes. In solution there is an equilibrium of Pd(0) complexes differing in their number of ligands (Scheme 6). Generally it can be said that the lower the number of ligands are, the higher is the reactivity of a Pd(0) complex, but also the more likely the remaining ligands dissociate and Pd(0) aggregates to those nanoparticles.

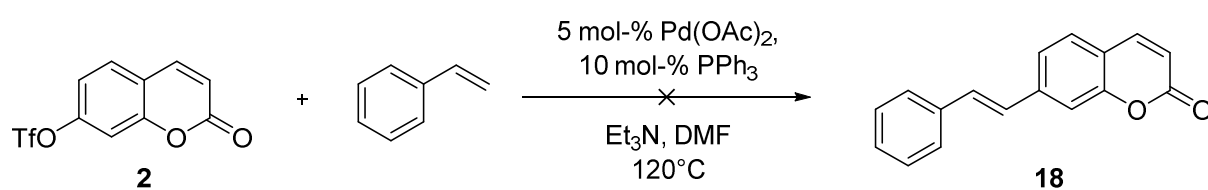


**Scheme 6: Equilibrium of Ligand dissociation in Pd(0) complexes; Number of valence electrons are shown below each complex**

As ligand dissociation is a process favored by entropy, aggregation is more likely at higher temperatures. Another parameter which influences the equilibrium is obviously the ligand concentration, its type and its steric demand. The choice of ligand depends highly on the reaction and a compromise between stability and reactivity has to be found in each case. As

substrates of a reaction additionally work as ligands, it makes sense that at the end of a reaction aggregation can occur, as substrate is consumed. Another reason for aggregation after prolonged reaction time is the irreversibility of nanoparticle formation. Even at incomplete conversion of substrates a formation of nanoparticles does not necessarily mean the end of reaction as Pd nanoparticles also have been reported to be catalytically active in some sorts of Pd cross coupling reactions.<sup>[66]</sup>

The first intent in the synthesis of the Glu-building block was to introduce the carbon skeleton of the phenylethyl side chain via a Heck reaction between **2** and styrene (Scheme 7).



**Scheme 7: Intended Heck reaction**

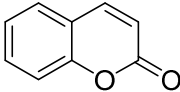
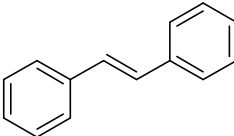
Although full conversion of **2** was obtained, no desired product **18** had formed. Also variation of reaction parameters (Table 2) did not lead to the desired product.

**Table 2: Varying parameters for the Heck reaction; in no entry **18** was formed**

| Entry    | Conversion of <b>2</b> | Solvent | Base              | T [°C]       | Precatalyst          | Ligand           | Pd loading [%] |
|----------|------------------------|---------|-------------------|--------------|----------------------|------------------|----------------|
| <b>1</b> | full                   | DMF     | Et <sub>3</sub> N | 120          | Pd(OAc) <sub>2</sub> | PPh <sub>3</sub> | 5              |
| <b>2</b> | full                   | DMAc    | Bu <sub>3</sub> N | 165 (reflux) | Pd(OAc) <sub>2</sub> | PPh <sub>3</sub> | 10             |
| <b>3</b> | full                   | DMF     | Et <sub>3</sub> N | 120          |                      |                  | 5              |
| <b>4</b> | full                   | DMF     | Et <sub>3</sub> N | 80           | Pd(OAc) <sub>2</sub> | PPh <sub>3</sub> | 10             |

In all different reaction conditions of Table 2 a mixture of various products had been formed. The harsh conditions in Entry 2 of Table 2 also led to decomposition to some amount of the educt to the coumarin **1**. None of the products have been isolated, but according to MS-database some peaks in the chromatogram could be related to possible compounds (Table 3).

Table 3: Compounds formed at the reaction, some with possible structure; Method: MT\_50\_S

| Entry | $t_R$ [min] | compound  | $m/z$ | certainty [%] |
|-------|-------------|---|-------|---------------|
| 1     | 5.66        |  | 146   | 94            |
| 2     | 6.44        |  | 180   | 92            |
| 3     | 9.07        | -   | 248   | -             |

Entry 1 in Table 3 could have been possibly formed over a hydride transfer via a reductive elimination of the metal, but this would raise the question of the hydride source. Generally the reduction of **2** by Pd catalysis is known in literature.<sup>[67,68]</sup> Another possibility would be over a radical mechanism. As it is very uncommon for Pd performing single-electron transfer, the radical source could be styrene, which is very prone to radical formation.

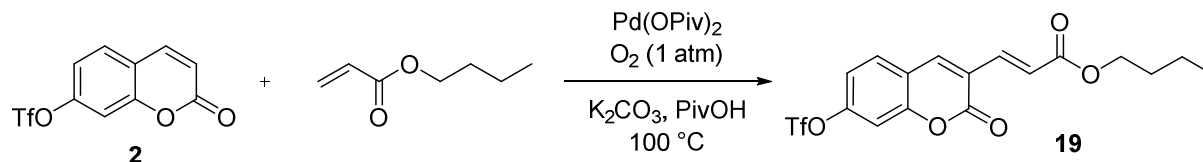
Entry 2 in Table 3 is very likely stilbene, because a reference of stilbene has been measured, which has the same fragmentation pattern and the same retention time with this method. On the one hand stilbene could have been formed by successful Heck reaction and rapid decomposition of the heterocyclic ring. This is rather unlikely as Suzuki reactions with **2** have been done in the past under similar conditions without any mentioning of degradation of the heterocyclic ring.<sup>[69,70]</sup> On the other hand stilbene could have been formed through metathesis. This would be very surprising as Schrock carbenes or NHC carbenes of early transition metals in high oxidation states are used as metathesis catalysts.<sup>[71]</sup> Pd is a very noble late transition metal and therefore not known for metathesis.

The last entry of Table 3 had a  $m/z$ , which would fit to the desired product **18**. The compound could not be isolated, but later experiments disproved that, because **18** was an intermediate in the hydration of **3** (Figure 18) and has a retention time of 8.20 min at the same method.

Suzuki and Sonogashira cross coupling have been reported for **2**,<sup>[69,70,72]</sup> but no Pd catalysed Heck reaction so far. As Heck chemistry failed for our substrate **2** an alternative for our synthesis was found in a Sonogashira reaction (see 4.1.3). One reason that the Heck reaction failed in our case could be the same reason why Heck chemistry actually works in general - Pd's affinity to  $\pi$ -systems. The highly delocalized  $\pi$ -system in **2** could act as a better ligand towards Pd than styrene. One example showing the affinity of Pd towards the  $\pi$ -system of **2** is



in an aerobic oxidative Heck reaction (Scheme 8). As an oxidative Heck reaction runs over a different mechanism, those reactions cannot be compared directly, but it is sufficient as an example for the affinity of Pd towards the  $\pi$ -system.<sup>[73]</sup>



**Scheme 8: Aerobic oxidative Heck reaction**<sup>[73]</sup>

Other examples have been published describing deactivation of Pd catalyst by coordination to substrates with  $\pi$ -systems.<sup>[74,75]</sup>

The oxidative addition of the leaving group and the aromatic ring to Pd has to be successful as other cross coupling reactions like Suzuki reaction<sup>[69,70]</sup> and Sonogashira<sup>[72]</sup> reaction (see 4.1.3) work with **2** as substrate. Another sign that the oxidative addition must have worked is the formed side product in Table 3 (entry 1).

If the oxidative addition of Ar-OTf to Pd is successful and the resulting species is coordinating to the delocalized  $\pi$ -system, dimers and/or oligomers of **2** could have been formed (Figure 17). As the formed products in our experiments have not been isolated and therefore have not been characterized, a formation of those compounds can neither be excluded nor verified.

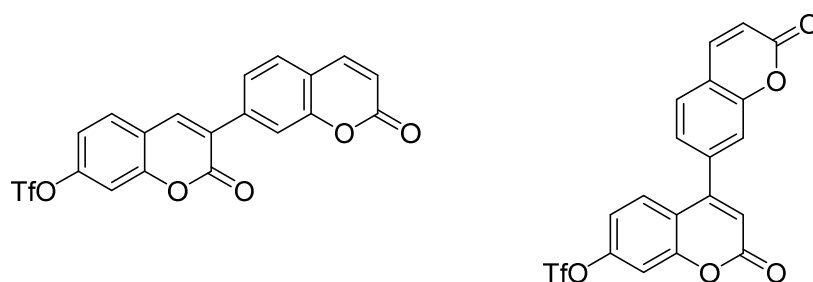


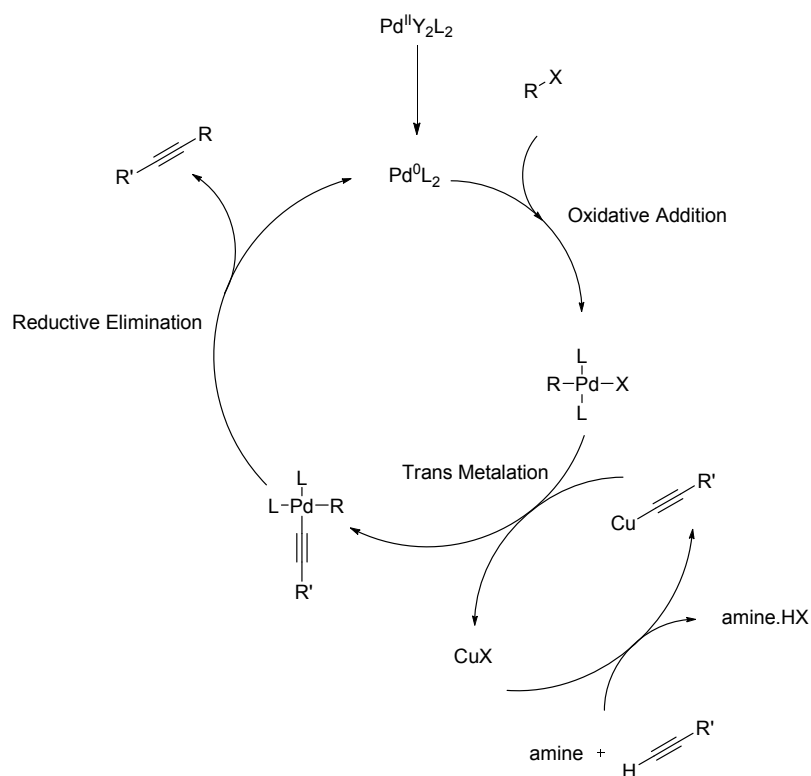
**Figure 17: Possible products of a Heck reaction of 2; Two possible dimers shown**

One example of a Ni-catalyzed Heck reaction with **2** as substrate has been published by Gøgsig *et al.*<sup>[76]</sup> As Ni is one period over Pd, Ni is a smaller metal and, speaking in a HSAB context, Ni is a harder metal than Pd and has therefore a lower affinity towards soft  $\pi$ -systems.

As we already had a working Sonogashira reaction as alternative, a Ni-catalyzed Heck reaction was not tested.

### 4.1.3 The Sonogashira reaction

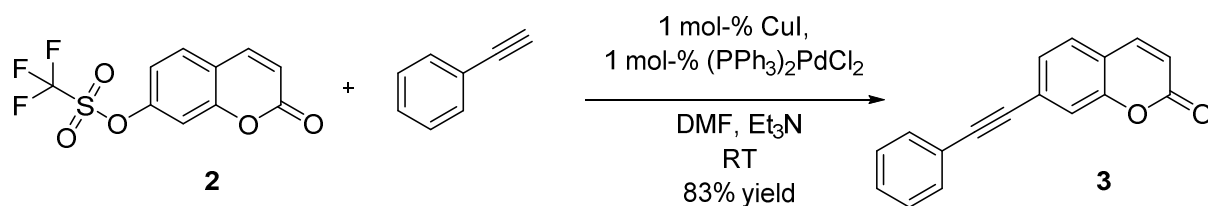
The Sonogashira reaction is a Pd cross coupling reaction between an aryl- or an alkenyl-halide or their corresponding triflates and an terminal alkyne in the presence of Cu(I) as a cocatalyst and an amine as base (Scheme 9).<sup>[65,75]</sup>



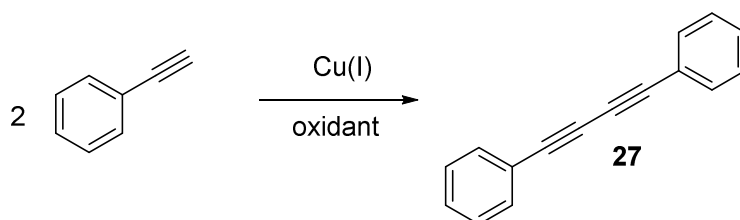
**Scheme 9: Catalytic cycle of a Sonogashira reaction**<sup>[65,75]</sup>

The catalytic cycle of Cu(I) is still poorly understood, but a transmetalation of a Cu(I) alkyne species is mainly considered.<sup>[75]</sup> Possible ways of Cu(I) alkyne formation are on the one hand a mechanism in which the terminal alkyne makes an oxidative addition to CuX resulting in a Cu(III) complex as an intermediate. After that a base supported reductive elimination could occur resulting in the Cu(I) alkyne. On the other hand Cu could act as a Lewis acid and withdraws electron density of the alkyne. That would lower the pK<sub>a</sub> of the alkyne, the amine would be strong enough to deprotonate the alkyne and after ligand exchange the Cu(I) alkyne complex would form.

Sonogashira reaction of our substrate **2** worked quite well with 83 % yield (Scheme 10).

Scheme 10: Sonogashira reaction of **2** with phenylacetylene

In the first attempts a high amount of oxidative Glaser coupling happened as an undesired side reaction. In a Glaser coupling two alkynes are oxidatively coupled via a Cu-catalyzed mechanism. This side reaction is widely known in Sonogashira reactions, especially for reactions with electron rich aryl halogenides. These react rather slowly in a Sonogashira reaction as an oxidative addition of electron rich compounds to the metal is more unfavorable than of an electron poor one. Therefore the Cu(I) alkynyl has enough time to react in a Glaser coupling. As a Glaser coupling is an oxidative coupling an oxidant has to be present (Scheme 11).<sup>[65,77]</sup>



Scheme 11: Glaser coupling

Table 4: Different parameters for Sonogashira coupling (Figure 34); base: Et<sub>3</sub>N, T = RT; solvent: DMF

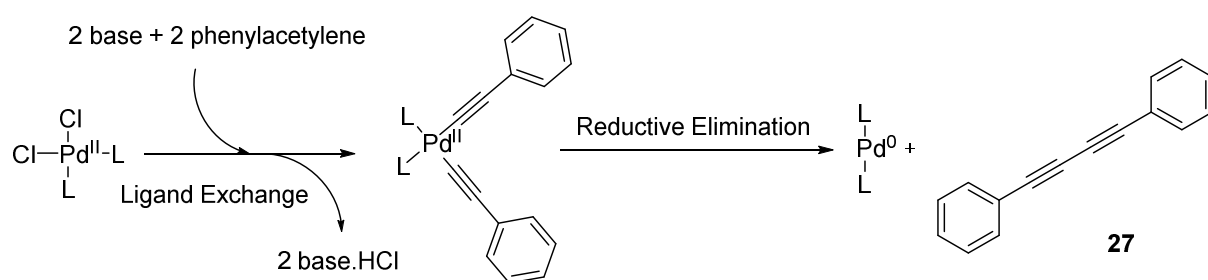
| Entry | 2 [mmol] | phenylacetylene [eq] | catalyst [mol-%] |  | Reaction time [d] | conversion [%] |
|-------|----------|----------------------|------------------|--|-------------------|----------------|
|       |          |                      | CuI              | Cl <sub>2</sub> Pd(PPh <sub>3</sub> ) <sub>2</sub> |                   |                |
| 1     | 0.070    | 2.6                  | 30               | 10   | 1                 | >99            |
| 2     | 0.343    | 1.3                  | 5                | 5  | 1                 | >99            |
| 3     | 0.768    | 1.3                  | 6                | 5  | 1                 | >99            |
| 4     | 5.47     | 1.1                  | 1                | 1  | 4                 | >99            |
| 5     | 36.4     | 1.1                  | 1                | 1  | 5                 | >99            |

At the very first experiment (Entry 1, Table 4) the solvent had been degassed, but the other liquid reagent have not been. Additional phenylacetylene had to be added as a lot of **27** had formed. As O<sub>2</sub> is very soluble in many organic compounds<sup>[78]</sup> and phenylacetylene is not stored under Ar, all liquid reagents (phenylacetylene and Et<sub>3</sub>N) were added to DMF and were then degassed together with Ar or N<sub>2</sub> in an ultrasonic bath. Also the catalyst loading and the excess of phenylacetylene were decreased. **27** was still forming, but in a lower amount than in entry

1. When the catalyst loading was decreased to 1 mol-% (Entry 4,5) the reaction time increased rapidly.

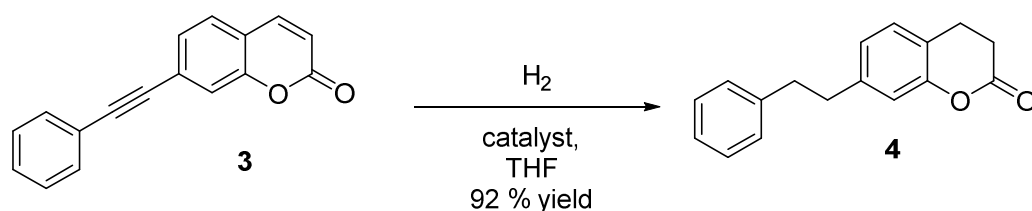
Studies have shown that  $\pi$ -systems can inactivate Pd catalysts through complexation,<sup>[75]</sup> therefore the reaction rate with lower Pd loading could be probably maintained by adding phenylacetylene via a syringe pump during the reaction. That would result in a low phenylacetylene concentration through the whole reaction time, which would lead to a smaller amount of inactive Pd-phenylacetylene complex.

A decrease of formed **27** with decreased catalyst loading was observed. Additionally **27** formation was detected at the beginning of the reaction and the amount of **27** stayed approximately constant through the whole reaction time. This could give a hint that the Pd(II) pre-catalyst is reduced to the Pd(0) catalyst (Scheme 12). If that is the case homocoupling of the alkyne could be avoided by using a Pd(0) precatalyst, for instance Pd(PPh<sub>3</sub>)<sub>4</sub>.



Scheme 12: Homocoupling through Pd(II)

#### 4.1.4 Heterogeneously catalyzed hydrogenation



Scheme 13: General reaction scheme of the hydrogenation of **3**

The first attempt to hydrogenate **3** was the classic approach with 5 mol-% 10%-Pd/C under a H<sub>2</sub> atmosphere with EtOAc as a solvent. GC-MS was used for reaction control and after 16 h all intermediates could be seen on GC-MS (Figure 18). Intermediates **18** and **28** have been identified through their mass spectra.

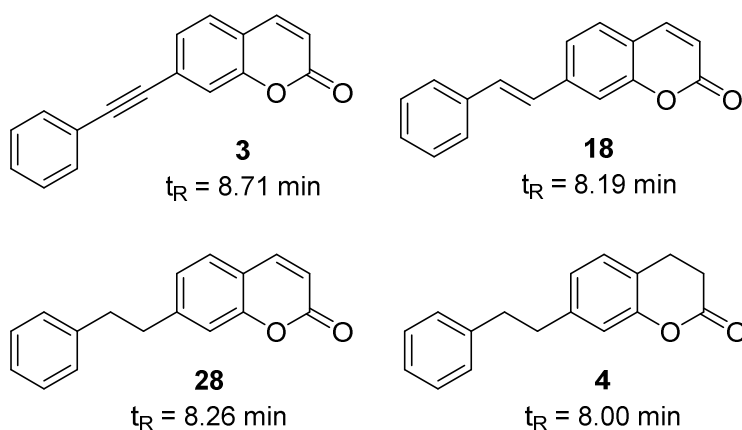


Figure 18: Educt **3**, product **4** and intermediates **18**, **28**;  $t_R$  with method MT\_50\_S

The reaction finally stopped after **28** was formed. **4** was detectable, but even after 4 additional days the amount of **4** had not increased. Another experiment had been tried out with the H-Cube. A solution of **3** in THF had been pumped in circle through the H-Cube at a flow rate of 0.5 mL/min, 60 °C, 60 bar H<sub>2</sub> and 10%-Pd/C as a catalyst. As in the previous experiment **4** was detectable, but the reaction stopped after the formation of **28**. When 5%-Pt/C was used as a catalyst further conversion to **4** was achieved. At 10 bar H<sub>2</sub> and after subsequent increasing the temperature (RT - 50°C) full conversion was achieved after 44 h. As this was a small scale experiment (260 μmol **3** in 5.2 mL THF) better reaction conditions had to be found, because otherwise the reaction on the H-Cube would take an unacceptable amount of time on larger scales. Therefore a screening for optimal reaction conditions was made (Table 5).

Table 5: Screening of ideal reaction conditions for catalytical hydrogenation on H-Cube; Single run of 20 mg **3** in 1.60 mL THF, flow = 0.5 mL/min, catalyst: 5%-Pt/C

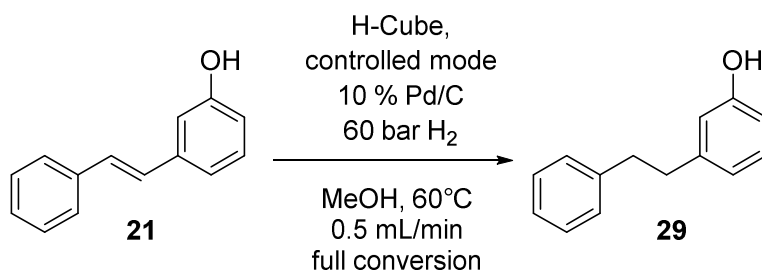
| Entry | T [°C] | p [bar] | area [%] |          |          |          |
|-------|--------|---------|----------|----------|----------|----------|
|       |        |         | 8.00 min | 8.19 min | 8.26 min | 8.71 min |
| 1     | RT     | 1       | -        | 61       | 39       | -        |
| 2     | RT     | 10      | -        | 61       | 39       | -        |
| 3     | 30     | 10      | -        | 61       | 39       | -        |
| 4     | 30     | 20      | -        | 66       | 34       | -        |
| 5     | 40     | 20      | -        | 64       | 36       | -        |
| 6     | 40     | 30      | -        | 62       | 38       | -        |
| 7     | 50     | 30      | <1       | 65       | 35       | -        |
| 8     | 50     | 40      | <1       | 65       | 35       | -        |
| 9     | 60     | 1       | 7        | 2        | 91       | -        |
| 10    | 60     | 20      | 3        | 21       | 76       | -        |
| 11    | 60     | 40      | 3        | 30       | 67       | -        |
| 12    | 60     | 60      | 3        | 36       | 61       | -        |
| 13    | 60     | 80      | 2        | 39       | 59       | -        |

The most interesting trend was the dependency on pressure. At the same temperature less **18** was transformed to **28** in most cases and also less **4** was formed by increasing pressure (compare Table 5; entries 3,4; .9-13). Normally the reaction rate accelerates with higher H<sub>2</sub> pressure. An explanation could be that adsorption of H<sub>2</sub> and substrate on the metal surface in this case is competitive. As every measurement was made just once, a failure in measurement cannot be excluded. In no experiment a reduction of the benzene ring was observed.

All reaction mixtures of Table 5 were combined (1.53 mmol in 31 mL THF) and then further hydrogenated on the H-Cube with the conditions of entry 9. Although the reaction was now faster at these conditions, conversion was not complete after 18 h (~90 % conversion). As this is very inefficient and as Thales Nano, the producer of H-Cube, recommends a concentration of 0.05 mol/L substrate a larger scale directly leads to higher reaction times. Therefore it was decided to make this reaction in batch with 5 mol-% 5%-Pt/C in THF under a H<sub>2</sub> atmosphere at 60°C. After 45 h full conversion was observed and **4** was isolated in 92 % yield (Scheme 13).

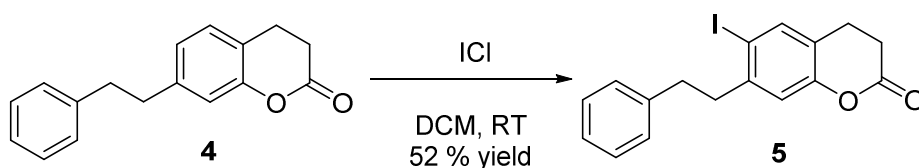
The H-Cube compared to the reaction in batch is at this case not a good choice, because longer hydrogenations on the H-Cube needs more attention of the operator. For instance the water reservoir has to be frequently refilled and also the solvent level has to be checked frequently, as the H-Cube must not run dry. Generally said, the H-Cube is the right choice for small scale reactions, with reaction conditions optimized to hydrogenate the substrate in one flow. Also parameters, like temperature and pressure, can be easily varied. For all larger scale reactions or in hydrogenations with low reaction rates, a hydrogenation in batch seems to be more favourable, as hydrogenation can be done more concentrated. The down side of a hydrogenation in batch is, that the catalyst has to be filtered off over celite and under inert conditions to avoid an ignition of the catalyst.

An example, in which full conversion was obtained in a single run on H-Cube, is the hydrogenation of **29** (Scheme 14).



Scheme 14: Hydrogenation of 29 on H-cube; Full conversion determined by GC-MS

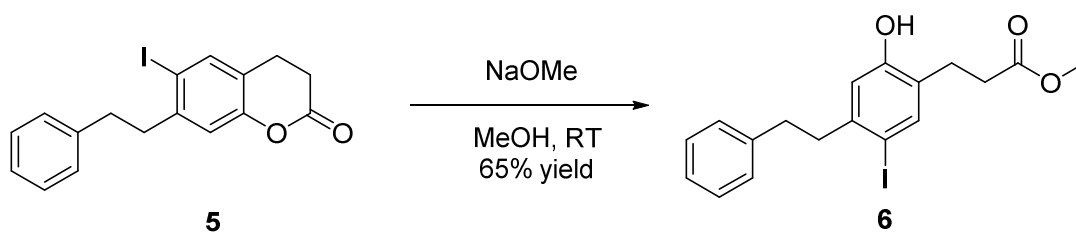
#### 4.1.5 Iodination



Scheme 15: Iodination of 4

The iodination of **4** worked selectively in para position to the oxygen (Scheme 15). Other isomers or diiodinated products have not been found by GC-MS. Nevertheless the reaction did not work absolutely clean, as some unidentified by-products had been formed. Therefore **5** was obtained in moderate yield after flash chromatography. The reason for the additional amount ICl (see 7.7.5) was a leakage of the dropping funnel, therefore the ICl-solution was not added quantitatively in the first place. In a previous experiment 1.1 equivalents of ICl were sufficient for complete conversion.

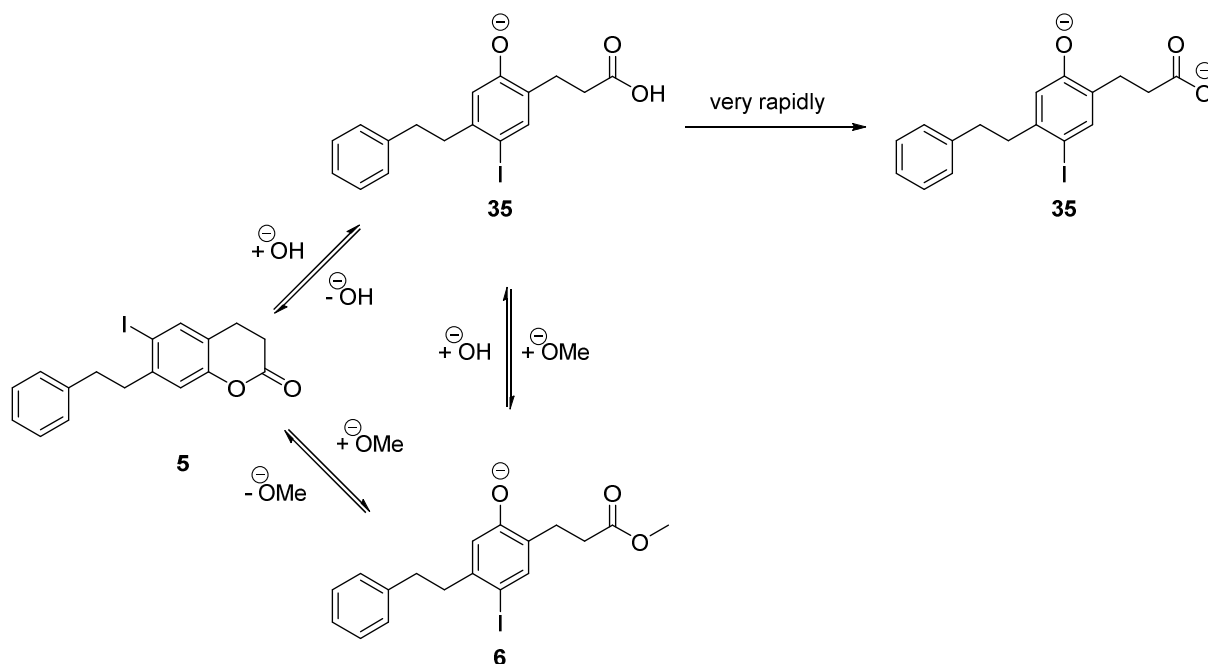
#### 4.1.6 Reesterification



Scheme 16: Transesterification of lactone 5 to methylester 6

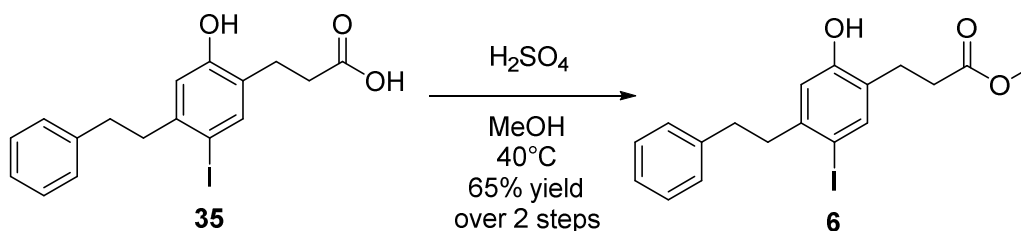
The reaction worked cleanly in short reaction times (Scheme 16). Our experiments have shown that the use of dry methanol is crucial. In one experiment technical methanol was used. At the first reaction control after 1.5 h full conversion to **6** was observed, the reaction was further stirred and the solvent was concentrated in oil pump vacuum to avoid emulsions during the work-up. It was then diluted with DCM and neutralized with 2 M HCl at 0 °C.

After the additional work-up another TLC showed that **6** completely had saponified to acid **35**. As between the reaction control and work-up no additional TLC had been measured, it could not be said at which stage that saponification happened. Rapid deprotonation of **35** removes the compound from the equilibrium. As this step is irreversible under these conditions the reaction is driving towards formation of **35** (Scheme 17).



Scheme 17: Equilibrium of reesterification/saponification

**35** was isolated and could be successfully transformed to **6** in a Fischer esterification in technical methanol (Scheme 18).



Scheme 18: Fischer esterification of **35**

After 19 h the reaction was cooled down to ambient temperature and poured on a DCM/ $NaHCO_3$ -solution/ice mixture after the work-up **6** was isolated in 65 % yield over all steps with traces of **5**. As at the first reaction control no **35**, but **5** and **6** could be seen on TLC the reaction may perhaps go mostly over the lactone **5** instead of the direct esterification of **35** to **6**. That would also explain why Fischer esterification is in that case a very fast reaction at

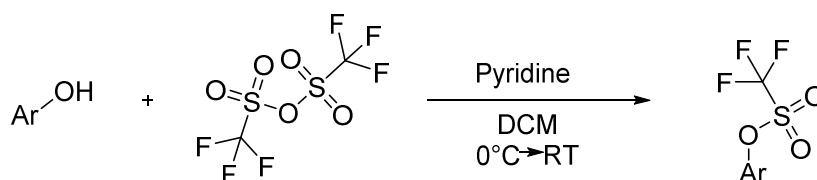


relatively low temperatures, whereas most commonly Fischer esterification is done at reflux and mostly several hours are required for high conversions. In the inlet of the GC-MS **6** quantitatively lactonizes to **5**, which also shows that the lactone **5** can easily be formed.

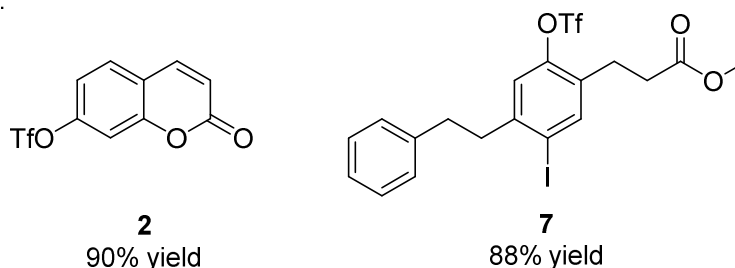
All in all that means a Fischer esterification would also be sufficient for the synthesis of **6** with **5** as starting material. As described above that reaction is also possible with technical methanol, but there is a downside on this reaction. In the above described Fischer esterification some cleavage of iodine had been recognized through the light pink colour of the solution after dilution with DCM. That could be removed through washing with 0.1 M Na<sub>2</sub>S<sub>2</sub>O<sub>3</sub> solution. As C<sup>Ar</sup>-I bonds are rather weak, elevated temperature and light exposure over longer times of such compounds should be avoided. Therefore the transesterification with NaOMe seems to be the better choice, as it has worked without any detected iodine cleavage.

#### 4.1.7 Introduction of the trifluoromethane sulfonate group

During the synthesis of the Glu-building block, the trifluoromethane sulfonate (TfO) group had been introduced twice by the same method (Scheme 19).



Method was used for:

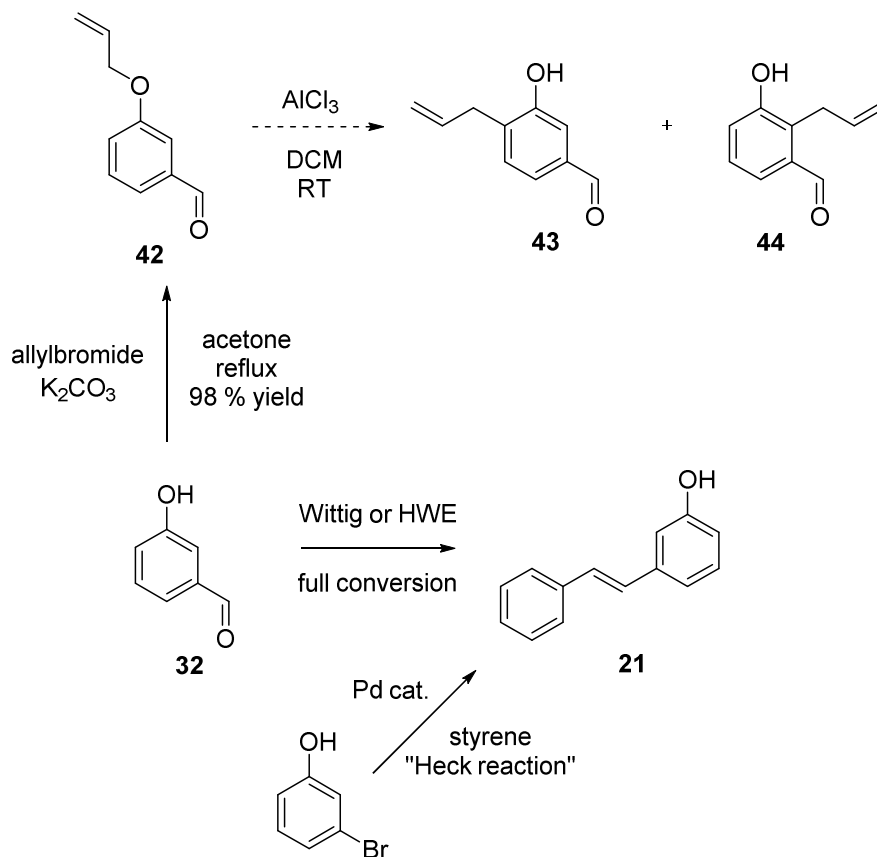


**Scheme 19: Used method for the introduction of the TfO-group**

The reactions were almost clean and resulted in high yields (90 % yield **2** and 88 % yield **7**). The purpose of the TfO-group in our synthesis is as a leaving group for later Pd cross-coupling (see 4.1.2 and 4.1.3).

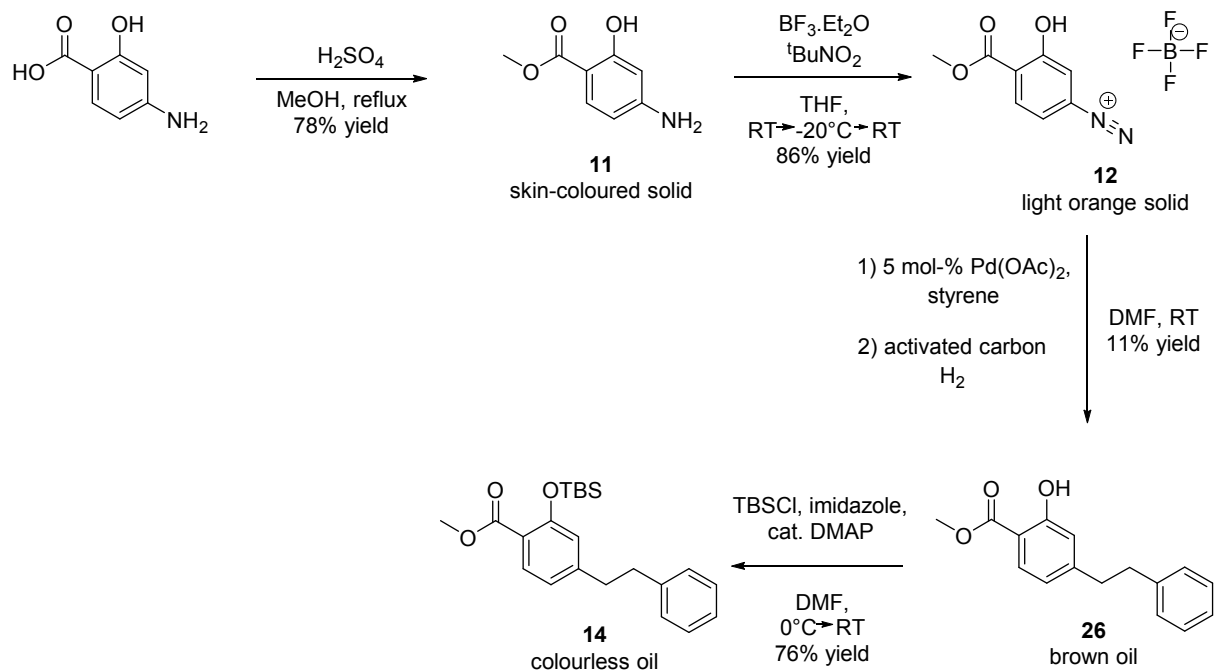
## 4.2 Synthesis of the Lys-building block

The first idea for the synthesis of the Lys-building block was from **32** or from 3-bromophenol as starting material (Scheme 20). The synthesis was dismissed later on, because of problems with the Claisen rearrangement.



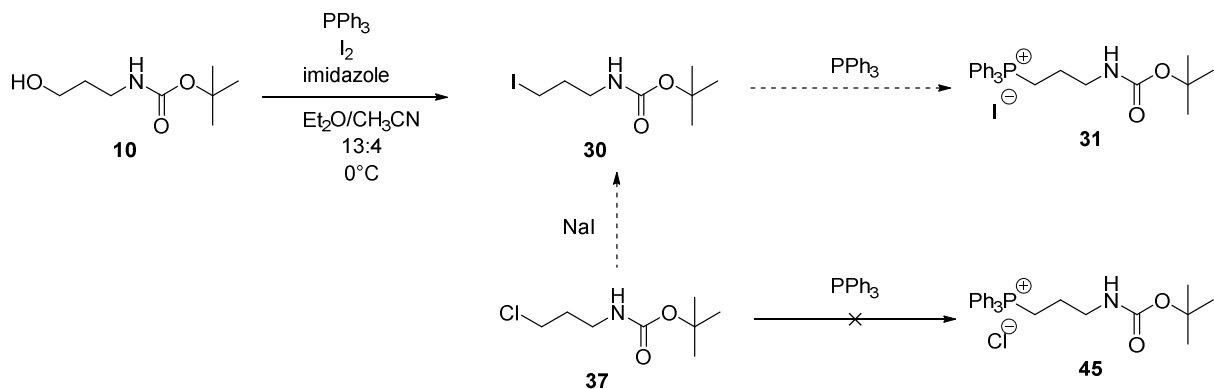
Scheme 20: Dismissed synthesis of the Lys-building block

The actual strategy of the Lys-building block starts with 4-aminosalicylic acid (Scheme 21) and was synthesized until compound **14** during this thesis.

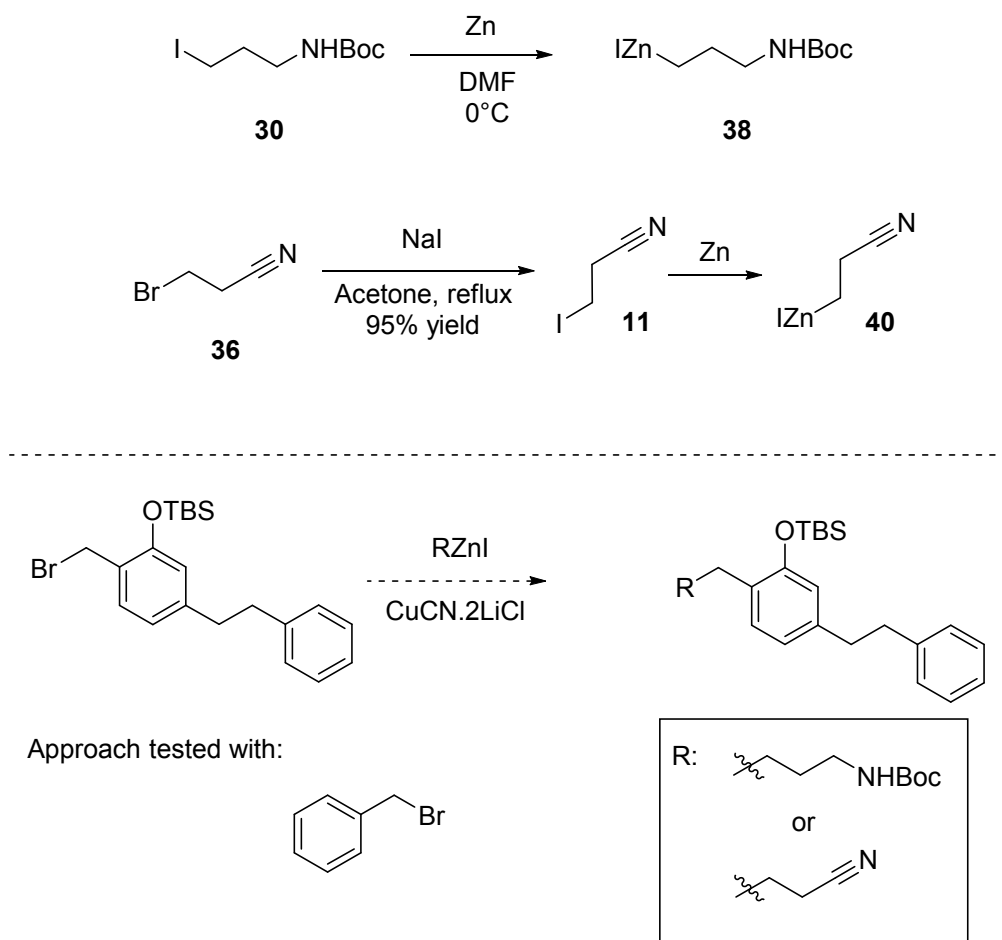


Scheme 21: Status quo of the Lys-building block

The Lys side chain was planned to be introduced via a Wittig reaction at first (Scheme 22). The latest strategy is now via organozinc chemistry (Scheme 23).



Scheme 22: Intended preparation of the Lys-side-chain fragment as a phosphonium salt



**Scheme 23: Preparation of various Lys-side-chain fragments as organozinc compounds**

All these approaches will be discussed now in more detail.

#### 4.2.1 Heck reaction of 3-bromophenol

In a former already dismissed synthesis route to the Lys-building block the carbon skeleton of the phenylethyl side chain was also planned to be introduced over a Heck reaction (Scheme 23).



**Scheme 24: Intended Heck reaction of 20 with styrene**

No desired product **21** had been formed. In literature a Heck reaction of **20** with styrene is known.<sup>[79]</sup> Those reaction conditions and the catalyst have been applied in one experiment

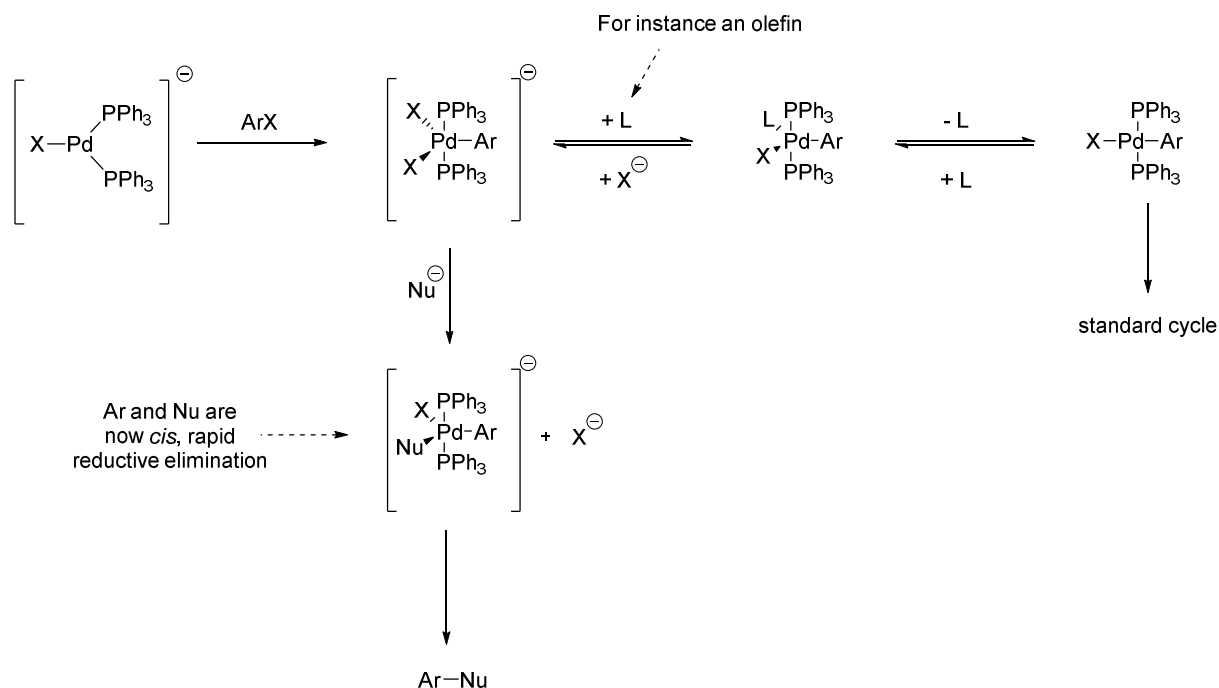
(Table 6, Entry 1) and **21** was obtained as product (determined by GC-MS). A closer look on the reaction conditions have shown that those are Jeffrey conditions.<sup>[80,81]</sup> Those conditions used with the cheaper Pd(OAc)<sub>2</sub> precatalyst also lead to the desired product **21** (Entry 2). In Entry 2 also formation of stilbene as a side product was detected, whereas in entry 1 just the desired product was detected. Maybe stilbene formation could have resulted from reductive desoxygenation of **21** or as mentioned in 4.1.2, metathesis had occurred. As that phenomena was now seen in many of our Heck reactions with styrene, that could be investigated with an additional experiment. If styrene substituted with a methyl in 3 position is used as substrate for the Heck reaction, a metathesis would be verified by the appearance of stilbene with a methyl substituent on each aromatic ring. Due to time issues such an experiment has not been performed yet.

As those reactions were just performed in a small scale for test purpose, the products have not been isolated.

**Table 6: Jeffrey conditions under which a successful Heck reaction with 20 was obtained**

| Entry | Base                | Solvent | T [°C] | Precatalyst  | Ligand           | Additive | Pd loading [%] |
|-------|---------------------|---------|--------|--|------------------|----------|----------------|
| 1     | Cy <sub>2</sub> NMe | DMAc    | 80     | [Pd( <sup>t</sup> Bu <sub>3</sub> P)Br] <sub>2</sub> | -                | TBAC     | 1              |
| 2     | Cy <sub>2</sub> NMe | DMAc    | 80     | Pd(OAc) <sub>2</sub>                                 | PPh <sub>3</sub> | TBAC     | 3              |

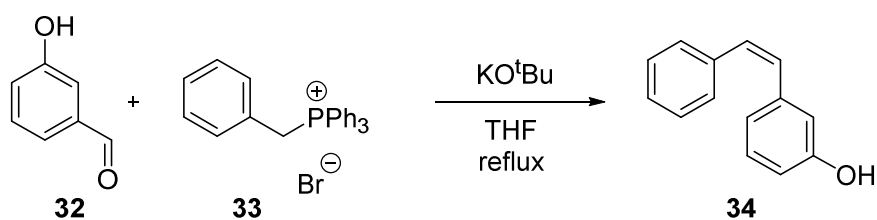
In Jeffrey conditions the reaction overcomes the standard cycle in an Amatore-Jutand mechanism (Scheme 25). Through the halide additives ate-complexes can be formed and pentacoordinated intermediates can occur in the catalytic pathway.<sup>[81,82]</sup>

Scheme 25: Amatore-Jutand mechanism<sup>[81,82]</sup>

In our case the addition of halide ions had a positive effect on the reaction, but that cannot be generalized, as it depends highly on the substrates and on the resulting rate determining step. Sometimes an addition of halide ions can also decelerate the reaction rate. All in all it can be said that Pd cross couplings are much more complicated as they are described in standard catalytic cycles. Dependent on the reaction system and reaction conditions different pathways could be followed. In Heck reactions the reaction mechanism can change during the reaction progress, as the starting olefin is consumed and a new olefin is formed, which also can coordinate to Pd with its  $\pi$ -system.<sup>[74]</sup>

#### 4.2.2 Wittig reaction with benzyltriphenylphosphonium bromide

A Wittig reaction is made by deprotonation of a phosphonium salt to the corresponding ylide, which reacts with a carbonyl-group to an olefin and phosphine oxide. In the classic Wittig reaction with unstabilized ylides mainly the *Z*-isomer results, whereas stabilized ones result in the *E*-isomer.<sup>[83]</sup>

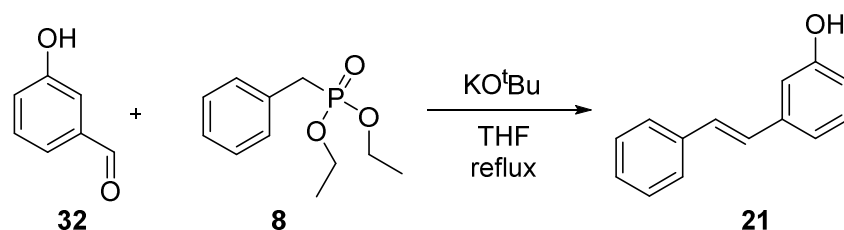


Scheme 26: Wittig reaction of 32

Wittig reaction of **32** with **33** (Scheme 26) leads to full conversion to **34**. The product was just determined by GC-MS. As the comparison of the mass spectrum with the mass spectrum from the data base fits with 87%, a successful Wittig reaction had been performed. The *Z*-isomer is the suggested isomer, as HWE (see 4.4.3) and Heck reaction (see 4.2.1) lead to the *E*-isomer, which had a  $t_R$  of 7.28 min, whereas **34** had a  $t_R$  of 6.64 min. Normally Wittig reactions with **33** results in *E*-olefins, *Z*-selectivity for **33** is reported for ortho-substituted aromatic aldehydes, but not for meta-substituted ones.<sup>[84]</sup> The crude product was tried to be separated from the triphenylphosphine oxide by crystallization and extraction, but neither of those approaches were successful. As the *E*- or *Z*-isomer or even mixtures of those would be sufficient for our synthesis, as the double bond would be hydrogenated anyway in a later step, HWE and Heck chemistry were considered as an alternative. Therefore further purification via flash chromatography and a further characterization by NMR were not executed. Therefore the formation of **34** cannot be ensured.

#### 4.2.3 Horner-Wadsworth-Emmons reaction

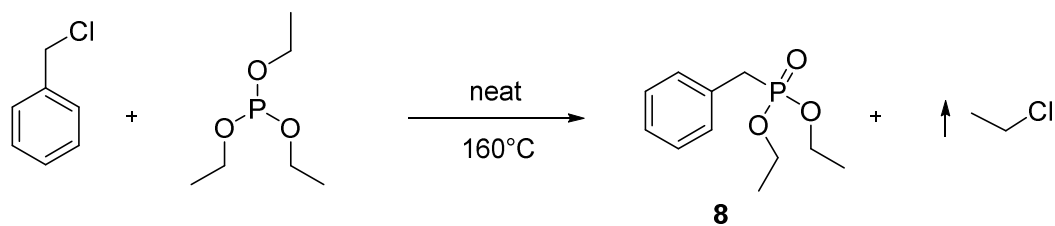
The Horner-Wadsworth-Emmons (HWE) reaction is a modification of the Wittig reaction, where EWG-substituted organophosphonates are transformed via deprotonation to the corresponding stabilized ylides and react with carbonyl compounds, which lead selectively to *E*-olefins.<sup>[83]</sup>



Scheme 27: HWE reaction of **32**

The HWE reaction of **32** (Scheme 27) led to full conversion (determined by GC-MS), although the reaction time was very long and more base and **8** had to be added after 3 d, as a small excess of 1.05 equivalents of **8** had proved to be little efficient. A longer reaction time compared to the corresponding Wittig reaction (Scheme 26) was predictable as the HWE reaction runs over a mechanism with reversible steps, until the elimination of the phosphate, which lead to the product. These reversible steps are also responsible for *E*-selectivity.<sup>[83]</sup>

The phosphonate **8** was prepared by a Michaelis-Arbuzow reaction (Scheme 28)



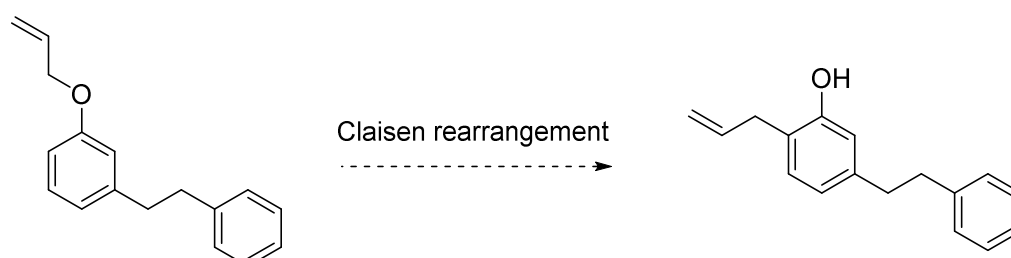
Scheme 28: Michaelis-Arbuzow reaction

The main reason for choosing HWE reaction was the forming phosphate ester, which is water soluble, even easily hydrolyzable respectively. Therefore the stoichiometric amount of phosphate ester is simply separated by the aqueous work-up, whereas the triphenylphosphine oxide mostly has to be separated via flash chromatography in Wittig reactions. After the work up all phosphate ester had been separated from the desired product, but several side products had not. As at this time the synthesis, in which **21** was needed, was already dismissed, the crude product was not further purified, but **21** could be identified by NMR as the main compound. By-products have not been identified, but there were several minor signals in the NMR.

#### 4.2.4 Claisen rearrangement

A Claisen rearrangement is a sigmatropic rearrangement of vinyl-allyl ethers to  $\gamma,\delta$ -unsaturated carbonyl or their corresponding enol form in cases of phenol ethers as starting materials. That reaction happens over a concerted six-membered transition state usually at high temperatures or with Lewis acids as catalysts.<sup>[85,86]</sup>

In a former planned synthesis of the Lys-building block an intended regio-selective Claisen rearrangement of a substituted allylic-phenoether was planned at later stage (Scheme 29).

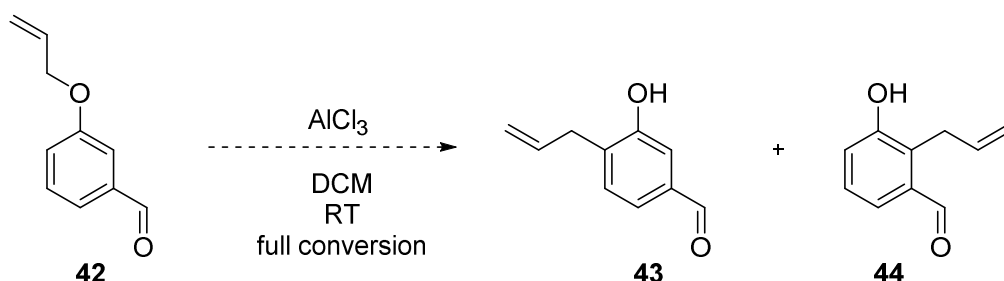


Scheme 29: Intended Claisen rearrangement

Regio-selective Claisen rearrangements are just known for resorcinol derivatives with  $\text{BCl}_3$  in literature.<sup>[86,87]</sup> As this was considered to be very risky, it was tried to test Claisen



rearrangement in an earlier step. An experiment was made with  $\text{AlCl}_3$  as a Lewis acid at ambient temperature (Scheme 30). The idea behind that was that the 2-position of **42** may be blocked by the Lewis acid and that therefore only **43** may be formed through Claisen rearrangement



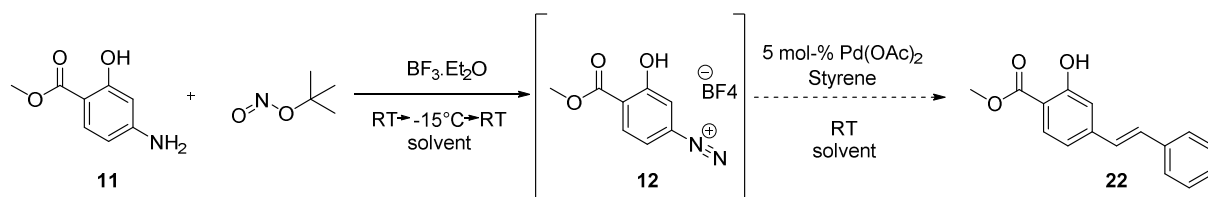
**Scheme 30: Attempted regioselective Claisen rearrangement; 43 was the desired compound**

Complete conversion was detected by GC-MS and two peaks were visible in the chromatogram ( $t_R = 5.36$  min,  $m/z = 162$ , relative area = 28 %;  $t_R = 5.64$  min,  $m/z = 162$ , relative area = 72%). That data indicated some sort of regio-selectivity, but later the compounds could not be isolated and so no further proof could be found, that those peaks are actually **43** and **44**, if so, which one is the major product? Therefore the whole synthesis of the Lys-building block with the Claisen rearrangement was dismissed and a new synthesis was planned.

#### 4.2.5 Heck reaction with a diazonium salt

One of the most reactive leaving groups is  $\text{N}_2$ . Therefore diazonium salts are very reactive electrophiles in Pd cross coupling reactions. Diazonium salts are prepared from anilines with treatment of a nitrite. Dependent on the counteranion the stability of the diazonium salt varies. Tetrafluoroborates of the corresponding diazonium compound have been shown to have good stability as they are readily isolable and air-stable.<sup>[65,88]</sup>

In our first attempts a one-pot synthesis (Scheme 31) was intended as some examples are reported in literature.<sup>[65,88]</sup> Although the desired product **22** had formed, most of the diazonium salt reacted with the solvent or hydrolyzed (Table 7).

Scheme 31: Attempted one-pot synthesis of a Heck reaction from the diazonium salt **11**; solvents in Table

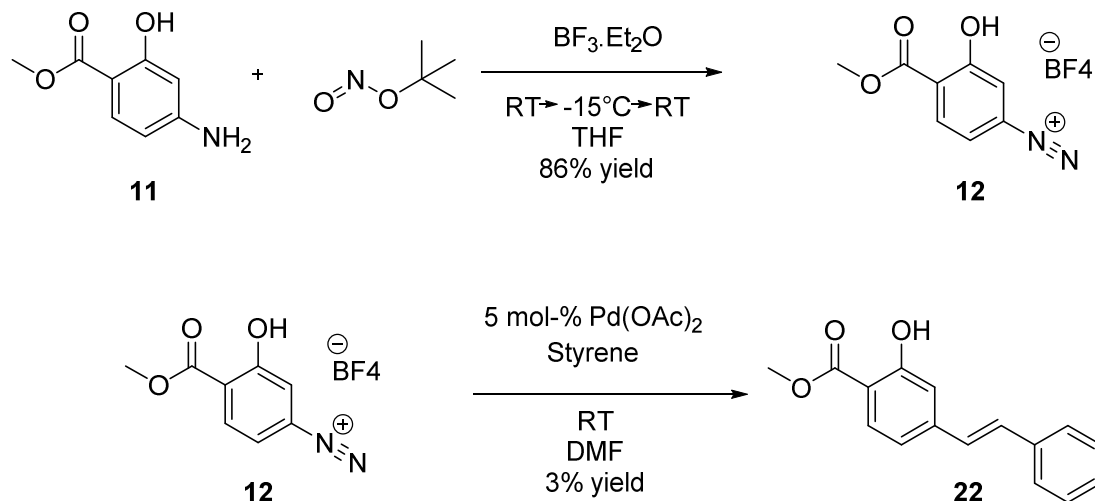
7

Table 7: Solvent screening of an one-pot attempt (Scheme 31); GC-MS method: MT\_50\_S; all products were just determined by GC-MS

| Entry    | Solvent | tR [min]     |                | main product  |
|----------|---------|--------------|----------------|---------------|
|          |         | main product | <b>22</b>      |               |
| <b>1</b> | MeOH    | 5.64         | 8.00           | <br><b>23</b> |
| <b>2</b> | THF     | 4.67         | 8.00           | <br><b>24</b> |
| <b>3</b> | DMF     | 5.85         | not detectable | <br><b>25</b> |

The hydrolysis product **25** was formed in all reactions of Table 7. As just dry solvents have been used the water must have brought in via a reagent. Most likely via the <sup>t</sup>BuNO<sub>2</sub> as it is stored in the fridge and has already been in use for several years. That MeOH can act as a nucleophile in that reaction was not surprising, but has not been reported in literature, where MeOH was also used as solvent.<sup>[65,88]</sup> In THF **12** is hardly soluble and so **24** was obtained as a main product. This could have been formed through a reductive elimination of the corresponding Pd-H complex. **24** has also been formed in the other two entries to some amount.

Despite those reactions GC-MS data had shown that styrene seems to react with the excess of  ${}^1\text{BuNO}_2$ . Therefore the one-pot attempt was dismissed and **22** was made from isolated **12** (Scheme 32).

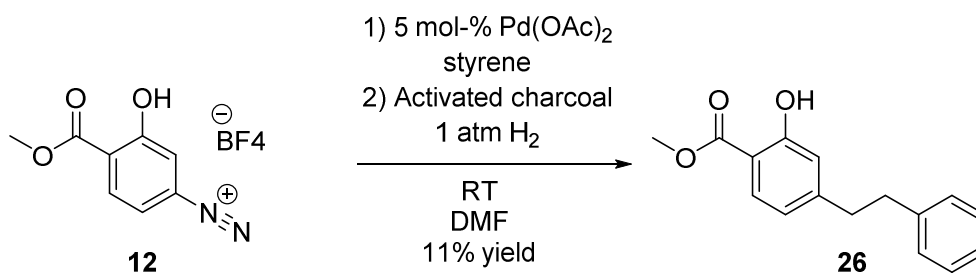


Scheme 32: Formation of diazonium salt **12** and Heck reaction with isolated **12**

In THF **12** precipitated and it could be isolated by simple filtration after addition of  $\text{Et}_2\text{O}$  in 86% yield. As **12** is very labile to hydrolysis in solution no NMR of **12** could be measured. **12** decomposed in every of our deuterated solvents under  $\text{N}_2$  evolution. A measurement of HRMS could also not be performed due to the thermal instability of **12**.

The following Heck reaction did work without any formation of the hydrolysis product **25**. **22** could be determined by NMR after work up and purification via flash chromatography. The yield (3%) was rather poor as this was a small test reaction with 263  $\mu\text{mol}$  **12**.

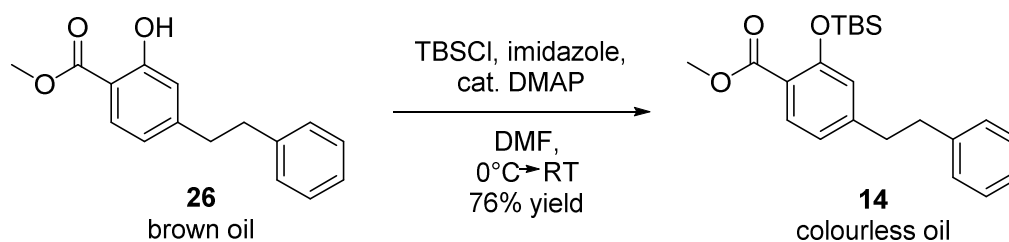
The Heck reaction was made on larger scale with a subsequent hydrogenation in one pot (Scheme 33). This approach has the advantage, that the Pd, which was previously used as catalyst for the Heck reaction, is then adsorbed on activated charcoal and is used as a hydrogenation catalyst. This approach is frequently used in Heck reactions where the double bond is not needed in the target molecule.<sup>[65,88]</sup>



Scheme 33: Heck reaction with following hydration in one pot

Unfortunately the DMF used for this reaction was not dry and therefore most of **12** hydrolyzed. Nevertheless, activated charcoal was added to the reaction mixture as no further N<sub>2</sub> formation was observed. A H<sub>2</sub> atmosphere was installed and **26** was formed. **26** could be isolated by treating the oily crude product with 3 M NaOH. The phenolate of **26** precipitated and could be filtrated. **26** was regenerated by treating the phenolate of **26** with saturated NH<sub>4</sub>Cl solution and following extraction with DCM. **26** could be characterized by NMR and was pure enough for the next step.

#### 4.2.6 Silylation

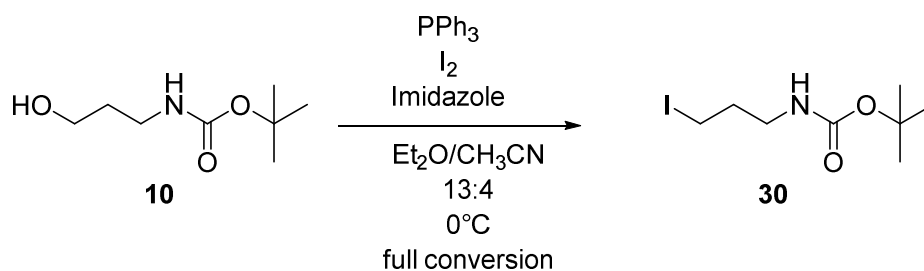


Scheme 34: Introduction of the TBS-protecting group

The silylation of **26** (Scheme 34) went as expected and **14** could be isolated in 76 % yield after flash chromatography. The reaction was done just once with a rather large excess of TBSCl (3.0 eq). NMR analysis of the crude product showed that the main impurity was at 0.92 ppm and 0.10 ppm, which is most likely 1,3-di-*tert*-butyl-1,1,3,3-tetramethyldisiloxane, the hydrolysis product of TBSCl. This could be avoided by using stoichiometric amount of TBSCl.

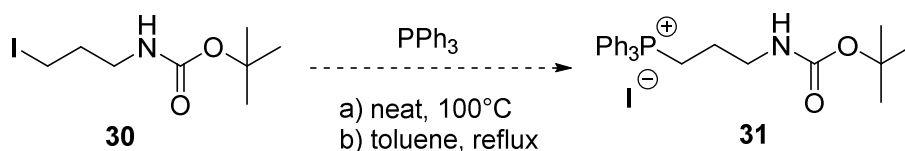
#### 4.2.7 Appel reaction

An Appel reaction is the substitution of a hydroxy group with a halogen. A hydroxy group is transformed in a leaving group with a halogen activated triphenylphosphine and than a S<sub>N</sub>2 reaction with a halogenide as nucleophile is happening. The corresponding halogenide is formed with triphenylphosphine oxide as a by-product.<sup>[89]</sup>

Scheme 35: Appel reaction of **10**

The conditions for the Appel reaction of **10** (Scheme 35) were done according to the literature known synthesis of *tert*-butyl (5-hydroxypentyl)carbamate, which differs to **10** just by the number of carbons between nitrogen and oxygen.<sup>[90]</sup> The reaction worked as described, **30** was determined by GC-MS and most of the produced triphenylphosphine oxide could be crystallized out from Et<sub>2</sub>O/cyclohexane. The crude product was used without further purification for the synthesis of the corresponding phosphonium salt (see 4.2.8).

#### 4.2.8 Synthesis of (3-((*tert*-butoxycarbonyl)amino)propyl)triphenylphosphonium iodide

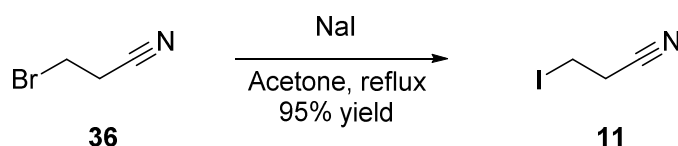
Scheme 36: Different reaction conditions for the synthesis of **31**

In the attempted synthesis of **31** the educt **30** was completely consumed (determined by TLC) under both reaction conditions (Scheme 36). Under solvent-free conditions a yellowish liquid had formed, which solidified during cooling to a yellowish amorphous solid. In toluene a two layer system had formed, which led to the same result as under solvent-free conditions. It seemed that an ionic liquid had been formed. Nevertheless, the crude product was very impure in both cases. Identified impurities were triphenylphosphine and triphenylphosphine oxide, which was brought in through the educt (see 4.2.7). Crystallization, extraction and even flash chromatography failed to purify the crude product. Therefore the characterization of the crude product is not clear, but NMR data indicates that **31** had been formed in this reaction.

Interestingly the synthesis of 5-(*tert*-butoxycarbonylamino)pentan-1-triphenylphosphonium iodide was reported in literature at the conditions of Scheme 36a. The reason why it did not work properly for the synthesis of **31** is not clear, as just the length of the alkyl chain between nitrogen and oxygen differs compared to the literature's synthesis.<sup>[90]</sup>

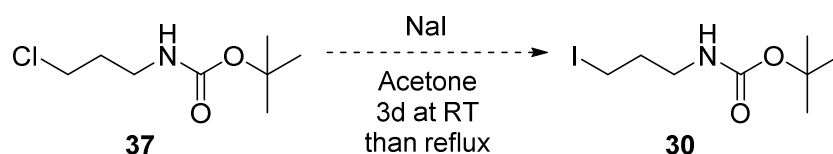
#### 4.2.9 Finkelstein reaction

In a Finkelstein reaction alkyl bromides or chlorides are exchanged to iodides through a nucleophilic substitution. The driving force behind this reaction is the insolubility of the forming NaBr or NaCl respectively, whereas NaI is soluble in acetone. The corresponding halogenide is thereby removed from the equilibrium.<sup>[85]</sup>



Scheme 37: Finkelstein reaction of **36**

The Finkelstein reaction of **36** to **11** worked almost quantitatively with 95 % yield (Scheme 37). **11** seems to be very light sensitive as the yellowish solution turned colourless after washing with 0.1 M Na<sub>2</sub>S<sub>2</sub>O<sub>3</sub>-solution, which turned light yellowish again after several minutes at evaporation on a rotary evaporator. Therefore **11** has to be stored under light exclusion, whereas room light exposure of several hours did not lead to detectable amount of degradation.



Scheme 38: Finkelstein reaction of **37**

At ambient temperature **30** was formed in the Finkelstein reaction of **37**, but after three days just 24 % conversion could be determined by GC-MS (Scheme 38). Therefore the reaction mixture was heated under reflux. Complete conversion of **37** was monitored by GC-MS after additional 2 d, but the amount of **30** stayed almost the same and another unknown compound had formed under these conditions as a main product. If **37** had decomposed or **37** had transformed to **30** and **30** had further decomposed is not clear. As an alkyl iodide is more reactive, the second hypothesis would be more likely, but that raises the question why the

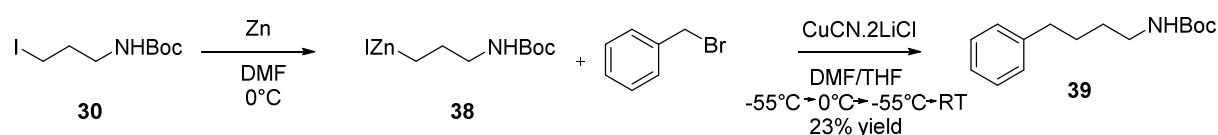
amount of **30** stayed almost the same. That could be explained by two reasons. First of all, the relative area of each compound on the GC chromatogram is strongly dependent on the ionization property of the compound and secondly, it could be by chance, that the second reaction control had been performed in that moment where the amount of **30** was relatively as much as in the first one at ambient temperature.

As **30** was better accessible through an Appel reaction (see 4.2.7), the above reaction was not investigated any further.

#### 4.2.10 Organozinc chemistry

The advantages of organozinc compounds are their relatively low basicity and their tolerance towards many functional groups. Therefore organozinc compounds can be made and act as nucleophiles, which would not be possible with organomagnesium or organolithium compounds. Organozinc are more tolerant, but they are less reactive compared to the previous mentioned ones. Sometimes organozinc compounds have to be transmetalated to obtain the desired reactivity or in some cases the electrophile has to be activated by a Lewis acid for successful reaction with the organozinc compound.<sup>[65]</sup>

The introduction of the side chain of the Lys-building block chain is planned through an organozinc reagent. Therefore some test experiments were done. In the following experiments commercially available Zn-dust was sufficient to generate the organozinc species.

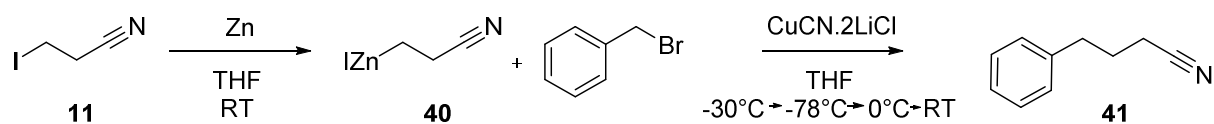


**Scheme 39: Nucleophilic substitution of benzylbromide by transmetalated **30****

The Zn metal in the reaction with **30** (Scheme 39) had been activated with chloro trimethylsilane. As this was a test reaction, **30** had been used as a crude product (impurity: triphenylphosphine oxide). Complete conversion of **30** was detected by TLC. The excess of Zn dust had to be filtered off to avoid undesired side reactions later on. In the solution of **38** was added to CuCN.2LiCl solution at -55°C and then warmed up to 0°C via an ice bath for several minutes to ensure transmetalation. Benzylbromide was added afterwards at -55°C. After an hour a sample was prepared for GC-MS analysis and the reaction mixture was warmed up stepwise from -55°C to 0°C and then to ambient temperature. The sample from -

55°C did not show any desired product formation, but a sample prepared after 15 h at ambient temperature did show formation of a compound, which fragmentation pattern in the mass spectrum did fit for **39**. To gain further proof the crude product was isolated after a work-up and purified via flash chromatography. NMR analysis gave additional confidence that the isolated compound is **39**. <sup>1</sup>H-NMR fits, in the ATP-spectrum the signal to noise ratio is too bad for the quaternary carbons, but the other carbon signals do match. HH-COSY and HSQC NMR experiments also support the structure of **39**.

1,2-Diphenylethane most likely formed through a Wurtz-coupling was detected by GC-MS as a side product.



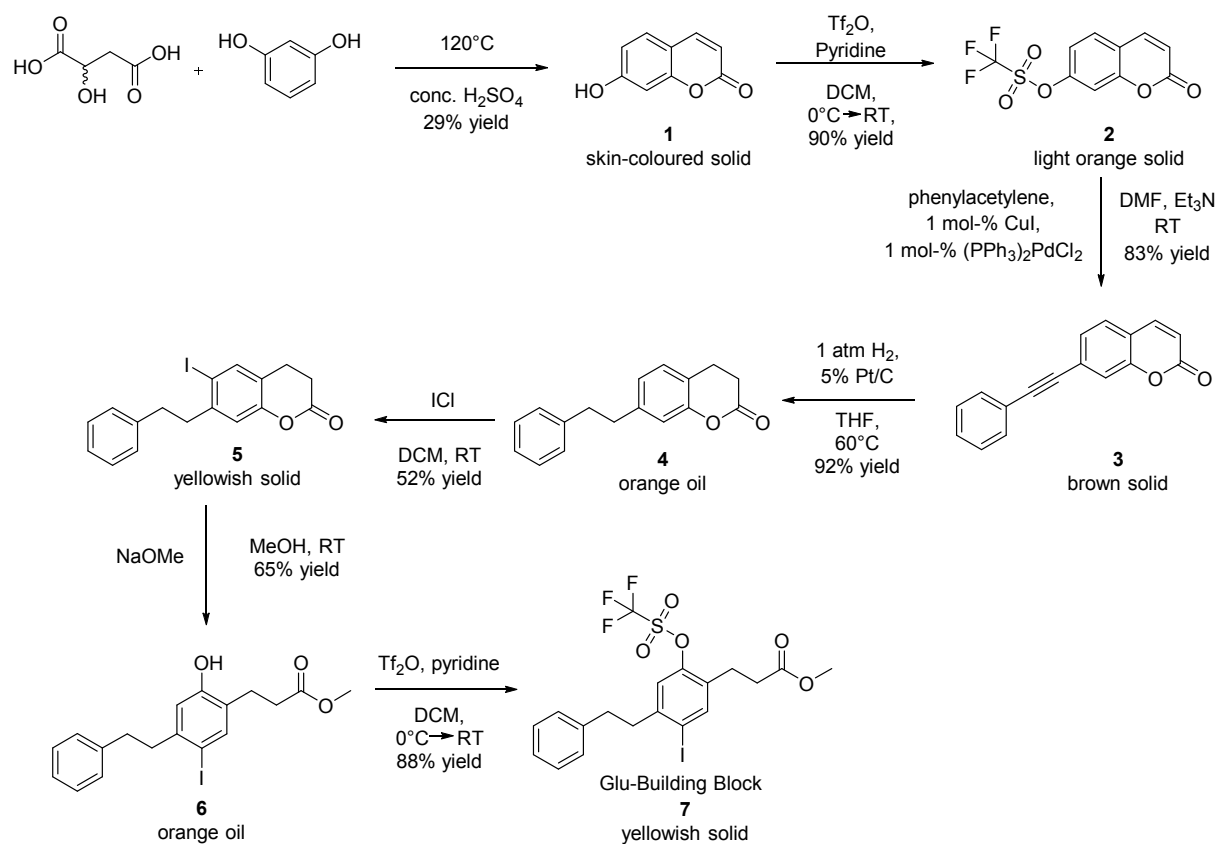
Scheme 40: Nucleophilic substitution of benzylbromide by transmetalated **40**

The preparation of **40** (Scheme 40) is known in the literature and therefore it was done according to the reported procedure.<sup>[91]</sup> Zn dust was activated with chlorotrimethylsilane and 1,2-dibromoethane. The complete conversion of **11** was detected after 35 min. As above the remaining Zn dust was filtered off and the filtrate was added to a CuCN·2LiCl solution. In contrast to the reaction in Figure 48 the reaction mixture was not warmed up, but cooled down to -78°C at which benzylbromide was added. As above the reaction was warmed up stepwise after an hour from -78°C to 0°C, at which temperature a sample for GC-MS analysis was prepared, to ambient temperature. No **41** was detected in the sample taken at 0°C. After 13 h at ambient temperature another sample for GC-MS was prepared, in which the formation of **41** could be detected. As **41** is known in the MS database and the mass spectrum fits to 90%, it was seen as sufficient proof for the formation of **41** and **41** was not isolated in that test reaction. As above 1,2-diphenylethane was detected as a side product.



## 5 Summary

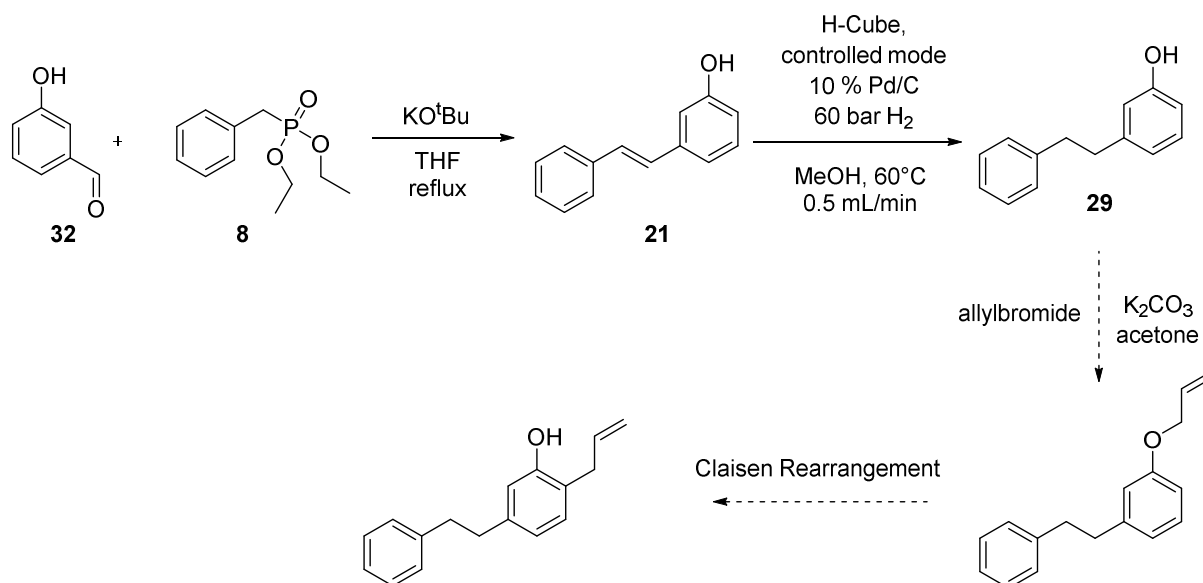
The aim of this thesis was the synthesis of the Glu- and Lys-building blocks.



**Scheme 41: Synthesis route of the Glu-building block**

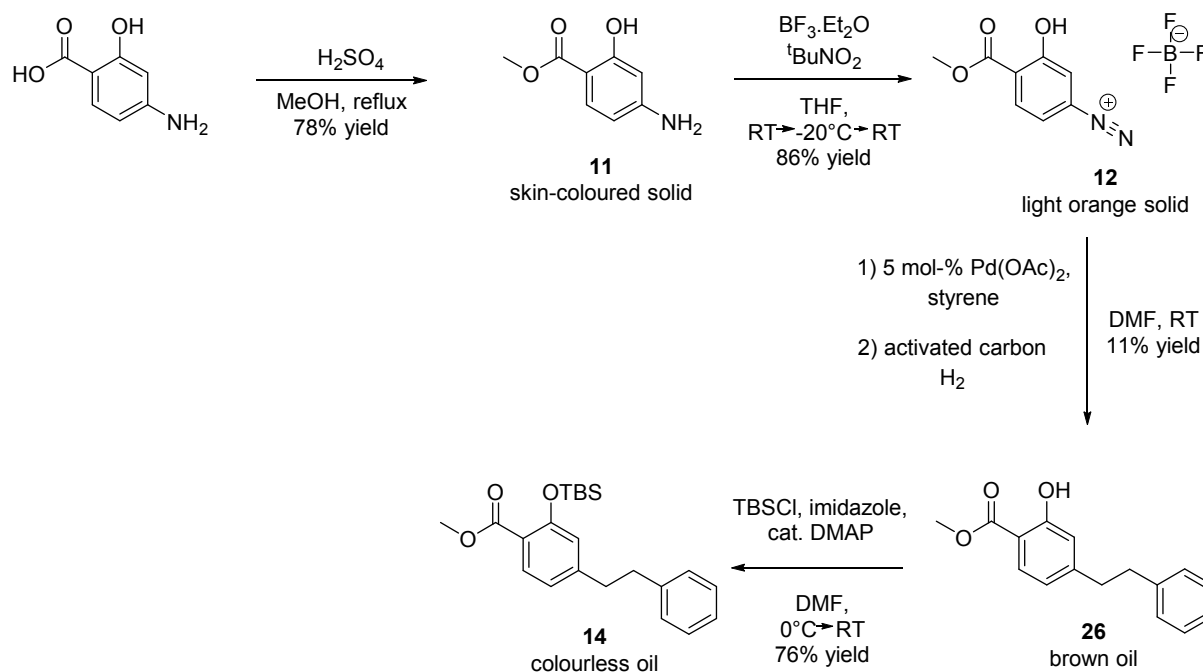
A synthesis of the Glu-building block was established with an overall yield of 6 % (Scheme 41).

One synthesis strategy for the Lys-building block contained a regioselective Claisen rearrangement (Scheme 42). As there is a high risk, that the desired regioselectivity could be achieved, the Claisen rearrangement was planned in an early step of the synthesis (Scheme 30). A test reaction showed that a regioselective Claisen rearrangement product could not be isolated (see 4.2.4).



**Scheme 42: Dismissed synthesis of the Lys-building block; no yields are given as all steps were just test reactions; planned steps are shown in dashed lines**

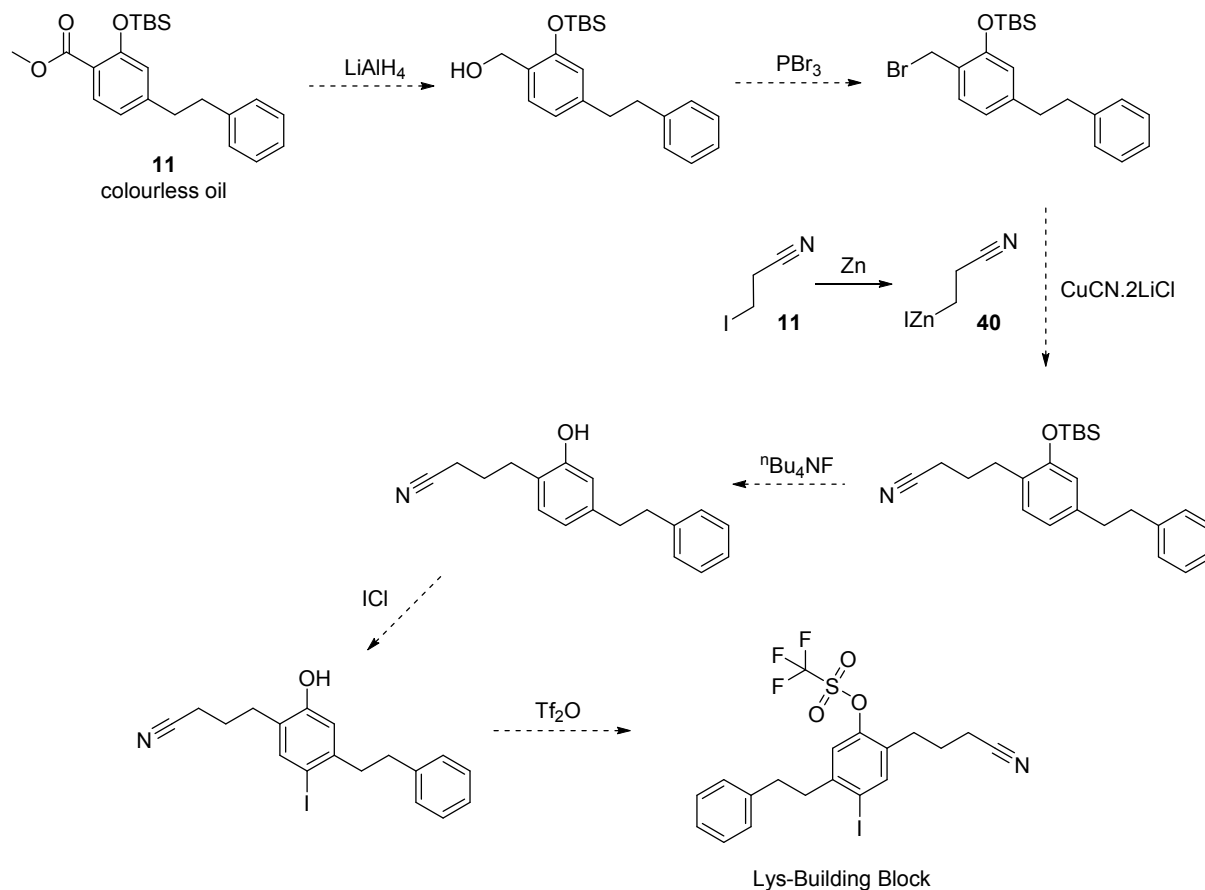
A synthesis of the Lys-building block was planned, in which the substitution pattern of the aromatic ring is already given in the starting material (Scheme 43). The synthesis of the Lys-building block could not be finished during this thesis and is therefore still under construction.



**Scheme 43: Status Quo in the synthesis of the Lys-building block**

## 6 Outlook

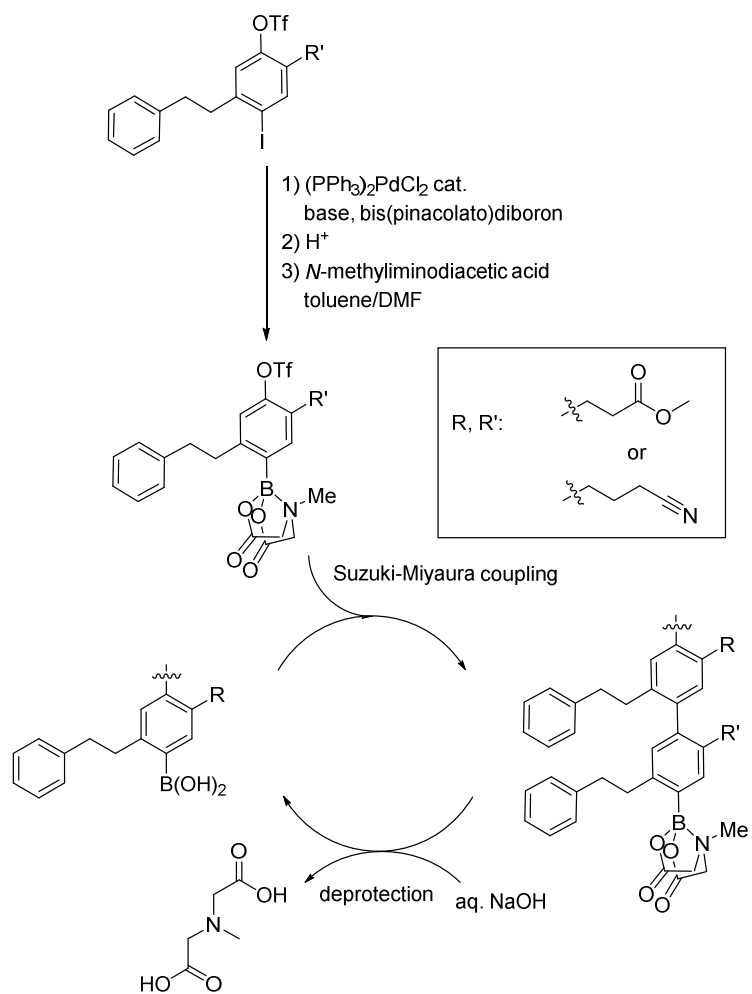
In short term the synthesis of the Lys-building block has to be finished (Scheme 44).



**Scheme 44: Planned steps of the Lys-building block synthesis**

In longer term the goal is to transform the iodide to the MIDA boronate via a Miyaura borylation to synthesize the ApoA1 mimetics through sequential Suzuki couplings (Scheme 45). After the ApoA1 mimetics are made from the building blocks the esters have to be cleaved to the corresponding acid and the nitriles have to be reduced to the corresponding amines. These mimetics will be then ready to be tested as drug carriers.

As the Glu-building block is already available the concept of the sequential Suzuki coupling could already be tested and optimized.



**Scheme 45: Sequential Suzuki coupling with previous Miyaura borylation**

## 7 Experimental Section

### 7.1 General

All chemicals were purchased from Merck, Sigma Aldrich, Fluka, Acros Organics or Alfa Aesar. All chemicals, if not mentioned otherwise, were used as purchased. Solvents were bought and/or prepared as described in 7.2.

When it was necessary to work under inert conditions, a Schlenk flask or a round-bottom flask with an attached Schlenk adapter was heated under vacuum with a heat gun. When the flask had cooled down, it was flushed with Ar or N<sub>2</sub>. All solids and dry solvents were added to the flask by an inert gas counter flow.

Every reaction, if not mentioned otherwise, was permanently stirred with a magnetic stir bar.

Hydrogenation catalysts were removed by filtration through celite under an inert atmosphere. The filter cake was washed with water and it was then disposed wet in a plastic bottle separated from flammable material.

Molecular sieves were activated by heating (~150°C) in a round-bottom flask under vacuum for several hours until a constant pressure was obtained.

### 7.2 Solvents

**Acetone:** Acetone was distilled over a rotary evaporator and stored in a brown glass bottle.

**Cyclohexane:** Cyclohexane was used as purchased and stored in 5 L plastic bottles.

**Diethylether:** Purchased diethylether was distilled over a rotary evaporator to remove the stabilizer. The distilled Et<sub>2</sub>O was stored in a brown glass bottle over KOH.

**DCM:** DCM was used as purchased and stored in 5 L plastic bottles.

Dry DCM was prepared by pre-drying DCM over phosphoric pentoxide and subsequent refluxing under an inert atmosphere over CaH<sub>2</sub>. After several hours of refluxing it was distilled off and stored in a brown glass bottle with a Schlenk adapter over 4 Å molecular sieves and under Ar.

**DMF:** Dry DMF was purchased and refilled in a brown glass bottle with a Schlenk adapter. It was stored over 3 Å molecular sieves and under Ar.

**Ethyl acetate:** Ethyl acetate was used as purchased and stored in 2.5 L brown glass bottles.

**Methanol:** Methanol was used as purchased and stored in 5 L plastic bottles.

Methanol was dried by refluxing over I<sub>2</sub> activated Mg under an inert atmosphere. After several hours of refluxing it was distilled off and stored in a brown glass bottle with a Schlenk adapter over 3 Å molecular sieves and under Ar.

**Pyridine:** Extra dry pyridine was used as purchased in a brown glass bottle over molecular sieves and under an Ar atmosphere closed by a septum. Every amount of pyridine was taken by using an Ar balloon as pressure equalization.

**THF:** Purchased THF was distilled over a rotary evaporator to separate it from the stabilizer. The distilled THF was stored in brown glass bottles over KOH.

THF was dried by refluxing stabilizer free THF over Na in an inert atmosphere. Benzophenone was used as indicator. THF was considered as dry when the indicator coloured purple and was then distilled off. Dry THF was stored in a brown glass bottle with a Schlenk adapter over 4 Å molecular sieves and under Ar.

**Triethylamine:** Triethylamine was used as purchased and stored in brown glass bottles.

Triethylamine was pre-dried by refluxing it over KOH for 2 h under an inert atmosphere. Pre-dried triethylamine was finally dried over CaH<sub>2</sub> under an inert atmosphere. Triethylamine was considered as dry after several hours of refluxing and subsequently distilled off and stored in a brown bottle with a Schlenk adapter over 4 Å molecular sieves and under Ar.

## 7.3 Separation techniques

### 7.3.1 Thin layer chromatography

For many reactions thin layer chromatography (TLC) was used for reaction control. Silica on aluminium plates were used for TLC. TLC plates were purchased from Merck (Merck silica gel 60-F<sub>254</sub>). Spots were visualised by UV ( $\lambda = 254$  nm or 366 nm) or by a CAM- or ninhydrin

solution as spraying reagent. TLC plates were gently heated with a heat gun to accelerate the reaction with the spraying reagent.  $R_f$ -values and eluent composition are each given.

**CAM:** 5.0 g phosphomolybdic acid and 15 mL conc.  $H_2SO_4$  were dissolved in 200 mL  $H_2O$ . 2.0 g  $Ce(SO_4)_2$  were added slowly and stirred until all solid parts had dissolved to form a yellow solution.

### 7.3.2 Flash chromatography

For purification via flash chromatography, 60 Å silica gel from Acros Organics was used. The particle size was distributed between 35 µm and 70 µm. Dependent on the separation problem 50 to 100 times as much  $SiO_2$  as the weight of the crude product was used. The column diameter was chosen that the resulting column height was between 15 and 30 cm. Chromatography was performed under elevated pressure applied by a hand pump. Hardly dissolvable compounds were usually former adsorbed on Celite®.

### 7.3.3 Gas chromatography

An Agilent Technologies 7890A GC-System with a polar HP-5MS capillary column (length: 30 m, diameter: 0.25 mm, film thickness: 0.25 µm) was used for analytical gas chromatography. Substance mixtures were separated by their differing boiling point and polarity. The samples were applied to the column by split mode. Helium 5.0 was used as a carrier gas. The detection of the compounds was achieved by the mass selective Agilent Technologies 5975C inert MSD with Triple-Axis Detector. Ionisation of the compounds for MS was achieved by an EI-ionisation source with a potential of  $E = 70$  eV. MT\_50\_S or MT\_50\_35S were used as methods.

**MT\_50\_S:** 50 °C 1 min; rampe 40 °C\*min<sup>-1</sup>; linear until 300 °C; 300 °C 5 min; solvent delay: 4.0 min.

**MT\_50\_35S:** 50 °C 1 min; rampe 40 °C\*min<sup>-1</sup>; linear until 300 °C; 300 °C 5 min; solvent delay: 3.5 min.

Integrals over the peak areas were considered for conversion control. These values have to be considered as relative, because in no measurement internal standards were used and the intensity of each peak is dependent on the ionization potential of each compound.

## 7.4 Nuclear Magnetic Resonance

All NMR spectra were measured by a Bruker AVANCE III (300.36 MHz- $^1\text{H}$ -NMR, 75.53 MHz- $^{13}\text{C}$ -NMR) with autosampler. The solvent peak of the residual protonated solvent was used as internal standard in each  $^1\text{H}$  and APT spectrum. To increase clarity, by decreasing the number of signals in APT spectra, all ATP spectra were  $^1\text{H}$ -decoupled. Signal multiplicities were written as s (singlet), bs (broad singlet), d (doublet), dd (doublet of a doublet), t (triplet), q (quadruplet), p (pentet) and m (multiplet). All signals were assigned to their binding situation ( $\text{C}_\text{q}$  for quaternary carbons,  $\text{C}^{\text{Ar}}$  for aromatic carbons,  $\text{H}^{\text{Ar}}$  for aromatic hydrogen, CF, CH,  $\text{CH}_2$ ,  $\text{CH}_3$ , OH, NH). The chemical shift  $\delta$  is given in ppm and the coupling constant  $J$  is given in Hz (Hertz).

## 7.5 Melting points

All melting points were determined by "MelTemp®" from Electrothermal with a built in microscope. Melting points were measured three times for each compound and they were not corrected with a standard.

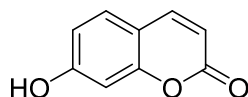
## 7.6 High resolution mass spectroscopy

All measurements of high resolution mass spectroscopy were done by Prof. Dr. Robert Saf and his group on a "Waters GCT Premier" system after ionisation with an EI-ionization source with a potential of  $E = 70$  eV. Calculated and measured masses are given each.



## 7.7 Experimental procedures

### 7.7.1 7-Hydroxy-2*H*-chromen-2-one (1)



CAUTION: This reaction has to be performed in a well-ventilated hood as CO-gas evolves! In a 1000 mL 3-neck-flask, equipped with a mechanical stirrer and an air cooler with gas exhaust, 80 mL conc. H<sub>2</sub>SO<sub>4</sub> were added to 25.6 g (232 mmol, 1.50 eq) resorcinol and 20.8 g (155 mmol, 1.00 eq) D/L-malic acid. The grey-brown suspension was heated to 120°C via an oil bath. During the heating process the colour of the reaction mixture changed over a skin coloured to a yellowish foamy suspension. At 120°C a strong gas evolution occurred resulting in yellow voluminous bubbles. After 85 min no further gas evolution (CO) could be seen, therefore the orange suspension was allowed to cool down to RT. When the reaction mixture had cooled down, the whole reaction mixture was poured on 1000 mL H<sub>2</sub>O/ice mixture. A greyish solid precipitated. The mixture was transferred to a separating funnel and extracted with 150 mL EtOAc. The two layers were separated and the aqueous layer was extracted with EtOAc (4 x 100 mL). The combined organic layers were washed with saturated NaHCO<sub>3</sub> solution (1 x 50 mL), brine (1 x 100 mL), dried over Na<sub>2</sub>SO<sub>4</sub> and filtered through a glass frit. The filter cake was washed with EtOAc (3 x 10 mL) and the filtrate was concentrated on a rotary evaporator. 10.4 g (64.1 mmol, 41 %) of a light orange solid was obtained as a crude product. The impure crude product (purity was checked by <sup>1</sup>H-NMR) was further purified by dissolving it in 200 mL EtOAc and washing it with saturated NaHCO<sub>3</sub> solution (3 x 30 mL). The combined organic layers were dried over Na<sub>2</sub>SO<sub>4</sub> and filtered through a glass frit. The filter cake was washed with EtOAc (3 x 5 mL), the filtrate was concentrated on a rotary evaporator and the obtained skin coloured solid was dried in vacuum. The product was used in the next step without further purification.

Yield: 7.41 g (45.7 mmol, 29%) skin coloured solid

C<sub>9</sub>H<sub>6</sub>O<sub>3</sub> [162.14 g/mol]

R<sub>f</sub> = 0.22 (Cyclohexane/EtOAc 2:1) (fluorescence in UV, CAM)

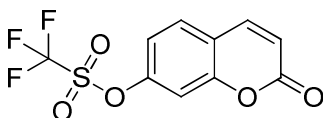
mp = 206 - 218°C (Lit.:<sup>[60]</sup> mp = 227 - 228°C)

**GC-MS** (MT\_50\_S):  $t_R$  = 6.78 min;  $m/z$  (%): 162 (70) [ $M^+$ ], 134 (100) [ $M^+$ -CO], 105 (24) [ $M^+$ -C<sub>2</sub>HO<sub>2</sub>]

**<sup>1</sup>H NMR** (300 MHz, DMSO):  $\delta$  = 10.57 (bs, 1H; OH), 7.92 (d, <sup>3</sup> $J_{HH}$  = 9.5 Hz, 1H; H<sup>Ar</sup>), 7.52 (d, <sup>3</sup> $J_{HH}$  = 8.5 Hz, 1H; H<sup>Ar</sup>), 6.78 (dd, <sup>3</sup> $J_{HH}$  = 8.5, 2.2 Hz, 1H; H<sup>Ar</sup>), 6.71 (d, <sup>3</sup> $J_{HH}$  = 1.9 Hz, 1H; H<sup>Ar</sup>), 6.19 (d, <sup>3</sup> $J_{HH}$  = 9.5 Hz, 1H; H<sup>ar</sup>) ppm.

**<sup>13</sup>C NMR** (76 MHz, DMSO):  $\delta$  = 161.2 (C<sub>q</sub>, C<sup>Ar</sup>), 160.41 (C<sub>q</sub>; C<sup>Ar</sup>), 155.5 (C<sub>q</sub>; C<sup>Ar</sup>), 144.49 (C<sup>Ar</sup>), 129.7 (C<sup>Ar</sup>), 113.1 (C<sup>Ar</sup>), 111.4 (C<sup>Ar</sup>), 111.3 (C<sub>q</sub>, C<sup>Ar</sup>), 102.12 (C<sup>Ar</sup>) ppm.

### 7.7.2 2-Oxo-2H-chromen-7-yl trifluoromethanesulfonate (2)



In an evacuated, flame-dried and N<sub>2</sub> flushed Schlenk flask 20 mL DCM and 740 μL (725 mg, 9.17 mmol, 1.44 eq) pyridine were added to 1.04 g (6.38 mmol, 1.00 eq) **1**. The orange suspension was cooled via an ice-bath to 0 °C. 1.35 mL (2.26 g, 8.02 mmol, 1.26 eq) trifluoromethanesulfonic anhydride were added dropwise via a septum within 10 min. The ice-bath was removed and the yellow-orange suspension was warmed up to RT. After another 4.75 h full conversion was detected via GC-MS and TLC. The reaction mixture was diluted with 100 mL DCM and quenched with 100 mL H<sub>2</sub>O. The layers were separated and the aqueous layer was extracted with DCM (2 x 50 mL). The combined organic layers were washed with brine (1 x 50 mL), dried over Na<sub>2</sub>SO<sub>4</sub> and filtered through a glass frit. The filter cake was washed with DCM (3 x 5 mL) and the filtrate was concentrated on a rotary evaporator. The resulting dark orange oil crystallized at RT to a light orange solid.

Yield: 1.70 g (5.76 mmol, 90 %) light orange solid

C<sub>10</sub>H<sub>5</sub>F<sub>3</sub>O<sub>5</sub>S [294.20 g/mol]

R<sub>f</sub> = 0.33 (Cyclohexane/EtOAc 2:1) (UV)

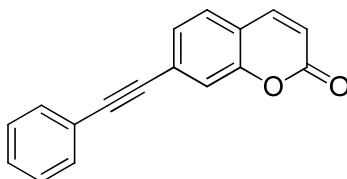
mp = 77 - 78°C (Lit.:<sup>[72]</sup> mp = 74-76°C)

**GC-MS** (MT\_50\_S): t<sub>R</sub> = 6.38 min; m/z (%): 294 (66) [M<sup>+</sup>], 161 (47) [M<sup>+</sup>-CF<sub>3</sub>O<sub>2</sub>S], 133 (100) [M<sup>+</sup>-C<sub>9</sub>H<sub>5</sub>O<sub>3</sub>], 69 (44) [M<sup>+</sup>-C<sub>9</sub>H<sub>5</sub>O<sub>5</sub>S]

**<sup>1</sup>H NMR** (300 MHz, CDCl<sub>3</sub>): δ = 7.72 (d, <sup>3</sup>J<sub>HH</sub> = 9.6 Hz, 1H; H<sup>Ar</sup>), 7.59 (d, <sup>3</sup>J<sub>HH</sub> = 8.6 Hz, 1H; H<sup>Ar</sup>), 7.28 (d, <sup>3</sup>J<sub>HH</sub> = 2.2 Hz, 1H; H<sup>Ar</sup>), 7.22 (dd, <sup>3</sup>J<sub>HH</sub> = 8.6, 2.3 Hz, 1H; H<sup>Ar</sup>), 6.49 (d, <sup>3</sup>J<sub>HH</sub> = 9.6 Hz, 1H; H<sup>Ar</sup>) ppm.

**<sup>13</sup>C NMR** (76 MHz, CDCl<sub>3</sub>): δ = 159.36 (C<sub>q</sub>, C<sup>Ar</sup>), 154.75 (C<sub>q</sub>, C<sup>Ar</sup>), 150.99 (C<sub>q</sub>, C<sup>Ar</sup>), 142.20 (C<sup>Ar</sup>), 129.56 (C<sup>Ar</sup>), 118.93 (C<sub>q</sub>, C<sup>Ar</sup>), 118.8 (d, <sup>1</sup>J<sub>CF</sub> = 321 Hz; CF<sub>3</sub>), 117.95 (C<sup>Ar</sup>), 117.88 (C<sup>Ar</sup>), 110.70 (C<sup>Ar</sup>).

### 7.7.3 7-(Phenylethynyl)-2*H*-chromen-2-one (3)



In a evacuated, flame dried and N<sub>2</sub> flushed Schlenk flask 5.0 mL (3.7 g, 36 mmol, 6.64 eq) Et<sub>3</sub>N and 630 μl (586 mg, 5.74 mmol, 1.06 eq) phenylacetylene were added to 10 mL dry DMF. The resulting mixture was degassed with a N<sub>2</sub>-ballon in an ultrasonic bath for 10 min. 38 mg (54 μmol, 0.01 eq) Pd(PPh<sub>3</sub>)<sub>2</sub>Cl<sub>2</sub> were added to the light yellow solution. To the resulting bright yellow solution 1.59 g (5.42 mmol, 1.00 eq) **2** were added. A darkish red solution resulted to which 10 mg (53 μmol, 0.0098 eq) CuI were added. After 115 h a brown solid had precipitated from the dark red solution. Full conversion was detected by TLC and GC-MS. A water bath was used to cool the reaction and 20 mL H<sub>2</sub>O and 5 mL 0.1M HCl were added to the reaction mixture. 20 mL DCM were added and the layers were separated. The aqueous phase was extracted with DCM (3 x 10 mL), the combined organic layers were washed with saturated NaHCO<sub>3</sub> solution (1 x 20 mL), dried over Na<sub>2</sub>SO<sub>4</sub> and filtrated through a glass frit. The filter cake was washed with DCM (3 x 5 mL). The filtrate was concentrated on a rotary evaporator and finally evaporated in the oil pump vacuum. 1.62 g brown solid was obtained as crude product, which was recrystallized from 74 mL EtOH. After the mother liquor was cooled down to RT the flask was put into a fridge at -23°C. After 5 d the overlapping liquor was decantated, the crystals were washed with cold EtOH (2 x 1.5 mL) and dried in vacuum. 857 mg of a chocolate brown solid were isolated. The mother liquor was evaporated and recrystallized a second time to give another 250 mg of product.

Yield: 1.11 g (4.50 mmol, 83%) chocolate brown solid

C<sub>17</sub>H<sub>10</sub>O<sub>2</sub> [246.27 g/mol]

R<sub>f</sub> = 0.48 (Cyclohexane/EtOAc 2:1) (UV/CAM)

mp = 175 - 176°C

---

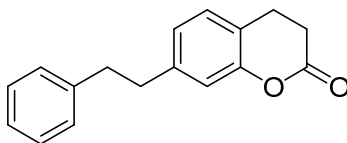
**GC-MS** (MT\_50\_S):  $t_R = 8.71$  min;  $m/z$  (%): 246 (100) [ $M^+$ ], 218 (93) [ $M^+ - CO$ ], 189 (61) [ $M^+ - C_2HO_2$ ]

**$^1H$  NMR** (300 MHz,  $CDCl_3$ ):  $\delta = 7.69$  (d,  $^3J_{HH} = 9.5$  Hz, 1H;  $H^{Ar}$ ), 7.59 – 7.52 (m, 2H;  $H^{Ar}$ ), 7.48 – 7.30 (m, 6H;  $H^{Ar}$ ), 6.42 (d,  $^3J_{HH} = 9.5$  Hz, 1H;  $H^{Ar}$ ) ppm.

**$^{13}C$  NMR** (76 MHz,  $CDCl_3$ ):  $\delta = 160.4$  ( $C_q$ ;  $C^{Ar}$ ), 153.9 ( $C_q$ ;  $C^{Ar}$ ), 142.8 ( $C^{Ar}$ ), 131.8 ( $C^{Ar}$ ), 129.0 ( $C^{Ar}$ ), 128.5 ( $C^{Ar}$ ), 127.8 ( $C^{Ar}$ ), 127.7 ( $C^{Ar}$ ), 127.0 ( $C_q$ ;  $C^{Ar}$ ), 122.4 ( $C_q$ ;  $C^{Ar}$ ), 119.6 ( $C^{Ar}$ ), 118.7 ( $C_q$ ;  $C^{Ar}$ ), 116.9 ( $C^{Ar}$ ), 93.0 ( $C_q$ ), 88.0 ( $C_q$ ) ppm.

**HRMS** (EI): calculated for [ $M^+$ ]: 246.0681; found: 246.0683

### 7.7.4 7-Phenethylchroman-2-one (4)



In a 50 mL round-bottom flask, equipped with a Schlenk adapter, 4.86 g (19.7 mmol, 1.00 eq) **3** were dissolved in 50 mL THF. To the dark brownish solution 3.85 g (987  $\mu$ mol, 0.05 eq) 5% Pt/C were added. A reflux condenser equipped with a H<sub>2</sub>-balloon was put on top and the apparatus was evacuated (2x) and flushed with H<sub>2</sub> (2x). Under vigorous stirring the reaction mixture was heated via an oil bath to 60 °C. After 23 h the H<sub>2</sub>-balloon was refilled. After additional 22 h full conversion was detected by GC-MS and the reaction mixture was cooled down to ambient temperature. The reaction mixture was filtrated through celite under inert conditions and the filter cake was washed with THF (4 x 10 mL). The filtrate was concentrated on a rotary evaporator and the resulted red-brown oil was further dried in vacuum.

Yield: 4.67 g (18.5 mmol, 94 %) red-brown, fruity smelling oil

C<sub>17</sub>H<sub>16</sub>O<sub>2</sub> [252.31 g/mol]

R<sub>f</sub> = 0.65 (cyclohexane/EtOAc 2:1) (UV/CAM)

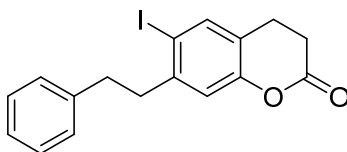
**GC-MS** (MT\_50\_S): t<sub>R</sub> = 8.01 min; m/z (%): 252 (45) [M<sup>+</sup>], 161 (93) [M<sup>+</sup>-C<sub>7</sub>H<sub>7</sub>], 91 (100) [M<sup>+</sup>-C<sub>10</sub>H<sub>9</sub>O<sub>2</sub>]

**<sup>1</sup>H NMR** (300 MHz, CDCl<sub>3</sub>):  $\delta$  = 7.26 - 7.21 (m, 2H), 7.19 – 7.09 (m, 3H), 7.04 (d, <sup>3</sup>J<sub>HH</sub> = 7.5 Hz, 2H), 6.88 – 6.81 (m, 2H), 2.92 (t, <sup>3</sup>J<sub>HH</sub> = 7.2 Hz, 2H), 2.86 (s, 4H), 2.72 (t, <sup>3</sup>J<sub>HH</sub> = 7.2 Hz, 2H) ppm.

**<sup>13</sup>C NMR** (76 MHz, CDCl<sub>3</sub>):  $\delta$  = 168.9 (C<sub>q</sub>), 152.1 (C<sub>q</sub>; C<sup>Ar</sup>), 142.6 (C<sub>q</sub>; C<sup>Ar</sup>), 141.4 (C<sub>q</sub>; C<sup>Ar</sup>), 128.53 (C<sup>Ar</sup>), 128.52 (C<sup>Ar</sup>), 127.9 (C<sup>Ar</sup>), 126.2 (C<sup>Ar</sup>), 124.7 (C<sup>Ar</sup>), 120.1 (C<sub>q</sub>; C<sup>Ar</sup>), 116.9 (C<sup>Ar</sup>), 37.7 (CH<sub>2</sub>), 37.4 (CH<sub>2</sub>), 29.5 (CH<sub>2</sub>), 23.5 (CH<sub>2</sub>) ppm.

**HRMS** (EI): calculated for [M<sup>+</sup>]: 252.1150; found: 252.1154

### 7.7.5 6-Iodo-7-phenethylchroman-2-one (**5**)



An evacuated flame dried and Ar flushed 250 mL 3-neck-flask, equipped with a 50 mL dropping funnel and a gas-inlet, was charged with 4.49 g (17.8 mmol, 1.00 eq) **4** and additionally evacuated (1x) and Ar flushed (1x). **4** was dissolved in 20 mL absolute DCM resulting in an orange-brown solution. 20 mL (3.25 g, 20 mmol, 1.12 eq) of a freshly prepared 1.0 M ICl-solution in DCM were filled into the dropping funnel. The ICl-solution was added dropwise within 10 min to the reaction vessel resulting in a deep red-brownish solution. After 24 h no further conversion (94% conversion) of **4** was detected and additional 300 mg (1.85 mmol, 0.090 eq) ICl were added to the reaction mixture. After additional 16.5 h it stopped at 96 % conversion, therefore another 320 mg (1.97 mmol, 0.099 eq) ICl were added to the reaction mixture. After additional 2.5 h full conversion was detected by GC-MS. The reaction mixture was diluted with 60 mL DCM and quenched with 100 mL 0.1 M Na<sub>2</sub>S<sub>2</sub>O<sub>3</sub> solution. The brownish mixture was transferred to a separating funnel and the layers were separated. The organic layer was washed with 0.1 M Na<sub>2</sub>S<sub>2</sub>O<sub>3</sub> solution (1 x 50 mL) and the combined aqueous layers were extracted with DCM (1 x 20 mL then 4 x 10 mL). The combined organic layers were washed with brine (1 x 50 mL), 0.1 M Na<sub>2</sub>S<sub>2</sub>O<sub>3</sub> solution (1 x 20 mL), dried over Na<sub>2</sub>SO<sub>4</sub> and then filtered through a glass frit. The filter cake was washed with DCM (4 x 5mL) and the filtrate was concentrated on a rotary evaporator. 6.59 g of a dark red-brownish oil was obtained as a crude product. The crude product was purified via flash chromatography (1100 mL SiO<sub>2</sub>; 25 x 8 cm, solvent mixture: cyclohexane/EtOAc 10:1, R<sub>f</sub> = 0.30; 250 mL fractions, pooled fractions: 10 and 11, 12 - 14, 15 and 16).

Yield: Fractions 12-14: 3.48 g (9.20 mmol, 52%) yellowish solid

C<sub>17</sub>H<sub>15</sub>O<sub>2</sub>I [378.21 g/mol]

R<sub>f</sub> = 0.72 (Cyclohexane/EtOAc 2:1) (UV/CAM)

mp = 64 - 71°C

---

**GC-MS** (MT\_50\_S):  $t_R = 9.31$  min);  $m/z$  (%): 378 (21) [ $M^+$ ], 287 (46) [ $M^+ - C_7H_7$ ], 251 (15) [ $M^+ - I$ ], 91 (100) [ $M^+ - C_{10}H_8O_2I$ ]

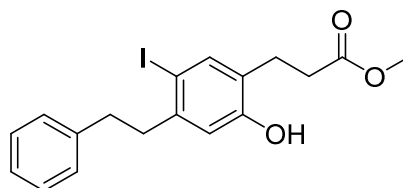
**$^1H$  NMR** (300 MHz,  $CDCl_3$ ):  $\delta = 7.58$  (s, 1H;  $H^{Ar}$ ), 7.24 – 7.13 (m, 5H;  $H^{Ar}$ ), 6.81 (s, 1H;  $H^{Ar}$ ), 2.95 – 2.77 (m, 6H;  $CH_2$ ), 2.69 (t,  $^3J_{HH} = 7.5$  Hz, 2H;  $CH_2$ ) ppm.

**$^{13}C$  NMR** (76 MHz,  $CDCl_3$ ):  $\delta = 168.0$  ( $C_q$ ), 152.4 ( $C_q$ ;  $C^{Ar}$ ), 144.7 ( $C_q$ ;  $C^{Ar}$ ), 140.9 ( $C_q$ ;  $C^{Ar}$ ), 138.4 ( $C^{Ar}$ ), 128.6 ( $C^{Ar}$ ), 128.6 ( $C^{Ar}$ ), 126.4 ( $C^{Ar}$ ), 122.7 ( $C_q$ ;  $C^{Ar}$ ), 117.9 ( $C^{Ar}$ ), 93.8 ( $C_q$ ;  $C^{Ar}$ ), 42.7 ( $CH_2$ ), 36.4 ( $CH_2$ ), 29.1 ( $CH_2$ ), 23.0 ( $CH_2$ ) ppm.

**HRMS** (EI): calculated for [ $M^+$ ]: 378.0117; found: 378.0127



### 7.7.6 Methyl 3-(2-hydroxy-5-iodo-4-phenethylphenyl)propanoate (6)



In an evacuated, flame dried and Ar flushed 10 mL two-neck flask, equipped with a gas inlet, 2 mL absolute MeOH were cooled via an ice bath to 0 °C. To the MeOH 33 mg (1.44 mmol, 26 eq) small Na pieces were added in small portions. Gas evolution was observed. After all Na had been consumed and no further gas evolution was detectable the whole NaOMe solution was added to 21 mg (56  $\mu$ mol, 1.0 eq) **5** in a 10 mL Schlenk flask. After 40 min full conversion was detected by TLC. The orange solution was diluted with 5 mL DCM and to the solution 2 mL H<sub>2</sub>O as well as 2 mL 2 M HCl were added. The mixture was transferred to a separating funnel. The layers were separated and the aqueous layer was extracted with DCM (2 x 5 mL). The combined organic layers were washed with saturated NaHCO<sub>3</sub> solution (1 x 5 mL), dried over MgSO<sub>4</sub> and filtrated through a glass frit. The filter cake was washed with DCM (2x 2 mL) and the filtrate was concentrated on a rotary evaporator. The orange oil was dried in vacuum.

Yield: 15 mg (37  $\mu$ mol, 65%) orange oil

C<sub>18</sub>H<sub>19</sub>IO<sub>3</sub> [410.25 g/mol]

R<sub>f</sub> = 0.60 (cyclohexane/EtOAc 2:1) (UV/CAM)

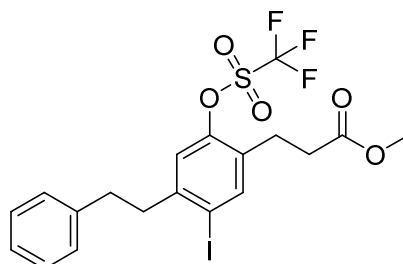
GC-MS (MT\_50\_S): lactonizes to **5** in the inlet.

<sup>1</sup>H NMR (300 MHz, CDCl<sub>3</sub>):  $\delta$  = 7.44 (s, 1H; OH), 7.29 (s, 1H; H<sup>Ar</sup>), 7.25 – 7.09 (m, 5H; H<sup>Ar</sup>), 6.72 (s, 1H; H<sup>Ar</sup>), 3.63 (s, 3H; CH<sub>3</sub>), 2.88 – 2.69 (m, 6H; CH<sub>2</sub>), 2.63 (t, <sup>3</sup>J<sub>HH</sub> = 5.9 Hz, 2H; CH<sub>2</sub>) ppm.

<sup>13</sup>C NMR (76 MHz, CDCl<sub>3</sub>):  $\delta$  = 176.3 (C<sub>q</sub>), 155.0 (C<sub>q</sub>; C<sup>Ar</sup>), 144.2 (C<sub>q</sub>; C<sup>Ar</sup>), 141.5 (C<sub>q</sub>; C<sup>Ar</sup>), 140.8 (C<sup>Ar</sup>), 128.6 (C<sup>Ar</sup>), 128.6 (C<sup>Ar</sup>), 127.9 (C<sup>Ar</sup>), 126.2 (C<sup>Ar</sup>), 118.7 (C<sup>Ar</sup>), 89.1 (C<sub>q</sub>; C<sup>Ar</sup>), 52.6 (CH<sub>3</sub>), 42.7 (CH<sub>2</sub>), 36.7 (CH<sub>2</sub>), 35.1 (CH<sub>2</sub>), 23.9 (CH<sub>2</sub>) ppm.

HRMS (EI): calculated for [M<sup>+</sup>]: 410.0379; found: 410.0378

### 7.7.7 Methyl-3-(5-iodo-4-phenethyl-2-(((trifluoromethyl)sulfonyl)oxy)phenyl)propanoate (7)



In an evacuated, flame dried and Ar flushed 100 mL Schlenk flask a solution of 2.32 g (5.65 mmol, 1.00 eq) **6** in 2 mL DCM was diluted with 20 mL absolute DCM. 1.4 mL (1.37 g, 17.3 mmol, 3.07 eq) pyridine were added to the light orange solution and the reaction mixture was cooled down via an ice bath to 0 °C. 1.45 mL (2.43 g, 8.62 mmol, 1.53 eq) Tf<sub>2</sub>O were added dropwise to the light orange solution within 10 min. During the Tf<sub>2</sub>O addition an orange solid formed, which dissolved after several seconds. After additional 10 min the ice bath was removed and the reaction mixture was allowed to warm up to RT. After another 45 min full conversion was detected by GC-MS and TLC. A water bath was put under the vessel for cooling purpose. The reaction mixture was diluted with 20 mL DCM and quenched slowly with 20 mL H<sub>2</sub>O. A solid precipitated, but dissolved after several seconds under vigorous stirring. The mixture was transferred to a separating funnel, the layers were separated and the aqueous layer was extracted with DCM (4 x 10 mL). The combined organic layers were washed with brine (1 x 20 mL), dried over MgSO<sub>4</sub>, and filtered through a glass frit. The filter cake was washed with DCM (3 x 2 mL) and the filtrate was concentrated on a rotary evaporator. The orange oil was further dried in vacuum. 3.04 g of an orange oil was obtained as a crude product. The crude product was adsorbed on 4.50 g Celite<sup>®</sup> and further purified via flash chromatography (600 mL SiO<sub>2</sub>, 20 x 6 cm, solvent mixture: cyclohexane/EtOAc 20:1, R<sub>f</sub> = 0.26; 150 mL fractions, pooled fractions: 6 - 9)

Yield: 2.70 g (4.98 mmol, 88%) light yellowish solid

C<sub>19</sub>H<sub>18</sub>F<sub>3</sub>IO<sub>5</sub>S [542.31 g/mol]

R<sub>f</sub> = 0.80 (cyclohexane/EtOAc 2:1) (UV/CAM)

mp = 34 - 36 °C

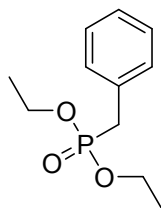
**GC-MS** (MT\_50\_S):  $t_R = 8.66$  min;  $m/z$  (%): 542 (3) [ $M^+$ ], 451 (6) [ $M^+ - C_7H_7$ ], 282 (13) [ $M^+ - C_8H_7F_3$ ], 91 (100) [ $M^+ - C_{12}H_{11}F_3IO_5S$ ].

**$^1H$  NMR** (300 MHz,  $CDCl_3$ ):  $\delta = 7.74$  (s, 1H;  $H^{Ar}$ ), 7.25 – 7.10 (m, 5H;  $H^{Ar}$ ), 6.94 (s, 1H;  $H^{Ar}$ ), 3.63 (s, 3H;  $CH_3$ ), 2.97 – 2.86 (m, 4H;  $CH_2$ ), 2.84 – 2.74 (m, 2H;  $CH_2$ ), 2.57 (t,  $^3J_{HH} = 7.6$  Hz, 2H;  $CH_2$ ) ppm.

**$^{13}C$  NMR** (76 MHz,  $CDCl_3$ ):  $\delta = 172.5$  ( $C_q$ ), 148.0 ( $C_q$ ;  $C^{Ar}$ ), 145.2 ( $C_q$ ;  $C^{Ar}$ ), 141.7 ( $C^{Ar}$ ), 140.5 ( $C_q$ ;  $C^{Ar}$ ), 132.9 ( $C_q$ ;  $C^{Ar}$ ), 128.7 ( $C^{Ar}$ ), 128.6 ( $C^{Ar}$ ), 126.5 ( $C^{Ar}$ ), 122.2 ( $C^{Ar}$ ), 118.6 (d,  $^1J_{CF} = 320$  Hz;  $CF_3$ ), 99.7 ( $C_q$ ;  $C^{Ar}$ ), 52.0 ( $CH_3$ ), 42.6 ( $CH_2$ ), 36.1 ( $CH_2$ ), 33.8 ( $CH_2$ ), 24.6 ( $CH_2$ ) ppm.

**HRMS** (EI): calculated for [ $M^+$ ]: 541.9872; found: 541.9875

### 7.7.8 Diethyl benzylphosphonate (8)



In a 100 mL round-bottom flask 6.2 mL (6.8 g, 54 mmol, 1.00 eq) benzyl chloride were added to 9.5 mL (9.1 g, 55 mmol, 1.02 eq) triethyl phosphite. An air cooler with gas exhaust was attached to the flask and the colourless reaction mixture was heated to 160°C via an oil bath. After 15 h 99% conversion was detected by GC-MS and the reaction mixture was allowed to cool down to ambient temperature. The reaction mixture was dried in vacuum.

Yield: 11.5 g (50.4 mmol, 93%) colourless oil

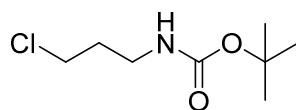
$C_{11}H_{17}O_3P$  [228.23 g/mol]

**GC-MS** (MT\_50\_35S):  $t_R = 5.91$  min;  $m/z$  (%): 228 (19) [ $M^+$ ], 91 (100) [ $M^+ - C_4H_{10}O_3P$ ]

**$^1H$  NMR** (300 MHz,  $CDCl_3$ ):  $\delta = 7.34 - 7.25$  (m, 5H;  $H^{Ar}$ ), 4.08 – 3.91 (m, 4H;  $CH_2$ ), 3.15 (d,  $^2J_{HP} = 21.6$  Hz, 2H), 1.24 (t,  $^3J_{HH} = 7.0$  Hz, 6H) ppm.

**$^{13}C$  NMR** (76 MHz,  $CDCl_3$ ):  $\delta = 131.8$  (d,  $^2J_{CP} = 9.2$  Hz;  $C_q$ ,  $C^{Ar}$ ), 129.9 (d,  $^3J_{CP} = 6.6$  Hz;  $C^{Ar}$ ), 128.6 (d,  $^4J_{CP} = 3.0$  Hz;  $C^{Ar}$ ), 127.0 (d,  $^5J_{CP} = 3.6$  Hz;  $C^{Ar}$ ), 62.2 (d,  $^2J_{CP} = 6.8$  Hz;  $CH_2$ ), 33.9 (d,  $^1J_{CP} = 138.1$  Hz;  $CH_2$ ), 16.5 (d,  $^3J_{CP} = 6.0$  Hz;  $CH_3$ ) ppm.

### 7.7.9 *tert*-Butyl (3-chloropropyl)carbamate (9)



In a 100 mL round-bottom flask 5.00 g (38.5 mmol, 1.05 eq) 3-chloropropylamine hydrochloride were dissolved in 15 mL DCM. A dropping funnel was attached to the reaction vessel and 6.0 mL (4.38 g, 43.3 mmol, 1.18 eq) Et<sub>3</sub>N were dropped to the light yellowish suspension within 5 min. The finely-granulated suspension was cooled via an ice-bath. 7.97 g (36.5 mmol, 1.00 eq) Di-*tert*-butyl dicarbonate (Boc<sub>2</sub>O) were dissolved in 50 mL DCM in the dropping funnel. A drying tube was attached to the top of the dropping funnel and the Boc<sub>2</sub>O solution was dropped to the reaction mixture within 17 min. After 10 min the skin coloured suspension was removed from the ice bath and the reaction mixture was allowed to warm up to RT. After 17 h full conversion was detected by TLC. 20 mL H<sub>2</sub>O were added dropwise to the reaction mixture. The solid had dissolved and the 2-phase-system was transferred to a separating funnel. The layers were separated and the aqueous layer was extracted with DCM (3 x 5 mL). The combined organic layers were washed with saturated NH<sub>4</sub>Cl solution, dried over Na<sub>2</sub>SO<sub>4</sub> and filtered through a glass frit. The filter cake was washed with DCM (3 x 2 mL) and the filtrate was concentrated on a rotary evaporator. The yellowish oil was dried in vacuum and was used without further purification in the next step.

Yield: 6.97 g (36.0 mmol, 99%) yellowish oil

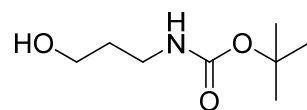
C<sub>8</sub>H<sub>16</sub>ClNO<sub>2</sub> [193.67 g/mol]

R<sub>f</sub> = 0.67 (cyclohexane/EtOAc 2:1) (ninhydrin)

**GC-MS** (MT\_50\_S): t<sub>R</sub> = 5.09 min; m/z (%): 138 (36) [M<sup>+</sup>-C<sub>4</sub>H<sub>7</sub>], 57 (100) [M<sup>+</sup>-C<sub>4</sub>H<sub>7</sub>ClNO<sub>2</sub>]

**<sup>1</sup>H NMR** (300 MHz, CDCl<sub>3</sub>): δ = 4.66 (bs, 1H; NH), 3.58 (t, <sup>3</sup>J<sub>HH</sub> = 6.4 Hz, 2H; CH<sub>2</sub>), 3.27 (bs, 2H; CH<sub>2</sub>), 1.96 (p, <sup>3</sup>J<sub>HH</sub> = 6.4 Hz, 2H; CH<sub>2</sub>), 1.43 (s, 9H; CH<sub>3</sub>) ppm.

**<sup>13</sup>C NMR** (76 MHz, CDCl<sub>3</sub>): δ = 156.10 (C<sub>q</sub>), 45.92 (C<sub>q</sub>), 42.48 (CH<sub>2</sub>), 38.09 (CH<sub>2</sub>), 32.75 (CH<sub>2</sub>), 28.52 (CH<sub>3</sub>) ppm.

**7.7.10 tert-Butyl (3-hydroxypropyl)carbamate (10)**

In a 500 mL round-bottom flask 10.0 g (133 mmol, 1.00 eq) 3-aminopropan-1-ol were dissolved in 50 mL DCM. The colourless solution was cooled to 0 °C via an ice bath. A dropping funnel was attached to the reaction vessel and 29.02 g (133 mmol, 1.00 eq) Boc<sub>2</sub>O were dissolved in 30 mL DCM in the dropping funnel. A drying tube was attached on top of the dropping funnel. The Boc<sub>2</sub>O solution was added dropwise within 30 min. A colourless solid had precipitated during the Boc<sub>2</sub>O addition. After additional 15 min the ice bath was removed and the reaction mixture was allowed to warm up to RT. After additional 15.75 h full conversion was detected by TLC. The solvent was evaporated on a rotary evaporator and dried afterwards in vacuum.

Yield: 22.4 g (128 mmol, 96%) light yellowish viscous oil

C<sub>8</sub>H<sub>17</sub>NO<sub>3</sub> [175.23 g/mol]

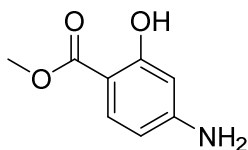
R<sub>f</sub> = 0.18 (cyclohexane/EtOAc 2:1) (ninhydrin)

**GC-MS** (MT\_50\_S): t<sub>R</sub> = 5.12 min; m/z (%): 119 (12) [M<sup>+</sup>-C<sub>4</sub>H<sub>8</sub>], 57 (100) [M<sup>+</sup>-C<sub>4</sub>H<sub>8</sub>NO<sub>3</sub>]

**<sup>1</sup>H NMR** (300 MHz, CDCl<sub>3</sub>): δ = 4.81 (bs, 1H; NH), 3.65 (t, <sup>3</sup>J<sub>HH</sub> = 5.5 Hz, 2H; CH<sub>2</sub>), 3.27 (q, <sup>3</sup>J<sub>HH</sub> = 5.9 Hz, 2H; CH<sub>2</sub>), 2.84 (bs, 1H; OH), 1.74 – 1.59 (m, 2H; CH<sub>2</sub>), 1.43 (s, 9H; CH<sub>3</sub>) ppm.

**<sup>13</sup>C NMR** (76 MHz, CDCl<sub>3</sub>) δ = 157.3 (C<sub>q</sub>), 79.8 (C<sub>q</sub>), 59.4 (CH<sub>2</sub>), 37.0 (CH<sub>2</sub>), 33.0 (CH<sub>2</sub>), 28.5 (CH<sub>3</sub>) ppm.

### 7.7.11 Methyl 4-amino-2-hydroxybenzoate (11)



In a 250 mL two-neck flask, equipped with an air cooler with a drying tube, 75 mL MeOH were added to 9.99 g (65.2 mmol, 1.00 eq) 4-aminosalicylic acid. To the skin coloured suspension 20 mL (36.8 g, 375 mmol, 5.75 eq) conc. H<sub>2</sub>SO<sub>4</sub> were added dropwise within 40 min. A colourless solid precipitated in an exothermic process. The reaction mixture was heated via an oil bath to light reflux. After several min at reflux all of the solid had dissolved resulting in a light orange solution. After 206 h almost full conversion was detected by TLC. The oil bath was removed and the orange-brownish solution was allowed to cool down to ambient temperature. The reaction mixture was poured on 150 mL H<sub>2</sub>O and a skin-coloured solid precipitated immediately. The mixture was cooled to 0 °C via an ice bath and then brought to a pH of 8 with 3 M NaOH. The precipitate was collected by filtration, washed with water (3 x 5 mL) and dried in vacuum.

Yield: 8.54 g (51.1 mmol, 78%) skin coloured solid

C<sub>8</sub>H<sub>9</sub>NO<sub>3</sub> [167.16 g/mol]

R<sub>f</sub> = 0.92 (DCM/MeOH/Et<sub>3</sub>N 20:1:2) (UV/ninhydrin)

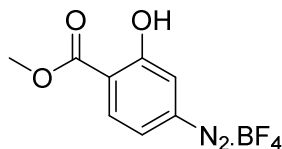
mp = 112-123°C (Lit.:<sup>[92]</sup> mp = 120 - 121°C

**GC-MS** (MT\_50\_S): t<sub>R</sub> = 6.10 min; m/z (%): 167 (86) [M<sup>+</sup>], 135 (100) [M<sup>+</sup>-H<sub>2</sub>NO], 107 (80) [M<sup>+</sup>-C<sub>2</sub>H<sub>4</sub>O<sub>2</sub>]

**<sup>1</sup>H NMR** (300 MHz, DMSO): δ = 10.77 (s, 1H; OH), 7.44 (d, <sup>3</sup>J<sub>HH</sub> = 8.7 Hz, 1H; H<sup>Ar</sup>), 6.16 – 6.08 (m, 3H; NH<sub>2</sub>; H<sup>Ar</sup>), 6.00 (d, <sup>3</sup>J<sub>HH</sub> = 1.8 Hz, 1H; H<sup>Ar</sup>), 3.78 (s, 3H; CH<sub>3</sub>) ppm.

**<sup>13</sup>C NMR** (76 MHz, DMSO): δ = 169.90 (C<sub>q</sub>), 162.84 (C<sub>q</sub>; C<sup>Ar</sup>), 156.02 (C<sub>q</sub>; C<sup>Ar</sup>), 131.01 (C<sup>Ar</sup>), 106.61 (C<sup>Ar</sup>), 99.54 (C<sub>q</sub>; C<sup>Ar</sup>), 98.54 (C<sup>Ar</sup>), 51.50 (CH<sub>3</sub>) ppm.

### 7.7.12 3-Hydroxy-4-(methoxycarbonyl)benzenediazoniumtetrafluoroborate (12)



In an evacuated, flame dried and Ar flushed 25 mL round-bottom flask, equipped with a Schlenk adapter, 1.01 g (6.01 mmol, 1.00 eq) **11** were dissolved in 5 mL absolute THF. To the orange solution 1 mL (1.12 g, 7.98 mmol, 1.31 eq)  $\text{BF}_3 \cdot \text{OEt}_2$  were added dropwise within 2 min. The reaction was exothermic and a skin coloured solid precipitated. After 1 h the reaction mixture was cooled down with an acetone/ $\text{CO}_2(\text{s})$  mixture to  $-20^\circ\text{C}$ . To the skin coloured suspension 950  $\mu\text{l}$  (824 mg, 7.99 mmol, 1.33 eq) *tert*-butyl nitrite were added dropwise within 2 min. More of an orange solid precipitated. After 20 min the cooling bath was removed and the reaction mixture was allowed to warm up to RT. After another 2 h 5 mL  $\text{Et}_2\text{O}$  were added to the reaction mixture. As no more solid had precipitated the precipitate was collected by filtration, washed with  $\text{Et}_2\text{O}$  (4 x 5 mL) and dried in vacuum.

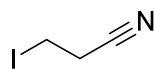
Yield: 1.37 g (5.15 mmol, 86%) light orange solid

$\text{C}_8\text{H}_7\text{BF}_4\text{N}_2\text{O}_3$  [265.96 g/mol]

mp =  $76 - 85^\circ\text{C}$  (decomposition) (Lit.:<sup>[93]</sup>  $93^\circ\text{C}$  (decomposition))



### 7.7.13 3-Iodopropanenitrile (13)



In a flame dried 250 mL round-bottom flask, equipped with an air cooler and a drying tube, 3.2 ml (5.17 g, 38.6 mmol, 1.00 eq) 3-bromopropanenitrile were dissolved in 50 mL distilled acetone. 11.3 g (75.5 mmol, 1.95 eq) NaI were added to the light yellowish solution. The yellowish suspension was covered with aluminium foil and it was heated in an oil bath to light reflux. After 89 h a great quantity of a white solid had precipitated. The oil bath was removed and the orange suspension was allowed to cool down to RT. The reaction mixture was concentrated on a rotary evaporator. 30 mL H<sub>2</sub>O and 20 mL EtOAc were added. The solid dissolved and the mixture was transferred to a separating funnel. The layers were separated and the aqueous layer was extracted with EtOAc (3 x 10 mL). The combined organic layers were washed with 0.1 M Na<sub>2</sub>S<sub>2</sub>O<sub>3</sub> solution (1 x 10 mL), saturated NaHCO<sub>3</sub> solution (1 x 10 mL), dried over Na<sub>2</sub>SO<sub>4</sub> and filtered through a glass frit. The filter cake was washed with EtOAc (1 x 5 mL) and the filtrate was concentrated on a rotary evaporator. The light yellowish oil was dried in vacuum.

Yield: 6.65 g (36.7 mmol, 95%) light yellowish oil

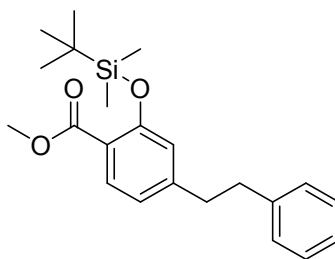
C<sub>3</sub>H<sub>4</sub>IN [180.98 g/mol]

R<sub>f</sub> = 0.64 (cyclohexane/EtOAc 2:1) (UV)

**GC-MS** (MT\_50\_35S): t<sub>R</sub> = 3.82 min; m/z (%): 181 (100) [M<sup>+</sup>], 127 (49) [M<sup>+</sup>-C<sub>3</sub>H<sub>4</sub>N], 54 (39) [M<sup>+</sup>-I]

**<sup>1</sup>H NMR** (300 MHz, CDCl<sub>3</sub>): δ = 3.28 (t, <sup>3</sup>J<sub>HH</sub> = 7.0 Hz, 2H), 3.01 (t, <sup>3</sup>J<sub>HH</sub> = 7.1 Hz, 2H) ppm.

**<sup>13</sup>C NMR** (76 MHz, CDCl<sub>3</sub>) δ = 118.3 (C<sub>q</sub>; CN), 22.7 (CH<sub>2</sub>), -6.8 (CH<sub>2</sub>) ppm.

**7.7.14 Methyl 2-((tert-butyldimethylsilyloxy)-4-phenethylbenzoate (14)**

In an evacuated, flame dried and Ar flushed 20 mL Schlenk flask 87 mg (339  $\mu\text{mol}$ , 1.00 eq) methyl 2-hydroxy-4-phenethylbenzoate, 127 mg (1.87 mmol, 5.50 eq) imidazole and 1 mg (8  $\mu\text{mol}$ , 0.02 eq) 4-(dimethylamino)pyridine were dissolved in 1 mL DMF. The brown-orange solution was cooled to 0  $^{\circ}\text{C}$  via an ice bath and 200 mg (1.33 mmol, 3.91 eq) *tert*-butyldimethylsilyl chloride were added to the reaction mixture. After 50 min the ice bath was removed and the brown-orange solution was allowed to warm up to RT. After an additional hour full conversion was detected by GC-MS. 5 mL saturated  $\text{NaHCO}_3$  solution were added to the reaction mixture. Gas evolution was detected and a colourless solid precipitated. After the gas evolution had finished, 5 mL  $\text{Et}_2\text{O}$  were added and the mixture was transferred to a separating funnel. The layers were separated and the aqueous layer was extracted with  $\text{Et}_2\text{O}$  (3 x 3 mL). The combined organic layers were washed with brine (1 x 5 mL), dried over  $\text{Na}_2\text{SO}_4$  and filtered through a glass frit. The filter cake was washed with  $\text{Et}_2\text{O}$  (2 x 2 mL), the filtrate was concentrated on a rotary evaporator and dried in vacuum. 115 mg of a colourless oil were obtained as crude product. The crude product was purified via flash chromatography (11.8 g  $\text{SiO}_2$ ; 20 x 4 cm, solvent mixture: cyclohexane/ $\text{EtOAc}$  50:1,  $R_f = 0.18$ ; 5 mL fractions, pooled fractions: 11 - 14, 15 and 16).

Yield: 84 mg (fractions 11-14, 227  $\mu\text{mol}$ , 67%) colourless oil, 11 mg (fractions 15 and 16, 30  $\mu\text{mol}$ , 9%) colourless oil

$\text{C}_{22}\text{H}_{30}\text{O}_3\text{Si}$  [370.56 g/mol]

$R_f = 0.85$  (cyclohexane/ $\text{EtOAc}$  2:1) (UV/CAM)

---

**GC-MS** (MT\_50\_S):  $t_R = 8.31$  min.;  $m/z$  (%): 313 (100) [ $M^+$ -C<sub>4</sub>H<sub>9</sub>], 222 (25) [ $M^+$ -C<sub>11</sub>H<sub>18</sub>], 115 (1) [ $M^+$ -C<sub>16</sub>H<sub>15</sub>O<sub>3</sub>], 91 (19) [ $M^+$ -C<sub>15</sub>H<sub>23</sub>O<sub>3</sub>Si]

**<sup>1</sup>H NMR** (300 MHz, CDCl<sub>3</sub>)  $\delta$  7.66 (d,  $^3J_{HH} = 8.0$  Hz, 1H; H<sub>Ar</sub>), 7.25 – 7.06 (m, 5H; H<sub>Ar</sub>), 6.77 (dd,  $^3J_{HH} = 8.0, 1.2$  Hz, 1H; H<sub>Ar</sub>), 6.59 (d,  $^3J_{HH} = 1.1$  Hz, 1H; H<sub>Ar</sub>), 3.82 (s, 3H; CH<sub>3</sub>), 2.87 (s, 4H; CH<sub>2</sub>), 0.96 (s, 9H; CH<sub>3</sub>), 0.12 (s, 6H; CH<sub>3</sub>) ppm.

**<sup>13</sup>C NMR** (76 MHz, CDCl<sub>3</sub>):  $\delta = 167.35$  (C<sub>q</sub>), 155.36 (C<sub>q</sub>; C<sup>Ar</sup>), 147.74 (C<sub>q</sub>; C<sup>Ar</sup>), 141.22 (C<sub>q</sub>; C<sup>Ar</sup>), 131.88 (C<sup>Ar</sup>), 128.6 (C<sup>Ar</sup>), 128.5 (C<sup>Ar</sup>), 126.2 (C<sup>Ar</sup>), 121.5 (C<sup>Ar</sup>), 121.5 (C<sup>Ar</sup>), 120.4 (C<sub>q</sub>; C<sup>Ar</sup>), 51.8 (CH<sub>3</sub>), 37.7 (CH<sub>2</sub>), 37.4 (CH<sub>2</sub>), 25.8 (CH<sub>3</sub>), 18.4 (C<sub>q</sub>), -4.2 (CH<sub>3</sub>) ppm.

**HRMS** (EI): calculated for [ $M^+$ ]: 369.1886; found: 369.1871 very low signal  
calculated for [ $M^+$ -CH<sub>3</sub>]: 355.1729; found: 355.1740

---

## 8 References

- [1] B. Alberts, A. Johnson, J. Lewis, M. Raff, K. Roberts, P. Walter, *The molecular Biology of the Cell*, 4<sup>th</sup> ed.; Garland Science, New York, **2002**.
- [2] J. Nielsen, *Curr. Opin. Chem. Biol.* **2002**, *6*, 297-305.
- [3] T. Berg, *Angew. Chem. Int. Ed.* **2003**, *42*, 2462-2481.
- [4] M. M. K. Shahzad, L. S. Mangala, H. D. Han, C. Lu, J. Bottsford-Miller, M. Nishimura, E. M. Mora, J.-W. Lee, R. L. Stone, C. V. Pecot, D. Thanappapasr, J.-W. Roh, P. Gaur, M. P. Nair, Y.-Y. Park, N. Sabnis, M. T. Deavers, J.-S. Lee, L. M. Ellis, G. Lopez-Berestein, W. J. McConathy, L. Prokai, A. G. Lacko, A. K. Sood, *Neoplasia* **2011**, *13*, 309-319.
- [5] Y. Ding, W. Wang, M. Feng, Y. Wang, J. Zhou, X. Ding, X. Zhou, C. Liu, R. Wang, Q. Zhang, *Biomaterials* **2012**, *33*, 8893-8905.
- [6] T. Nakayama, J. S. Butler, A. Sehgal, M. Severgnini, T. Racie, J. Sharman, F. Ding, S. S. Morskaya, J. Brodsky, L. Tchangov, V. Kosovrasti, M. Meys, L. Nechev, G. Wang, C. G. Peng, Y. Fang, M. Maier, K. G. Rajeev, R. Li, J. Hettinger, S. Barros, V. Clausen, X. Zhang, Q. Wang, R. Hutabarat, N. V. Dokholyan, C. Wolfrum, M. Manoharan, V. Kotelianski, M. Stoffel, D. W. Y. Sah, *Mol. Ther.* **2012**, *20*, 1582-1589.
- [7] A. G. Lacko, M. Nair, S. Paranjape, L. Mooberry, W. J. McConathy, *Chemotherapy* **2006**, *52*, 171-173.
- [8] M. Zamanian-Daryoush, D. Lindner, T. C. Tallant, Z. Wang, J. Buffa, E. Klipfell, Y. Parker, D. Hatala, P. Parsons-Wingter, P. Rayman, M. S. S. Yusufihaq, E. A. Fisher, J. D. Smith, J. Finke, J. A. DiDonato, S. L. Hazen, *J. Biol. Chem.* **2013**, *288*, 21237-21252.
- [9] P. Natarajan, T. M. Forte, B. Chu, M. C. Phillips, J. F. Oram, J. K. Bielicki, *J. Biol. Chem.* **2004**, *279*, 24044-24052.
- [10] G. Datta, M. Chaddha, S. Hama, M. Navab, A. M. Fogelman, D. W. Garber, V. K. Mishra, R. M. Epan, S. Lund-Katz, M. C. Phillips, J. P. Segrest, G. M. Anantharamaiah, *J. Lipid. Res.* **2001**, *42*, 1096-1104.
- [11] Z. Wu, M. A. Wagner, L. Zheng, J. S. Parks, J. S. Parks, J. M. Shy III, J. D. Smith, V. Gogonea, S. L. Hazen, *Nat. Struct. Mol. Biol.* **2007**, *14*, 861-868.
- [12] I. Lorenzi, A. von Eckardstein, C. Cavelier, S. Radosavljevic, L. Rohrer, *J. Mol. Med.* **2008**, *86*, 171-183.
- [13] L. J. Leman, B. E. Maryanoff, M. R. Ghadiri, *J. Med. Chem.* **2014**, *57*, 2169-2196.

- 
- [14] Y. Huang, Z. Wu, M. Riwanto, S. Gao, B. S. Levison, X. Gu, X. Fu, M. A. Wagner, C. Besler, G. Gerstenecker, R. Zhang, X.-M. Li, A. J. DiDonato, V. Gogonea, W. H. W. Tang, J. D. Smith, E. F. Plow, P. L. Fox, D. M. Shih, A. J. Lusic, E. A. Fisher, J. A. DiDonato, U. Landmesser, S. L. Hazen, *J. Clin. Invest.* **2013**, *123*, 3815-3828.
- [15] J. K. Qiang, Y. C. Wong, A. Siderowf, H. I. Hurtig, S. X. Xie, V. M.-Y. Lee, J. Q. Trojanowski, D. Yearout, J. B. Leverenz, T. J. Montine, M. Stern, S. Mendick, D. Jennings, C. Zabetian, K. Marek, A. S. Chen-Plotkin, *Ann. Neurol.* **2013**, *74*, 119-127.
- [16] S. As, S. Sahukar, J. Murthy, K. Kumar, *J. Clin. Diagn. Res.* **2013**, *7*, 1303-1306.
- [17] K. L. Gillotte, M. Zaiou, S. Lund-Katz, G. M. Anantharamaiah, P. Holvoeti, A. Dhoesti, M. N. Palgunachari, J. P. Segrest, K. H. Weisgraber, G. H. Rothblat, M. C. Phillips, *J. Biol. Chem.* **1999**, *274*, 2021-2028.
- [18] I. Saraogi, A. D. Hamilton, *Biochem. Soc. Trans.* **2008**, *36*, 1414-1417.
- [19] J. M. Davis, L. K. Tsou, A. D. Hamilton, *Chem. Soc. Rev.* **2007**, *36*, 326-334.
- [20] D. A. Guarracino, B. N. Bullock, P. S. Arora, *Biopolymers* **2010**, *95*, 1-7.
- [21] A. Shaginian, L. R. Whitby, S. Hong, I. Hwang, B. Farooqi, M. Searcey, J. Chen, P. Vogt, D. L. Boger, *J. Am. Chem. Soc.* **2009**, *131*, 5564-5572.
- [22] L. Zheng, B. Nukuna, M.-L. Brennan, M. Sun, M. Goormastic, M. Settle, D. Schmitt, X. Fu, L. Thomson, P. L. Fox, H. Ischiropoulos, J. D. Smith, M. Kinter, S. L. Hazen, *J. Clin. Invest.* **2004**, *114*, 529-541.
- [23] K. N. Liadaki, T. Liu, S. Xu, B. Y. Ishida, P. N. Duchateaux, J. P. Krieger, J. Kane, M. Krieger, V. I. Zannis, *J. Biol. Chem.* **2000**, *275*, 21262-21271.
- [24] Y. Che, B. R. Brooks, G. R. Marshall, *Biopolymers* **2007**, *86*, 288-297.
- [25] J. Garner, M. M. Harding, *Org. Biomol. Chem.* **2007**, *5*, 3577-3585.
- [26] D. A. Guarracino, B. N. Bullock, P. S. Arora, *Biopolymers* **2010**, *95*, 1-7.
- [27] R. J. Simon, R. S. Kania, R. N. Zuckermann, V. D. Huebner, D. A. Jewell, S. Banville, S. Ng, L. Wang, S. Rosenberg, C. K. Marlowe, D. C. Spellmeyer, R. Tans, A. D. Frankelo, D. V. Santi, F. E. Cohen, P. A. Bartlett, *Proc. Natl. Acad. Sci. USA* **1992**, *89*, 9367-9371.
- [28] B. P. Orner, J. T. Ernst, A. D. Hamilton, *J. Am. Chem. Soc.* **2001**, *123*, 5382-5383.
- [29] M. Peters, M. Trobe, H. Tan, R. Kleineweischede, R. Breinbauer, *Chem. Eur. J.* **2013**, *19*, 2442-2449.
- [30] P. Restorp, J. Rebek, Jr., *Bioorg. Med. Chem. Lett.* **2008**, *18*, 5909-5911.
- [31] J. M. Rodriguez, N. T. Ross, W. P. Katt, D. Dhar, G. Lee, A. D. Hamilton, *ChemMedChem* **2009**, *4*, 649-656.
-

- 
- [32] M. Peters, M. Trobe, R. Breinbauer, *Chem. Eur. J.* **2013**, *19*, 2450-2456.
- [33] M. Ditiatkovski, W. D'Souza, R. Kesani, J. Chin-Dusting, J. B. de Haan, A. Remaley, D. Sviridov, *PLoS ONE* **2013**, *8*, e68802.
- [34] M. Navab, G.M. Anantharamaiah, S. T. Reddy, S. Hama, G. Hough, V. R. Grijalva, N. Yu, B. J. Ansell, G. Datta, D. W. Garber, A. M. Fogelman, *Arterioscler. Thromb. Vasc. Biol.* **2005**, *25*, 1325-1331.
- [35] F. Tabet, A. T. Remaley, A. I. Segaliny, J. Millet, L. Yan, S. Nakhla, P. J. Barter, K.-A. Rye, G. Lambert, *Arterioscler. Thromb. Vasc. Biol.* **2010**, *30*, 246-252.
- [36] A. A. Sethi, J. A. Stonik, F. Thomas, S. J. Demosky, M. Amar, E. Neufeld, H. B. Brewer, W. S. Davidson, W. D'Souza, D. Sviridov, A. T. Remaley, *J. Biol. Chem.* **2008**, *283*, 32273–32282.
- [37] W. D'Souza, J. A. Stonik, A. Murphy, S. J. Demosky, A. A. Sethi, X. L. Moore, J. Chin-Dusting, A. T. Remaley, D. Sviridov, *Circ. Res.* **2010**, *107*, 217-227.
- [38] E. Carballo-Jane, Z. Chen, E. O'Neill, J. Wang, C. Burton, C. H. Chang, X. Chen, S. Eveland, B. Frantz-Wattley, K. Gagen, B. Hubbard, M. Ichetovkin, S. Luell, R. Meurer, X. Song, A. Strack, A. Langella, S. Cianetti, F. Rech, E. Capitò, S. Bufali, M. Veneziano, M. Verdirame, F. Bonelli, E. Monteagudo, A. Pessi, R. Ingenito, E. Bianchi, *Bioorg. Med. Chem.* **2010**, *18*, 8669–8678.
- [39] M. Navab, G.M. Anantharamaiah, S. T. Reddy, B. J. Van Lenten, G. M. Buga, A. M. Fogelman, *J. Clin. Lipidol.* **2007**, *1*, 142–147.
- [40] S. Imaizumi, M. Navab, C. Morgantini, C. Charles-Schoeman, F. Su, F. Gao, M. Kwon, E. Ganapathy, D. Meriwether, R. Farias-Eisner, A. M. Fogelman, S. T. Reddy, *Circ. J.* **2011**, *75*, 1533 – 1538.
- [41] F. Sua, K. R. Kozak, S. Imaizumi, F. Gao, M. W. Amneus, V. Grijalva, C. Ng, A. Wagner, G. Hough, G. Farias-Eisner, G. M. Anantharamaiah, B. J. Van Lenten, M. Navab, A. M. Fogelman, S. T. Reddy, R. Farias-Eisner, *Proc. Natl. Acad. Sci. USA* **2010**, *107*, 19997-20002.
- [42] H. Gupta, L. Dai, G. Datta, D. W. Garber, H. Grenett, Y. Li, V. Mishra, M. N. Palgunachari, S. Handattu, S. H. Gianturco, W. A. Bradley, G. M. Anantharamaiah, C. R. White, *Circ. Res.* **2005**, *97*, 236-243.
- [43] J. Cao, N. Puri, K. Sodhi, L. Bellner, N. G. Abraham, A. Kappas, *Int. J. Hypertens.* **2012**, *2012*, 1-8.
- [44] A. L. Kruger, S. Peterson, S. Turkseven, P. M. Kaminski, F. F. Zhang, S. Quan, M. S. Wolin, N. G. Abraham, *Circulation* **2005**, *111*, 3126-3134.
-

- 
- [45] S. J. Peterson, D. Husney, A. L. Kruger, R. Olszanecki, F. Ricci, L. F. Rodella, A. Stacchiotti, R. Rezzani, J. A. McClung, W. S. Aronow, S. Ikehara, N. G. Abraham, *JPET* **2007**, *322*, 514-520.
- [46] J. M. P. Woo, Z. Lin, M. Navab, C. Van Dyck, Y. Trejo-Lopez, K. M. T. Woo, H. Li, L. W. Castellani, X. Wang, N. Iikuni, O. J. Rullo, H. Wu, A. La Cava, A. M. Fogelman, A. J. Lulis, B. P. Tsao, *Arthritis Res. Ther.* **2010**, *12*, R93.
- [47] C. E. Watson, N. Weissbach, L. Kjems, S. Ayalasomayajula, Y. Zhang, I. Chang, M. Navab, S. Hama, G. Hough, S. T. Reddy, D. Soffer, D. J. Rader, A. M. Fogelman, A. Schechter, *J. Lipid Res.* **2011**, *52*, 361–373.
- [48] E. Fattala, A. Bochota, *Int. J. Pharm.* **2008**, *364*, 237-248.
- [49] A. Fire, *Trends Genet.* **1999**, *15*, 358-363.
- [50] S. M. Elbashir, J. Harborth, W. Lendeckel, A. Yalcin, K. Weber, T. Tuschl, *Nature* **2001**, *411*, 494-498.
- [51] J. E. Darnell Jr., *Science* **1997**, *277*, 1630-1635.
- [52] J. Turkson, *Exp. Opin. Ther. Targets* **2004**, *8*, 409-422.
- [53] B. Ozpolat, A. K. Sood, G. Lopez-Berestein, *Adv. Drug Deliv. Rev.* **2014**, *66*, 110-116.
- [54] C. Zhang, M. Jugold, E. C. Woenne, T. Lammers, B. Morgenstern, M. M. Mueller, H. Zentgraf, M. Bock, M. Eisenhut, W. Semmler, F. Kiessling, *Cancer Res.* **2007**, *67*, 1555-1562.
- [55] K. F. Pirollo, E. H. Chang, *Cancer Res.* **2008**, *68*, 1247-1250.
- [56] W. M. Merritt, Y. G. Lin, W. A. Spannuth, M. S. Fletcher, A. A. Kamat, L. Y. Han, C. N. Landen, N. Jennings, K. De Geest, R. R. Langley, G. Villares, A. Sanguino, S. K. Lutgendorf, G. Lopez-Berestein, M. M. Bar-Eli, A. K. Sood, *J. Natl. Cancer. Inst.* **2008**, *100*, 359-372.
- [57] J. Halder, A. A. Kamat, C. N. Landen Jr., L. Y. Han, S. K. Lutgendorf, Y. G. Lin, W. M. Merritt, N. B. Jennings, A. Chavez-Reyes, R. L. Coleman, D. M. Gershenson, R. Schmandt, S. W. Cole, G. Lopez-Berestein, A. K. Sood, *Clin. Cancer Res.* **2006**, *12*, 4916-4924.
- [58] E. P. Gillis, M. D. Burke, *J. Am. Chem. Soc.* **2007**, *129*, 6716-6717.
- [59] J. A. Joule, K. Mills, *Heterocyclic Chemistry*, 5<sup>th</sup> ed.; Wiley, Chichester, **2010**.
- [60] W. Bridge A. J. Crocker, T. Cubin, A. Robertson, *J. Chem. Soc.* **1937**, 1530-1535.
- [61] S.-S. Xie, X.-B. Wang, J.-Y. Li, L. Yang, L.-Y. Kong, *Eur. J. Med. Chem.* **2013**, *64*, 540-553.
- [62] A. Robertson, R. B. Waters, E. T. Jones, *J. Chem. Soc.* **1932**, 1681-1688.
-

- 
- [63] J. Daru, A. Stirling, *J. Org. Chem.* **2011**, *76*, 8749-8755.
- [64] M. Bulut, Ç. Erk, *Dyes and Pigments* **1996**, *30*, 99-104.
- [65] M. Schlosser (Ed.), *Organometallics in Synthesis: Third Manual*, 1<sup>st</sup> ed.; John Wiley & sons, New Jersey, **2013**.
- [66] M. T. Reetz, R. Breinbauer, K. Wanninger, *Tetrahedron Lett.* **1996**, *37*, 4499-4502.
- [67] S. Cacchi, P. G. Ciattini, E. Morera, G. Ortar, *Tetrahedron Lett.* **1986**, *27*, 5541-5544.
- [68] A. L. S. Thompson, G. W. Kabalka, M. R. Akula, J. W. Huffman, *Synthesis* **2005**, *4*, 547-550.
- [69] W.-J. Huang, Y.-C. Wang, S.-W. Chao, C.-Y. Yang, L.-C. Chen, M.-H. Lin, W.-C. Hou, M.-Y. Chen, T.-L. Lee, P. Yang, C.-I. Chang, *ChemMedChem* **2012**, *7*, 1815 – 1824.
- [70] Š. Starčević, P. Brožič, S. Turk, J. Cesar, T. L. Rižner, S. Gobec, *J. Med. Chem.* **2011**, *54*, 248-261
- [71] C. Elschenbroich, *Organometallchemie*, 6<sup>th</sup> ed.; B. G. Teubner Verlag, Wiesbaden, **2008**.
- [72] M. Chtchigrovsky, A. Primo, P. Gonzalez, K. Molvinger, M. Robitzer, F. Quignard, F. Taran, *Angew. Chem. Int. Ed.* **2009**, *48*, 5916-5920.
- [73] M. Min, Y. Kim, S. Hong, *Chem. Commun.* **2013**, *49*, 196-198.
- [74] C. Amatore, E. Carré, A. Jutand, Y. Medjour, *Organometallics* **2002**, *21*, 4540-4545.
- [75] A. Jutand, *Pure Appl. Chem.* **2004**, *76*, 565-576.
- [76] T. M. Gøgsig, J. Kleimark, S. O. N. Lill, S. Korsager, A. T. Lindhardt, P.-O. Norrby, T. Skrydstrup, *J. Am. Chem. Soc.* **2012**, *134*, 443-452.
- [77] X.-Y. Chen, C. Barnes, J. R. Dias, T. C. Sandreczki, *Chem. Eur. J.* **2009**, *15*, 2041-2044.
- [78] M. Quaranta, M. Murkovic, I. Klimant, *Analyst* **2013**, *138*, 6243-6245.
- [79] P. M. Murray, J. F. Bower, D. K. Cox, E. K. Galbraith, J. S. Parker, J. B. Sweeney, *Org. Process Res. Dev.* **2013**, *17*, 397-405.
- [80] T. Jeffery, *J. Chem. Soc., Chem. Commun.* **1984**, 1287-1289.
- [81] C. Amatore, A. Jutand, A. Suarez, *J. Am. Chem. Soc.* **1993**, *115*, 9531-9541.
- [82] C. Amatore, M. Azzabi, A. Jutand, *J. Am. Chem. Soc.* **1991**, *113*, 1670-1677.
- [83] J. Clayden, N. Greeves, S. Warren, P. Wothers, *Organic Chemistry*, 1<sup>st</sup> ed.; Oxford, New York, **2001**.
- [84] P. A. Byrne, D. G. Gilheany, *J. Am. Chem. Soc.* **2012**, *134*, 9225-9239.
-



- 
- [85] T. Laue, A. Plagens, *Namen- und Schlagwort-Reaktionen der Organischen Chemie*, 5<sup>th</sup>ed.; Vieweg+Teubner, Wiesbaden, **2009**.
- [86] F. Ito, K. Fusegi, T. Kumamoto, T. Ishikawa, *Synthesis* **2007**, *12*, 1785–1796.
- [87] N. Cairns, L. M. Harwood, D. P. Astles, A. Orr, *J. Chem. Soc. Perkin Trans.1* **1994**, *21*, 3095-3100.
- [88] A. Roglans, A. Pla-Quintana, M. Moreno-Mañas, *Chem. Rev.* **2006**, *106*, 4622–4643.
- [89] R. Appel, *Angew. Chem Int. Ed.* **1975**, *14*, 801-811.
- [90] S. Bonazzi, B. Cheng, J. S. Wzorek, D. A. Evans, *J. Am. Chem. Soc.* **2013**, *135*, 9338–9341.
- [91] S. C. Berk, M. C. P. Yeh, N. Jeong, P. Knochel, *Organometallics* **1990**, *9*, 3053-3064.
- [92] D. J. Drain, D. D. Martin, B. W. Mitchell, D. E. Seymour, F. S. Spring, *J. Chem. Soc.* **1949**, 1498-1503.
- [93] F. Zuber, E. Sorkin H. Erlenmeyer, *Helv. Chim. Acta* **1950**, *33*, 1269-1271.

---

## 9 Abbreviations

### Analytical methods:

|                |  |
|----------------|--|
| ATP            | attached proton test                   |
| bs             | broad singlet                          |
| C <sub>q</sub> | quaternary carbon                      |
| COSY           | Correlated Spectroscopy                |
| d              | doublet                                |
| dd             | doublet of a doublet                   |
| EI             | electron impact ionization             |
| eV             | electron Volt                          |
| FT             | Fourier transform                      |
| GC-MS          | Gas chromatography-mass spectrometry   |
| HSQC           | Heteronuclear Single Quantum Coherence |
| HRMS           | high resolution mass spectrometry      |
| <i>J</i>       | coupling constant                      |
| m              | multiplet                              |
| m.p.           | melting point                          |
| <i>m/z</i>     | mass-charge ratio                      |
| MSD            | mass sensitive detector                |
| NMR            | nuclear magnetic resonance             |
| ppm            | parts per million                      |
| p              | pentet                                 |
| q              | quadruplet                             |
| R <sub>f</sub> | retardation factor                     |
| s              | singlet                                |
| t              | triplet                                |
| TIC            | total ion count                        |
| TLC            | thin layer chromatography              |
| t <sub>R</sub> | retention time                         |
| UV             | ultraviolet                            |
| δ              | chemical shift                         |

---

**Chemical abbreviations:**

|                   |   |
|-------------------|---|
| ABCA1             | ATP-binding cassette transporter A1         |
| ApoA1             | Apolipoprotein A1                           |
| ApoB              | Apolipoprotein B                            |
| ApoE3             | Apolipoprotein E3                           |
| Ar                | aryl  |
| Boc               | <i>tert</i> -butyloxycarbonyl               |
| brine             | saturated sodium chloride solution in water |
| CAM               | cerium-ammonium-molybdate                   |
| CDCl <sub>3</sub> | deuterated chloroform                       |
| DCM               | dichloromethane                             |
| d-DMSO            | D <sub>6</sub> -dimethyl sulfoxide          |
| DMSO              | dimethyl sulfoxide                          |
| dsRNA             | double stranded RNA                         |
| <i>E</i>          | entgegen                                    |
| Et                | ethyl                                       |
| Et <sub>2</sub> O | diethyl ether                               |
| EtOAc             | ethyl acetate                               |
| FAK               | focal adhesion kinase                       |
| Glu               | glutamate                                   |
| HDL               | high-density lipoprotein                    |
| HDM2              | Human Double Minute 2 protein               |
| HO-1              | heme oxygenase 1                            |
| <i>i</i> Pr       | isopropyl                                   |
| LCAT              | lecithin-cholesterol acyltransferase        |
| LDL               | low-density lipoprotein                     |
| LPA               | lysophosphatidic acid                       |
| Lys               | lysine                                      |
| Me                | methyl                                      |
| MPO               | Myeloperoxidase                             |
| mRNA              | messenger RNA                               |
| OAc               | acetate                                     |
| <i>p</i>          | para  |
| PTX               | paclitaxel                                  |

---

|             |  |
|-------------|--|
| PDB         | protein data base                                  |
| Pin         | 2,3-dimethyl-2,3-butanediol                        |
| PON1        | paraoxonase-1                                      |
| PPI         | protein-protein interaction                        |
| Pro         | proline  |
| rHDL        | reconstituted high-density lipoprotein             |
| RNA         | ribonucleic acid                                   |
| siRNA       | small interfering RNA                              |
| SR-B1       | scavenger receptor B1                              |
| smMLCK      | smooth muscle myosine light-chain kinase           |
| STAT3       | Signal Transducer and Activator of Transcription 3 |
| TBS         | <i>tert</i> -butyldimethylsilyl                    |
| <i>t</i> Bu | 1,1-dimethylethyl                                  |
| Tf          | triflate   |
| THF         | tetrahydrofurane                                   |
| Thr         | threonine  |
| Trp         | tryptophan   |
| Val         | valine   |
| VLDL        | very-low-density lipoprotein                       |
| Z           | zusammen   |

**Others:**

|    |                |
|----|----------------|
| %  | percent        |
| °C | degree Celsius |
| µm | micrometer     |
| Å  | angstrom       |
| cm | centimeter     |
| d  | day            |
| eq | equivalents    |
| g  | gramm          |
| h  | hour           |
| Hz | Hertz          |
| IV | intravenous    |
| KO | knock-out      |

|             |                  |
|-------------|------------------|
| m           | meter            |
| M           | molar (mol/L)    |
| mbar        | millibar         |
| mg          | milligram        |
| MHz         | megaHertz        |
| min         | minute           |
| mL          | milliliter       |
| mmol        | millimole        |
| Mol%        | mole percent     |
| nm          | nanometer        |
| RT          | room temperature |
| SC          | subcutaneously   |
| T           | temperature      |
| <i>tert</i> | tertiary         |
| V           | Volt             |

## 10 Danksagung

Das Wichtigste kommt zum Schluss; die Zeit danken zu sagen! An erster Stelle möchte ich vor allem meinen Eltern, Michaela Dobrounig und Erich Dobrounig, danken. Nur dank ihrer großzügigen Unterstützung, sowohl auf persönlicher als auch auf finanzieller Ebene, war es mir überhaupt erst möglich, dieses Studium zu beginnen und auch durchzustehen. Selbstverständlich möchte ich mich auch bei allen anderen Verwandten für ihre stete Hilfsbereitschaft und auch für ihre bereitwillige Unterstützung bedanken. Besonders hervorheben möchte ich an dieser Stelle meinen Cousin Mag. Dr. Christian Kazianka, der viele Teile dieser Arbeit auf sprachliche Korrektheit überprüfte.

Weiters möchte ich Prof. Dr. Rolf Breinbauer danken. Dafür, dass er es mir ermöglichte meine Arbeit an seinem Institut durchzuführen und es mir ermöglichte, mich mit diesem äußerst interessanten Thema auseinanderzusetzen. Selbstverständlich danke ich auch für die stete Unterstützung und den interessanten und hilfreichen Gesprächen über chemische Problemstellungen. Weiters danke ich auch dafür, dass er es mir, gemeinsam mit meinen Kollegen, ermöglichte, das 14<sup>th</sup> Belgian Organic Synthesis Symposium zu besuchen. Vielen Danke auch für alles, das du mir in deinen Vorlesungen und darüber hinaus über organische Chemie beigebracht hast.

Ich möchte mich auch beim gesamten Arbeitskreis bedanken. Danke dafür, dass ihr mich so freundlich aufgenommen habt, stets Hilfsbereitschaft an den Tag gelegt habt und dass ihr die Grenze zwischen Arbeit und Vergnügen verschwinden habt lassen. Besonders hervorheben möchte ich hier Melanie Trobe, MSc, die seit meiner Bachelorarbeit stets für alle Probleme ein offenes Ohr hat. Ich möchte Melanie, Nikolaus Guttenberger, MSc und selbstverständlich auch Xuepu Yu für den Spaß im Labor danken. Weiters danken möchte ich Carina Doler, BSc, die seit dem ersten Semester meine Laborpartnerin ist und seitdem für ständigen Spaß sorgt und auch immer mit Rat und Tat zur Seite steht. Danke auch an Felix Anderl, BSc. Mit ihm geben wir uns schon seit der allerersten Matheklausur im 1. Semester gelegentlichen Erfrischungen hin. Wenn wir nicht gerade "Abzugstetris" spielen oder sonstige geistreiche Gespräche führen, unterhalten wir uns über chemische Problemstellungen, die sich für mich immer als sehr lehrreich herausgestellt haben. Danke Felix für alles was ich von dir lernen durfte und vor allem dafür, dass du mir viele Arbeitstechniken gezeigt hast, die zwar hin und

wieder etwas fragwürdig waren, die aber über das Standardrepertoire von den Laborübungen hinausgingen und sich oft als sehr hilfreich erwiesen haben.

Weiters möchte ich Dipl.-Ing. Marko Kljajic für die ständigen gegenseitigen Neckereien danken und für den tollen Spaß den wir sehr oft, sowohl beim Kaffee, Bier als auch im Labor gemeinsam haben.

Selbstverständlich auch ein herzliches Dankeschön an Ing. Carina Illaszewicz-Trattner und Prof. Dr. Hansjörg Weber für die NMR-Messungen. Weiters möchte ich Ing. Peter Plachota für seine unersetzbare Hilfe bei allem rund um die Computerwelt danken. Selbstverständlich auch ein großes Danke an Mag. Astrid Nauta für ihre unglaubliche Geduld und Hilfe in allen organisatorischen Angelegenheiten.

Abschließend möchte ich noch meiner Freundin Sarah Lenart danken. Danke dafür, dass du stets hinter mir stehst und mir in allen Dingen eine unersetzbare Stütze bist. Vielen Dank für die Unterstützung vor allem in schwierigeren Zeiten. Danke auch dafür, dass du in arbeitsreichen Zeiten so viel Verständnis für mich aufgebracht hast und immer darum bemüht warst mich bestmöglich zu unterstützen.

---

## **EIDESSTATTLICHE ERKLÄRUNG**

### *AFFIDAVIT*

Ich erkläre an Eides statt, dass ich die vorliegende Arbeit selbstständig verfasst, andere als die angegebenen Quellen/Hilfsmittel nicht benutzt, und die den benutzten Quellen wörtlich und inhaltlich entnommenen Stellen als solche kenntlich gemacht habe. Das in TUGRAZonline hochgeladene Textdokument ist mit der vorliegenden Masterarbeit identisch.

*I declare that I have authored this thesis independently, that I have not used other than the declared sources/resources, and that I have explicitly indicated all material which has been quoted either literally or by content from the sources used. The text document uploaded to TUGRAZonline is identical to the present master's thesis.*

---

Datum / Date

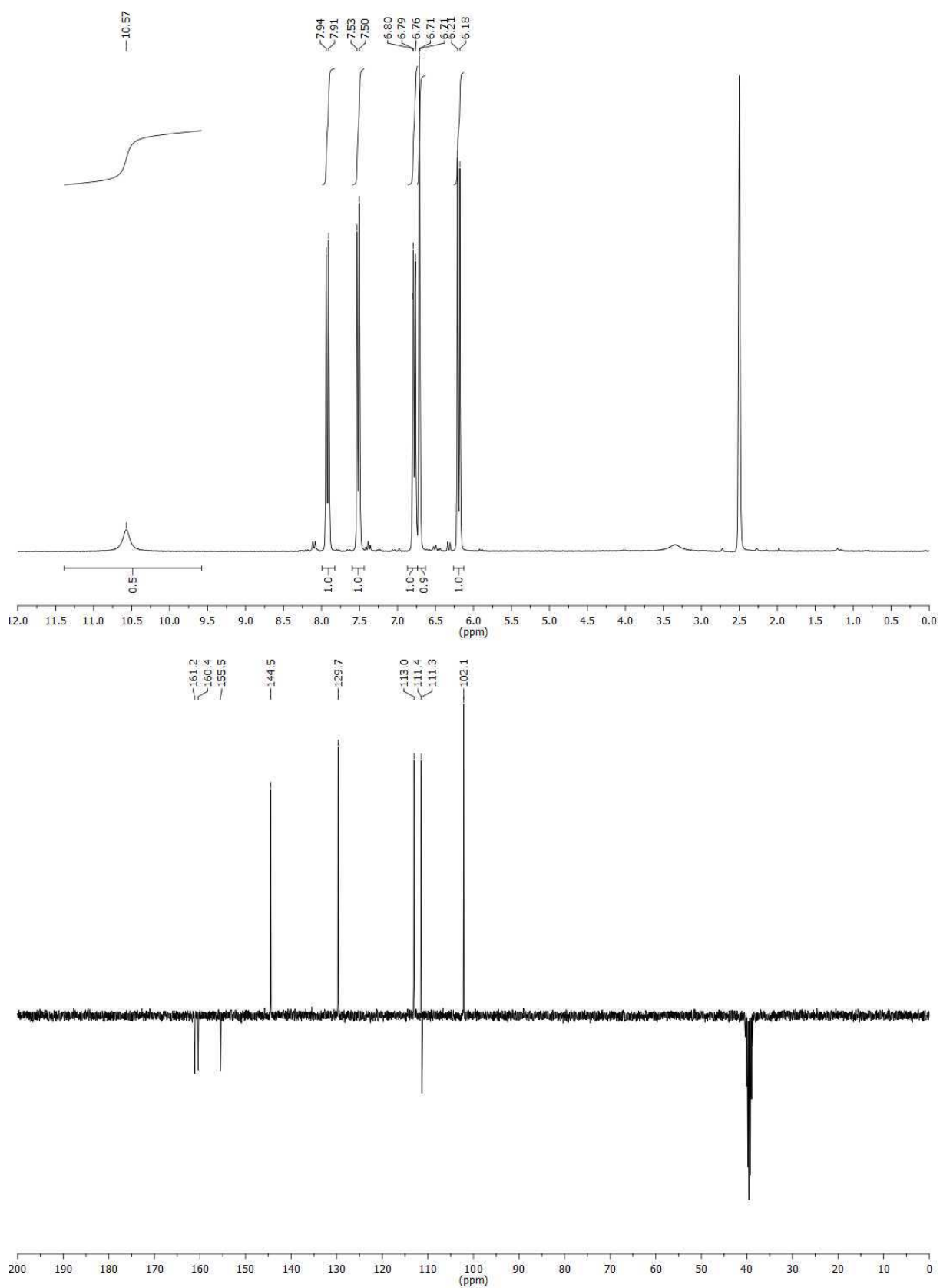
---

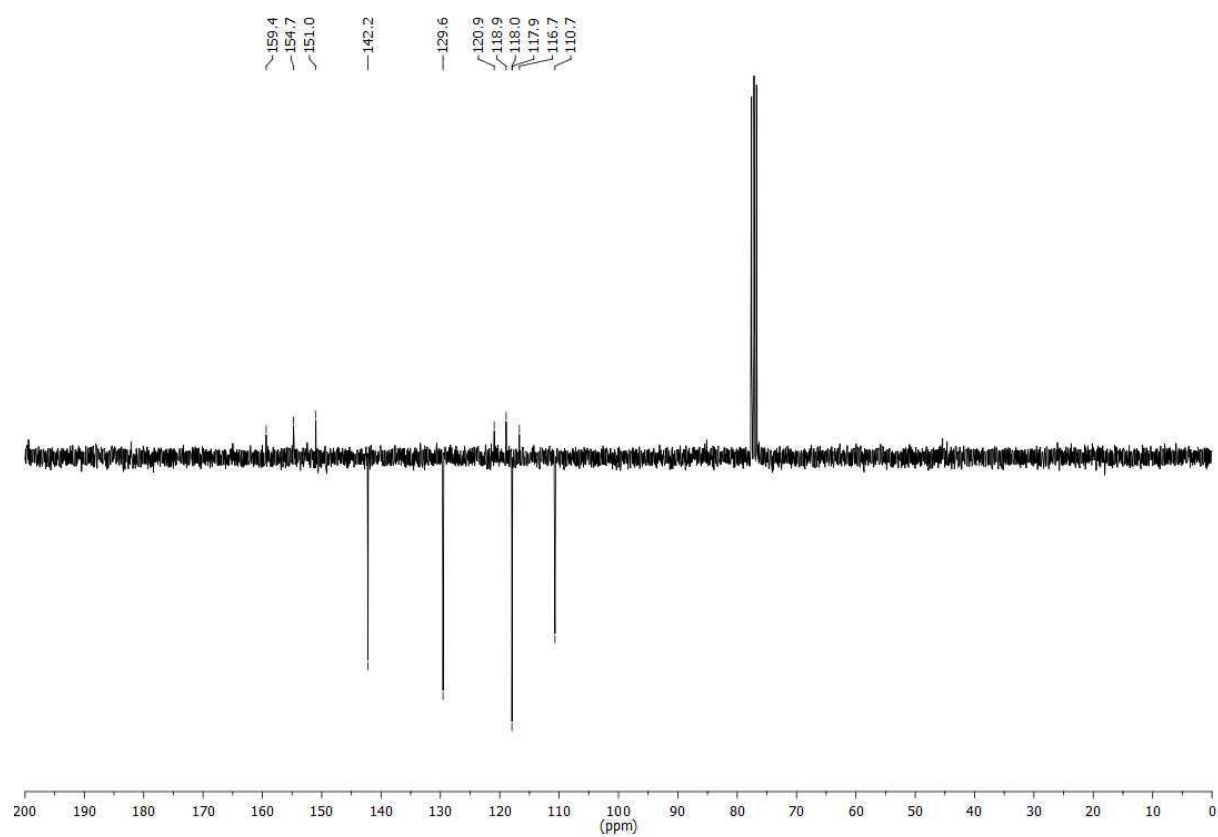
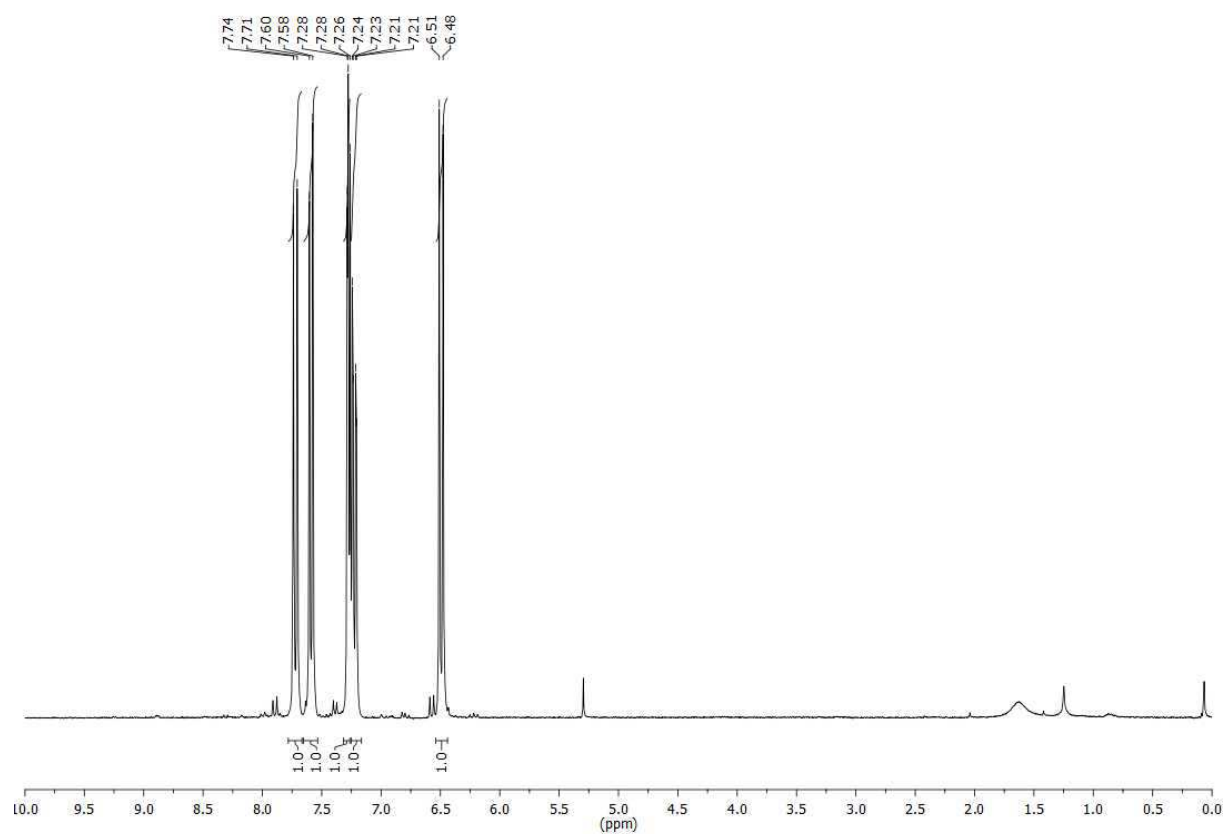
Unterschrift / Signature

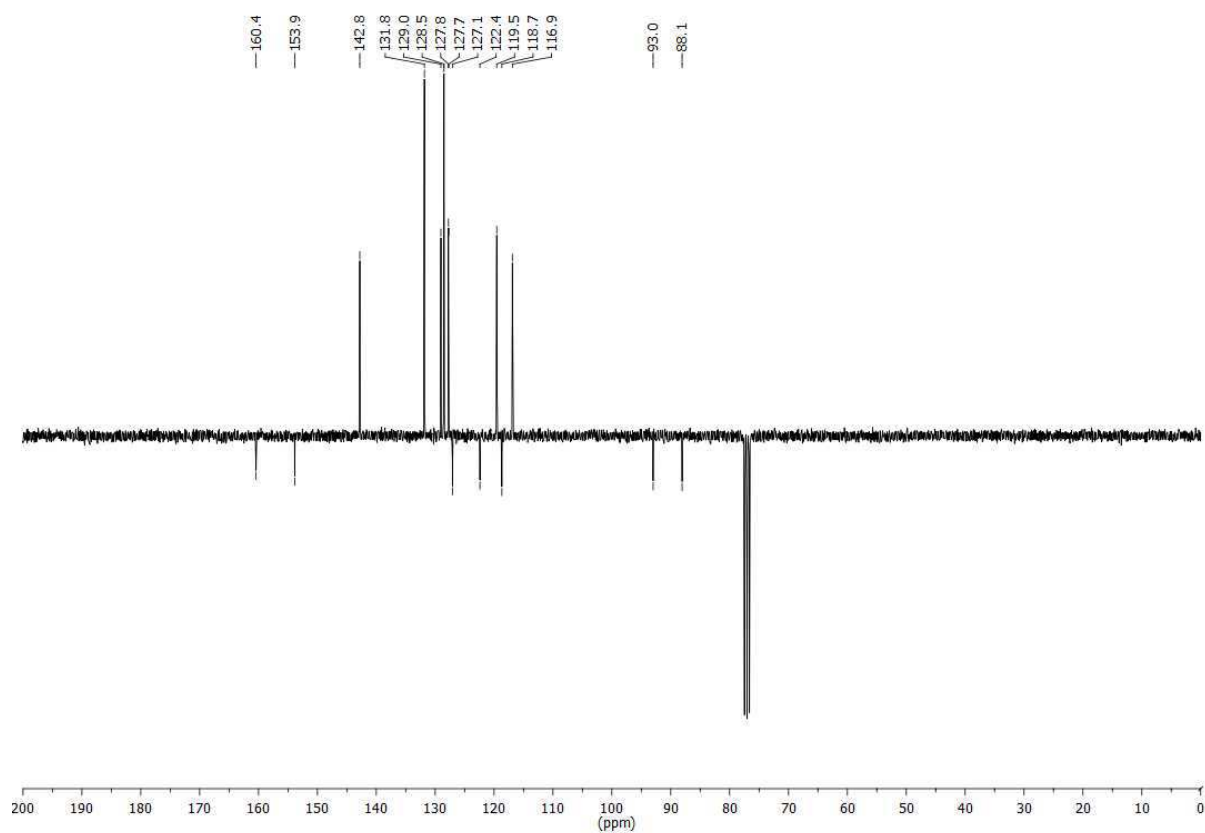
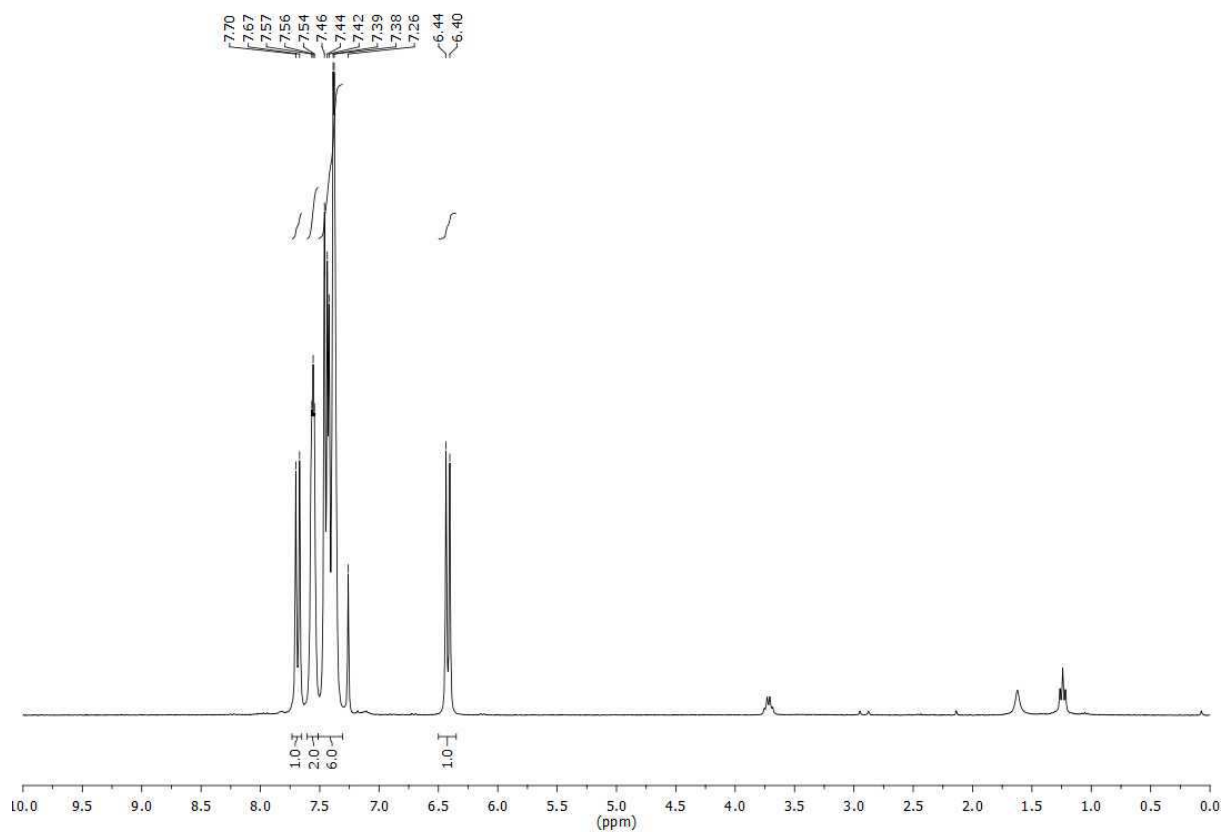


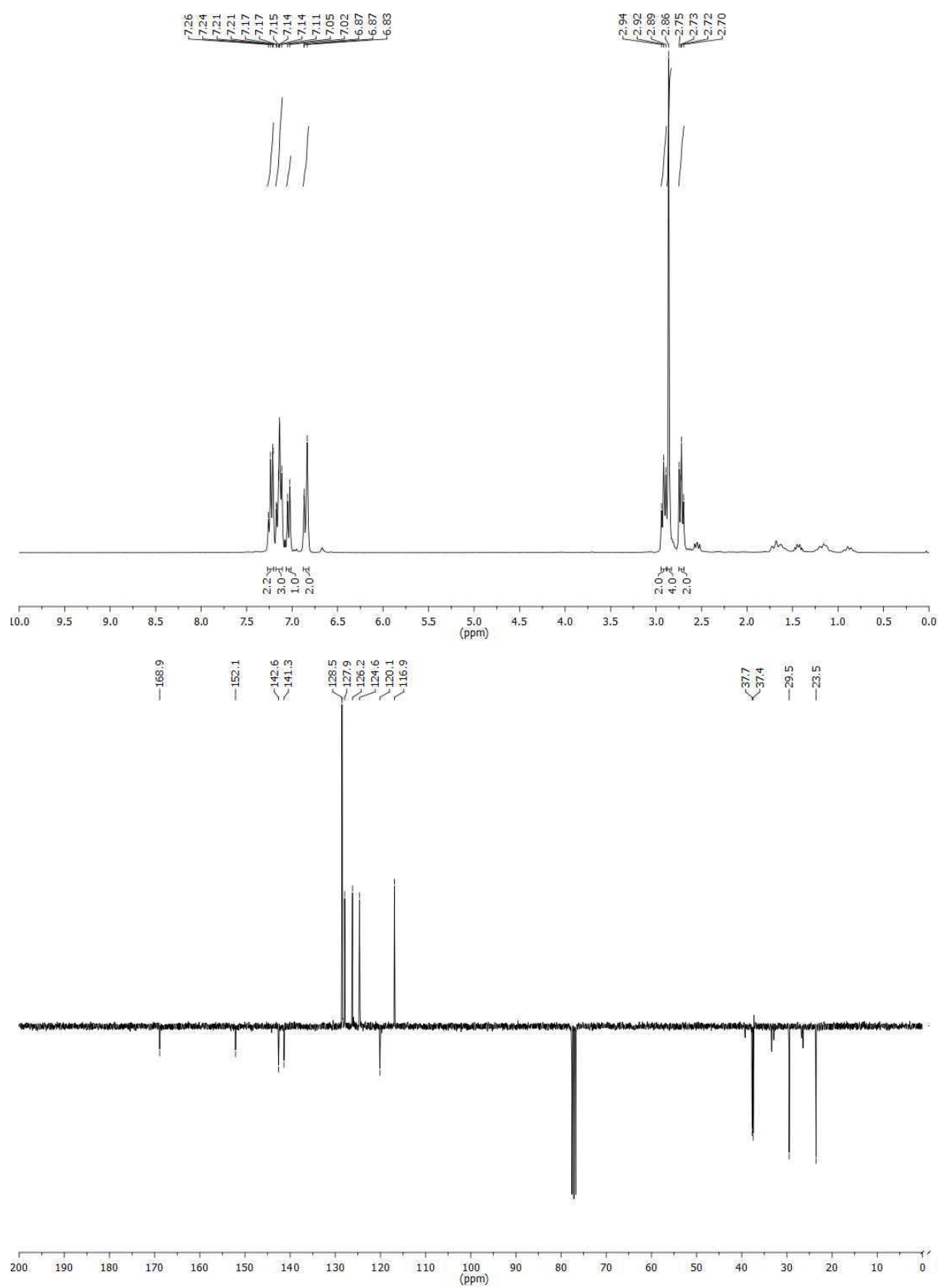
## 11 Appendix

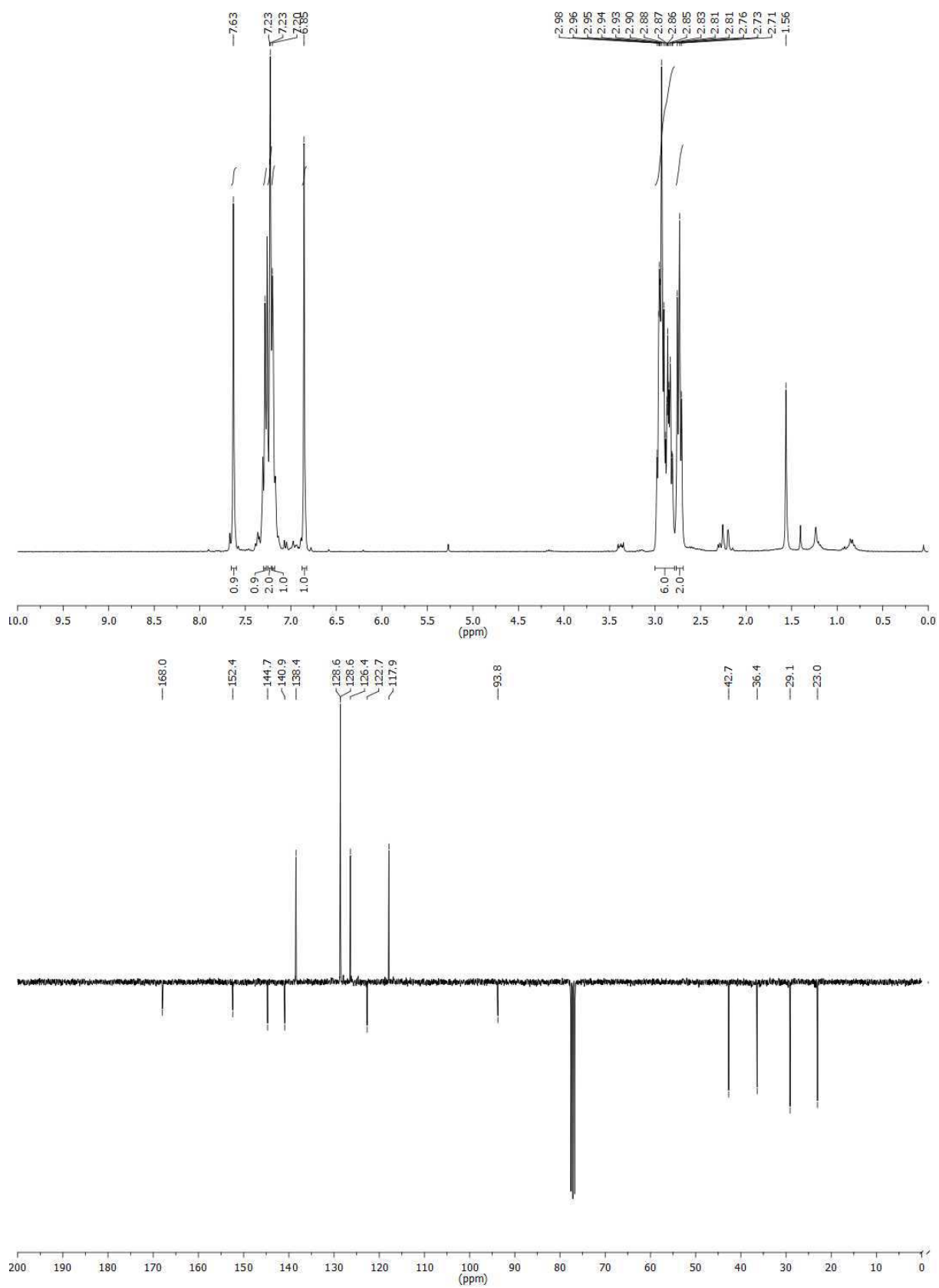
$^1\text{H}$ - and APT spectrum of 7-hydroxy-2*H*-chromen-2-one (**1**)

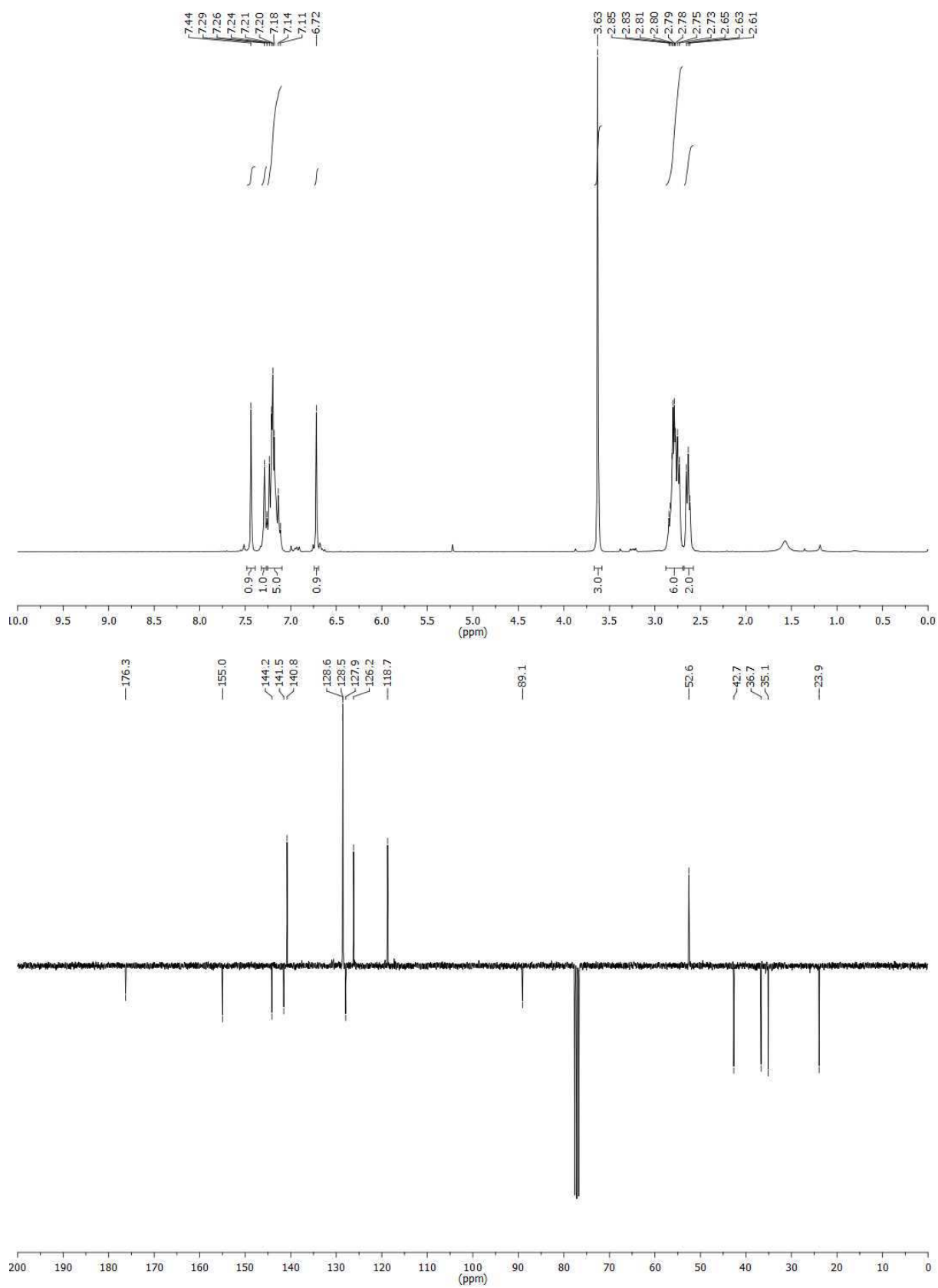


$^1\text{H}$ - and APT spectrum of 2-oxo-2*H*-chromen-7-yl trifluoromethanesulfonate (**2**)

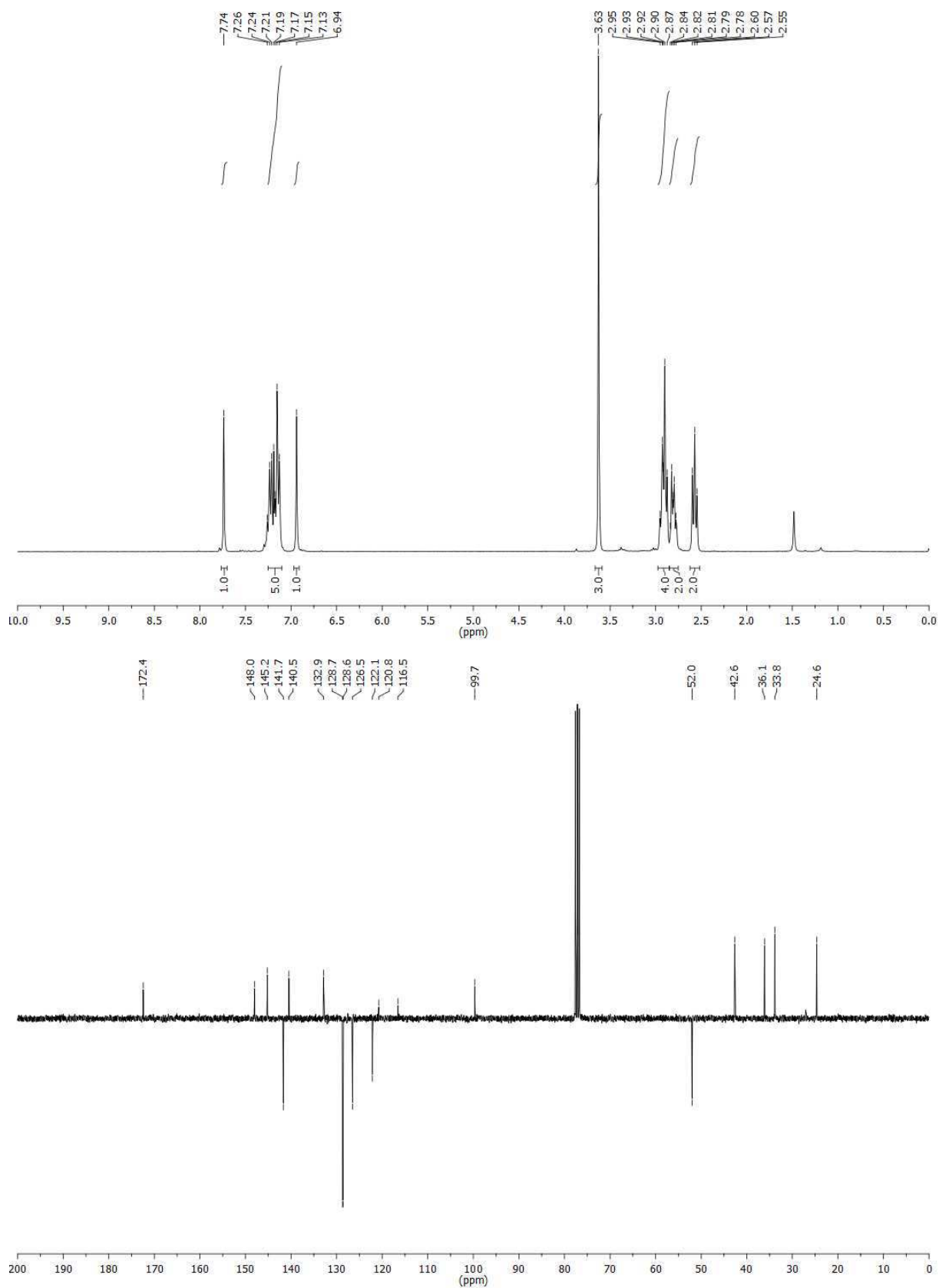
<sup>1</sup>H- and APT spectrum of 7-(phenylethynyl)-2*H*-chromen-2-one (**3**)

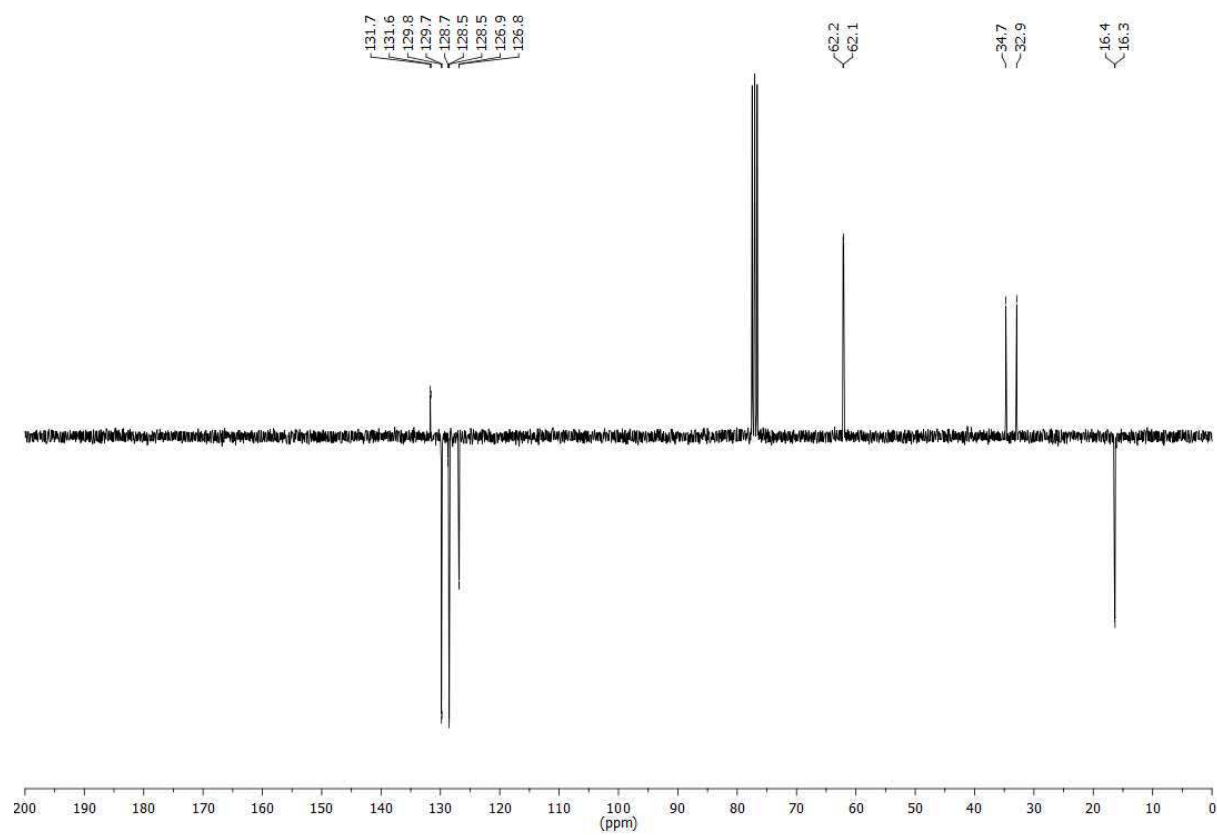
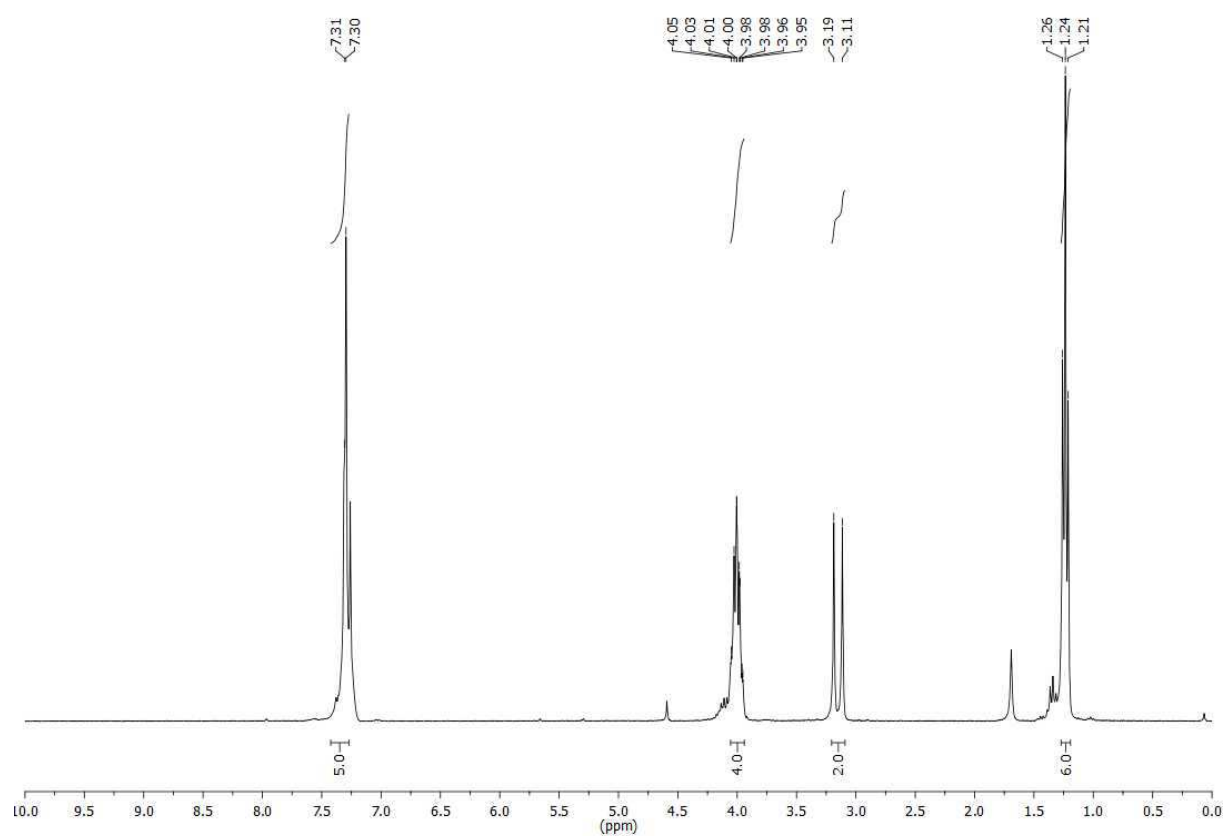
$^1\text{H}$ - and APT spectrum of 7-phenethylchroman-2-one (**4**)

<sup>1</sup>H- and APT spectrum of 6-iodo-7-phenethylchroman-2-one (**5**)

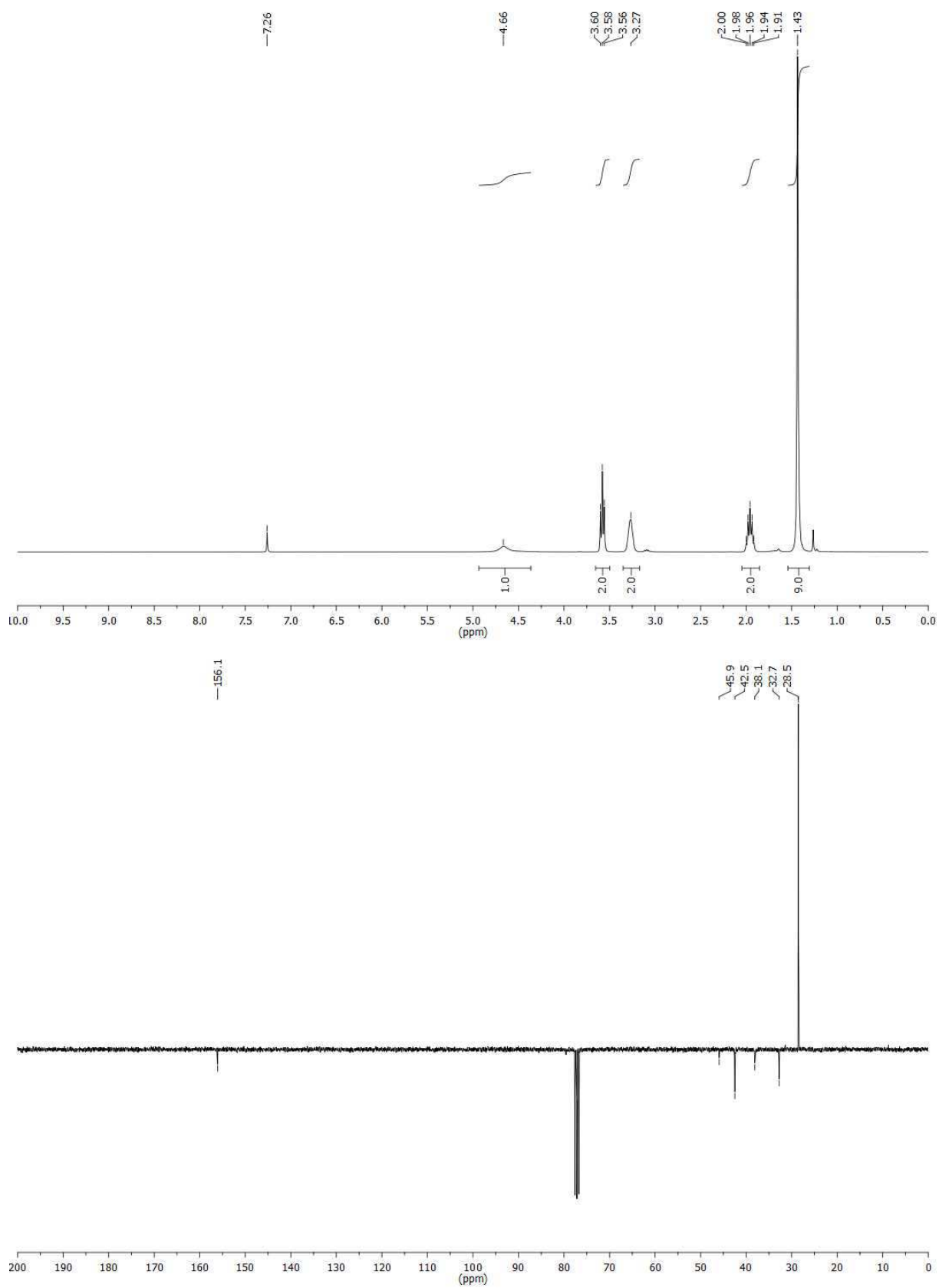
$^1\text{H}$ - and APT spectrum of methyl 3-(2-hydroxy-5-iodo-4-phenethylphenyl)propanoate (**6**)

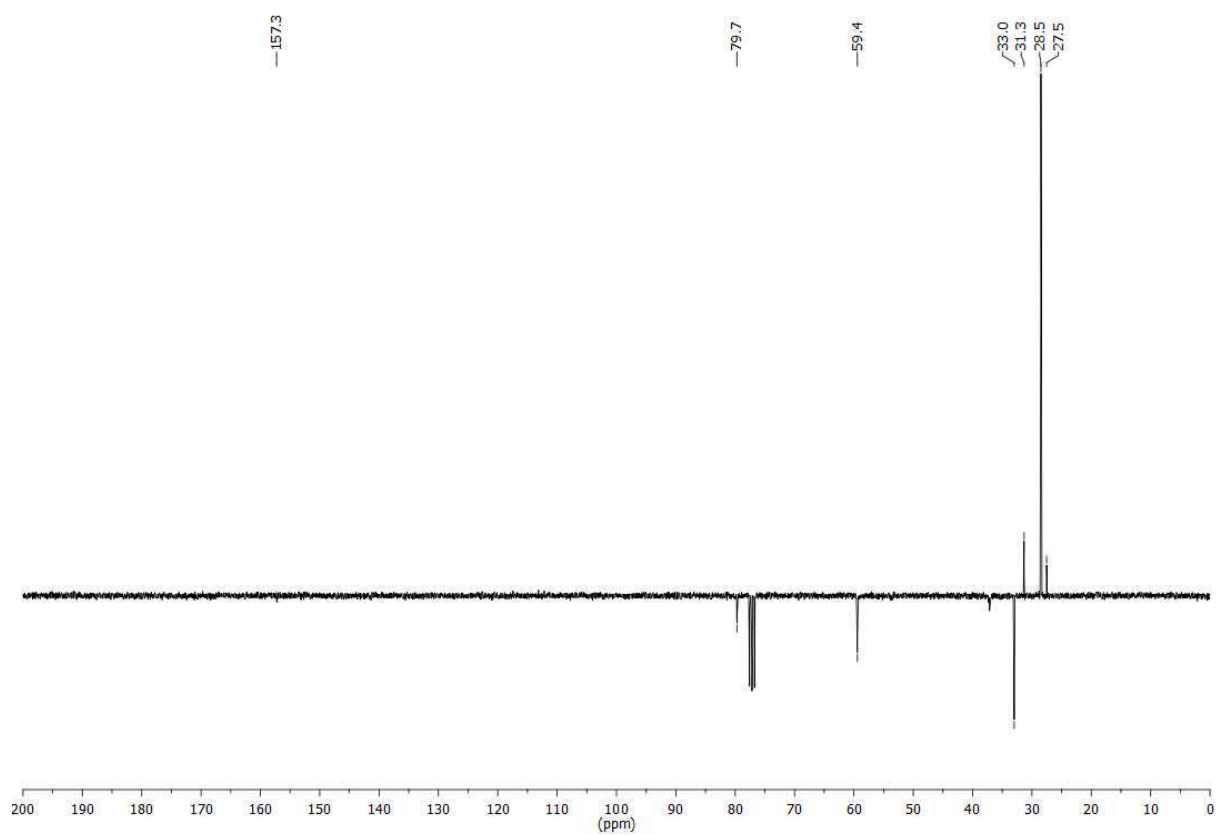
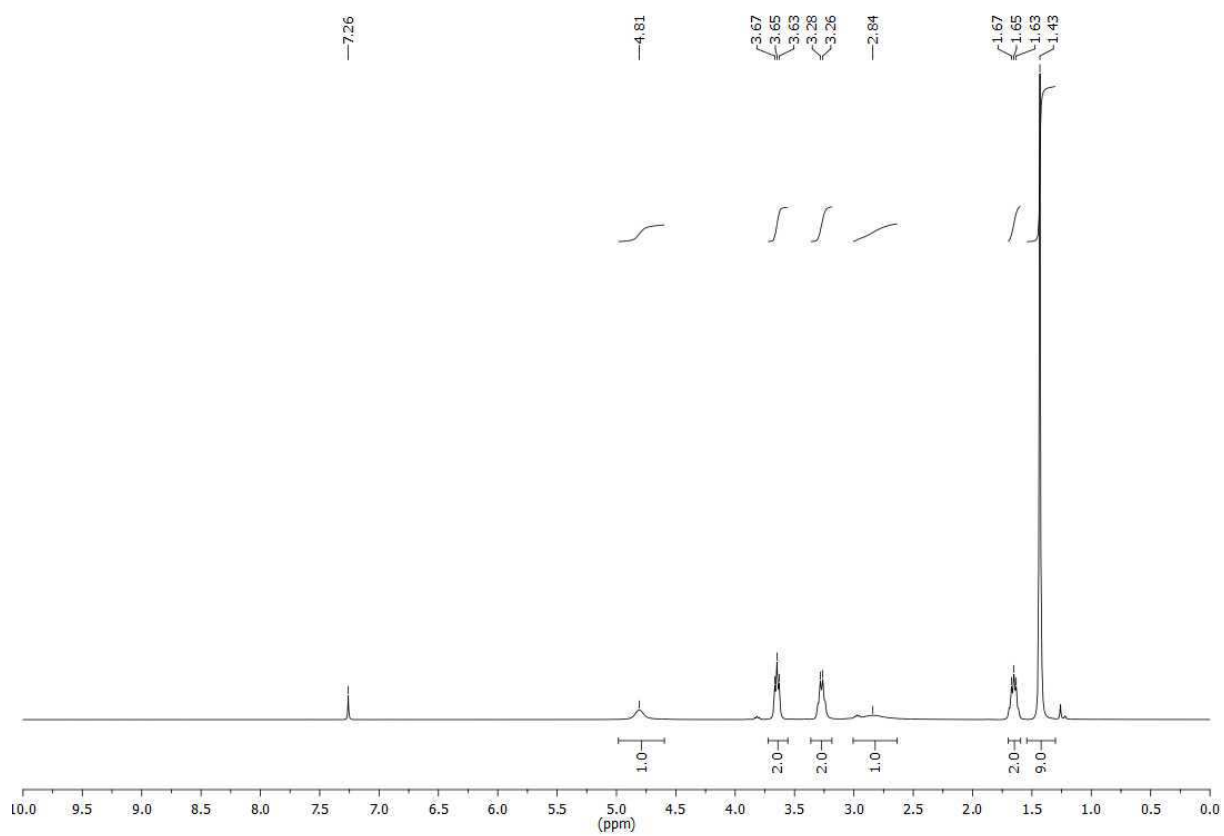
$^1\text{H}$ - and APT spectrum of methyl-3-(5-iodo-4-phenethyl-2-(((trifluoromethyl)sulfonyl)oxy)phenyl)propanoate (**7**)

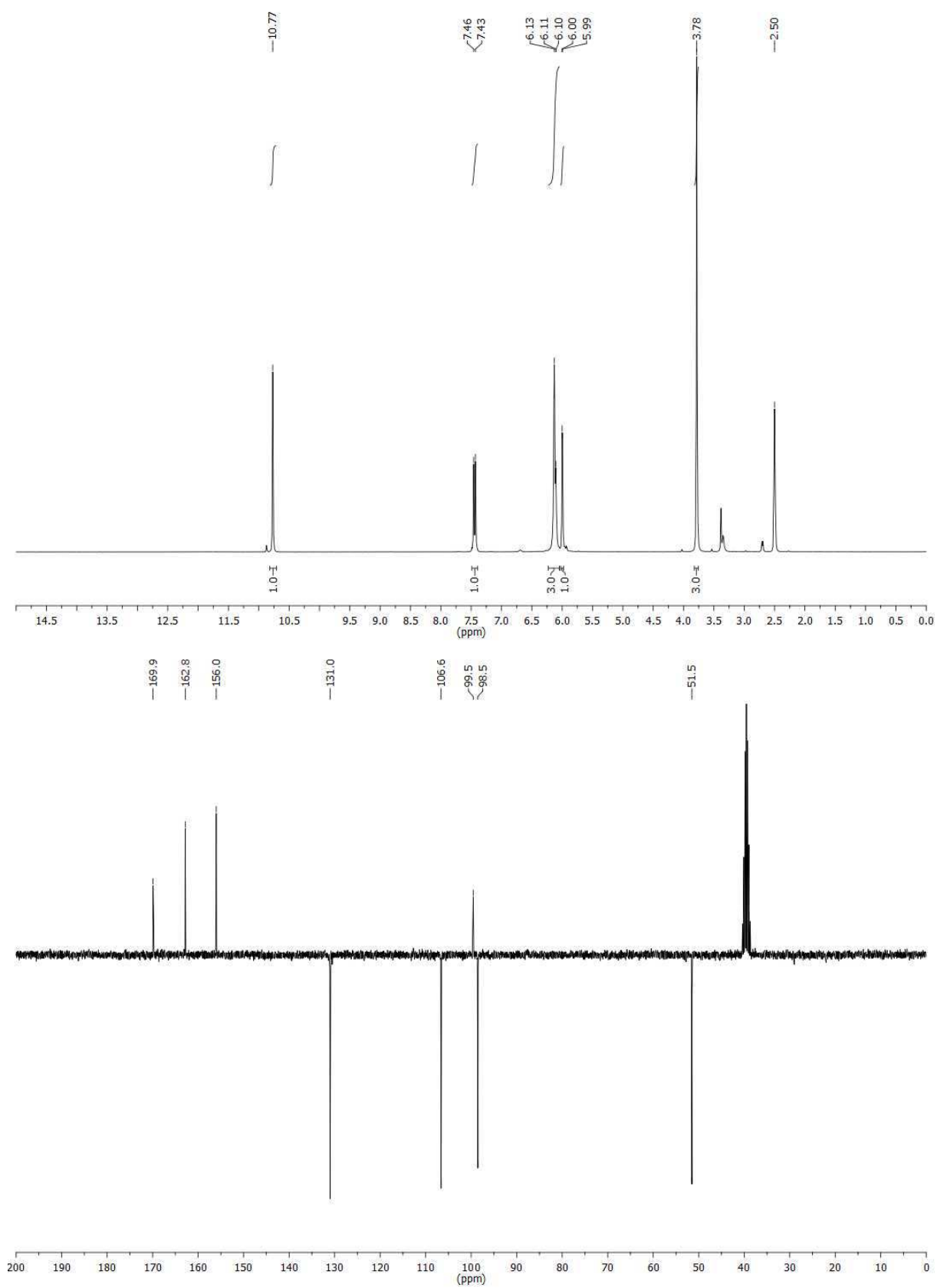


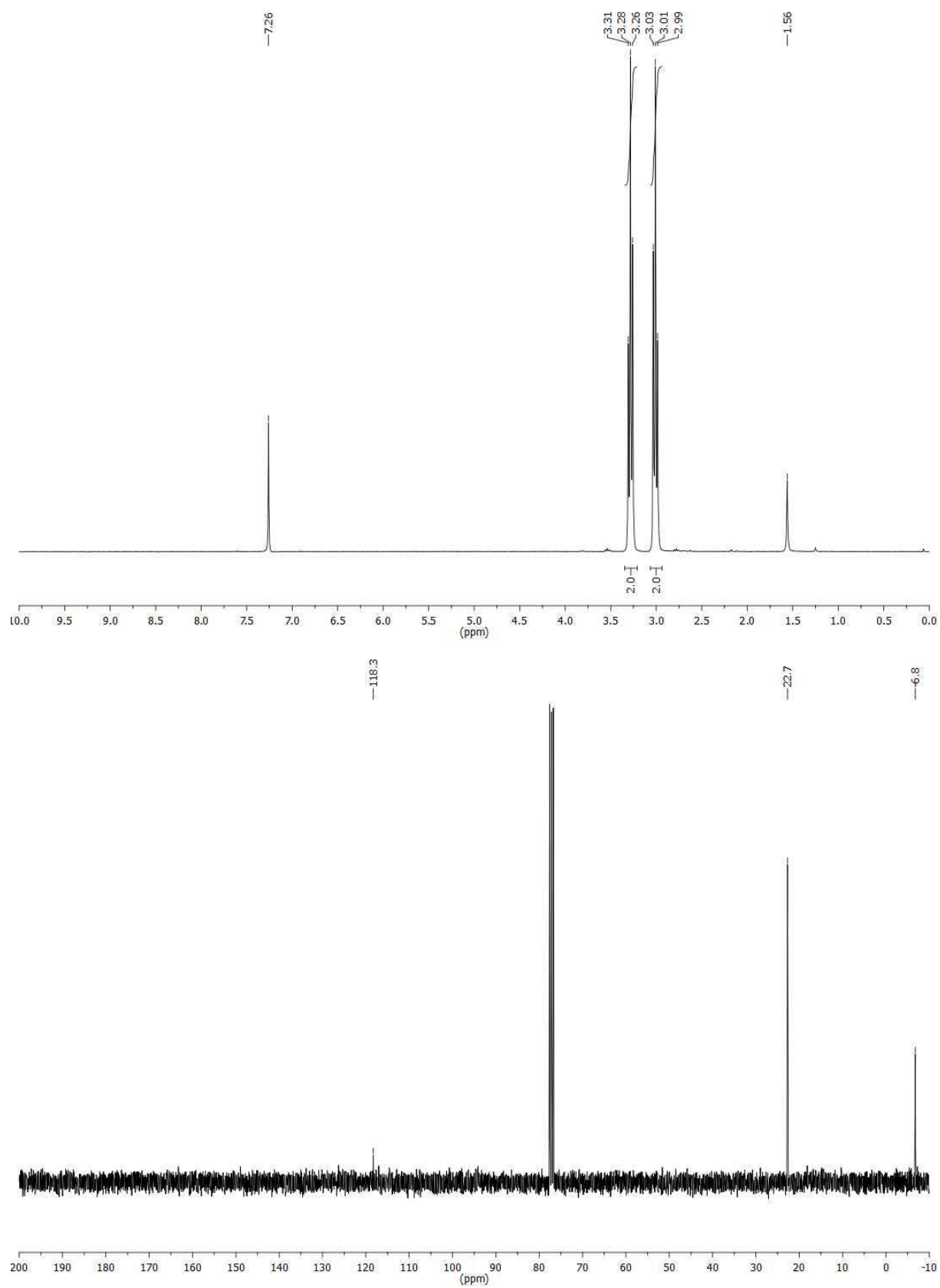
$^1\text{H}$ - and APT spectrum of diethyl benzylphosphonate (**8**)



$^1\text{H}$ - and APT spectrum of *tert*-butyl (3-chloropropyl)carbamate (**9**)

$^1\text{H}$ - and APT spectrum of *tert*-butyl (3-hydroxypropyl)carbamate (**10**)

<sup>1</sup>H- and APT spectrum of methyl 4-amino-2-hydroxybenzoate (**11**)

$^1\text{H}$ - and APT spectrum of 3-iodopropanenitrile (**13**)

$^1\text{H}$ - and APT spectrum of methyl 2-((tert-butyldimethylsilyl)oxy)-4-phenethylbenzoate (**14**)